Exploring the Performance of a PV-Supplied Cooking System with Hybrid Electric-Thermal Energy Storage

by

Learn Leago Chiloane

School of Electrical & Information Engineering, University of the Witwatersrand, Johannesburg, South Africa

A dissertation submitted to the Faculty of Engineering and the Built Environment at the University of the Witwatersrand, Johannesburg in fulfilment of the requirements for the degree of Master of Science in Engineering.

May 2024

Johannesburg, South Africa

Declaration

I declare that this dissertation is my own, unaided work, except where otherwise acknowledged. It is being submitted for the degree of Master of Science in Engineering to the University of the Witwatersrand, Johannesburg. It has not been submitted before for any degree or examination to any other university.

Signed this 22nd day of May 2024

Learn Leago Chiloane

Abstract

This research explores the extent to which the addition of a thermal storage tank can reduce the electrical cooking energy in solar Photo-Voltaic (PV) supplied cooking systems. The aim is to consider a smaller battery size to store the decreased electrical cooking energy and the rest of the solar energy is stored in a low-cost thermal storage tank. This is done to reduce the cost of the storage unit to address the challenges of clean-cooking access in rural African households without grid electricity. The energy performance of the system is evaluated considering a small-scale solar system that powers a storage water heater as the thermal storage tank and a slow cooker as the cooking appliance. A thermal-electrical analogy and experimental tests are employed to model and validate the effectiveness of the system under different cooking conditions. Rice is chosen as the cooking medium because it is the fastest growing staple in Africa, and its cooking process benefits from starting it with pre-heated water. It is shown that starting with pre-heated water accelerates the readiness of rice, and reduces the additional electrical energy to complete the cooking process which translates to a similar battery size reduction. The results from three cooking scenarios indicate that a hybrid cooking system incorporating a battery and thermal storage tank can reduce the battery capacity requirements by up to 24.3% for one meal, 14.7% for two meals, and 10.6% for three meals in comparison to a pure electrical cooking system with a battery only.

Acknowledgments

My acknowledgements go out to the following individuals and organizations whose assistance made the completion of this dissertation possible.

Firstly, I would like to thank Dr. Yu-Chieh (Jessie) Yen for her continued guidance and supervision throughout this research project. Your motivation and encouragement played a vital role in helping me reach this milestone.

To Prof. Willie Cronje and Mr. Muhammed Aswat, thank you for imparting your knowledge and engaging in insightful discussions on renewable energy related topics. The weekly meetings were a significant source of motivation that kept me on track and pushed me to deliver my tasks efficiently.

This work was also completed because of the significant contribution of the technical staff in the Goldfields Laboratory at the University of the Witwatersrand. A special thanks to Mr. Muzi Mabaso for his assistance in building some of the equipment I required to conduct experiments for this work.

I am thankful to Peco Power's Research and Development team for the opportunity and willingness to allow me to develop products with them during the dissertation period. I gained not only research but practical skills that became useful in completing this work.

Lastly, I would like to acknowledge my family, friends, and Ms. Tlotlo Marakalla for their support and encouragement throughout my postgraduate university life. Your proofreading contributions played a significant role in this final work as well. I thank you all from the bottom of my heart.

Table of Contents

List of Tables

List of Figures

Chapter 1

Introduction

This research focuses on exploring the performance of renewable-based cooking systems with hybrid storage to address the challenges of clean-cooking access in rural Africa. The explored cooking system topology involves supplementing a battery with a thermal storage system to influence the cooking process. This integration aims to reduce the required energy stored in the batteries, consequently reducing the overall system cost, as thermal storage systems typically use cost-effective materials than electrochemical battery storage systems.

This chapter introduces the research by providing the key reasoning and motivation behind it in *Section 1.1*. The main research question is then presented in *Section 1.2*, followed by the detailed research objectives in *Section 1.3*. The research scope and high-level assumptions made are given in *Section 1.4*. The guide of the dissertation using its chapters and appendices is outlined in *Section 1.5*.

1.1 Research Introduction

Access to energy in households is a multi-faceted challenge typically comprising of three key components: lighting, cooking, and heating, all of which are necessary for overall progress and to enhance the quality of life. In some households, multiple energy sources are used to achieve all three components. While there has been a significant progress in lighting, access to cooking and heating with clean energy has not been able to keep pace with the population growth [1]. It is estimated that by 2030, 2.3 billion people globally will still lack access to clean-cooking solutions [1–3].

According to the International Energy Agency (IEA), approximately 64% of the population in Africa relies on solid biomass sources such as wood, charcoal, agricultural and animal wastes for cooking [4]. The lack of access to electricity and socio-economic factors such as poverty and preference contribute to the continued use of these sources [4, 5]. However, these sources have serious negative impacts on human health and the environment [1, 3–7]. Therefore, there is a need for innovative alternatives to address the clean-cooking challenges.

Cooking using renewable energy sources (such a solar and wind) with an electrical cooking appliance provides potential solutions for clean and sustainable alternatives [3, 8]. Two distributed renewable energy schemes are represented in *Figure 1.1* each employing distinct energy storage systems. A singular energy storage system, as shown in *Figure 1.1(a)*, typically uses either a battery or thermal storage system, depending on the intended application. Batteries are commonly used in singular energy storage systems to directly power electrical loads. At small-scale, these systems can meet the requirements of low power and energy applications, such as lighting, charging of small appliances, and television. However, cooking demands high power and energy necessitating high-cost batteries to cook during periods of low renewable energy generation [9, 10]. This poses a challenge for these alternatives in rural areas of Africa because of limited finances. To address these barriers, low-cost methods to store and use the harnessed renewable energy are necessary.

A hybrid energy storage system, as shown in *Figure 1.1(b)*, incorporates a secondary storage system that can be charged when the primary storage system reaches maximum capacity. Thermal storage systems are typically cheaper than battery storage systems and are well-suited for thermal loads such as cooking, space heating or cooling [11]. This approach could also be implemented to store more energy from renewable energy sources during days of higher energy generation [12, 13]. Therefore, the selection of an appropriate low-cost thermal storage system is important to achieve the effective use of renewable energy in the context of cooking.

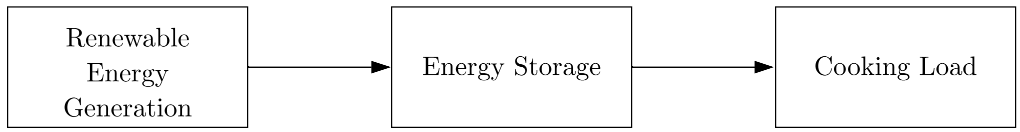

(a) Singular energy storage.

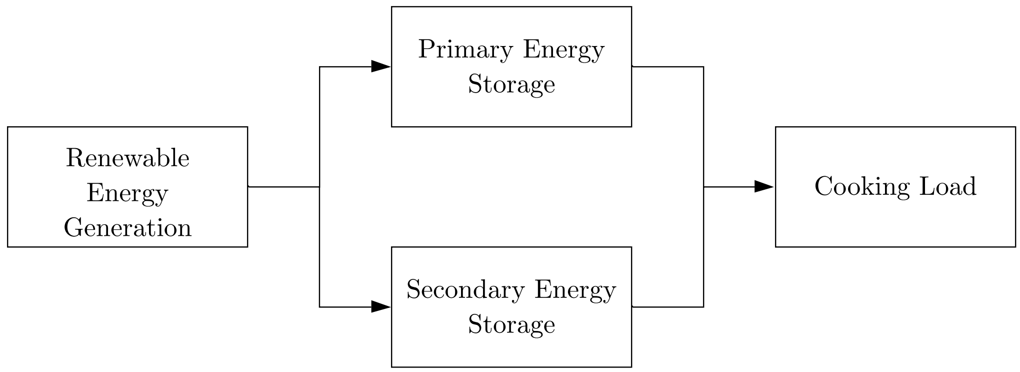

(b) Hybrid energy storage.

Figure 1.1: Representation of energy storage system configurations. (a) Singular energy storage. (b) Hybrid energy storage.

This dissertation explores the performance of a cooking system that stores solar Photo-Voltaic (PV) energy in the form of hot water, which is used in the cooking process. A storage water heater tank, as a supplement to a battery acts as a low-cost thermal storage tank. Cooking initially with hot water is expected to shorten the cooking duration and reduce the additional electrical energy required for cooking staple foods. This cooking system topology could allow for the use of reduced battery capacities in PV cooking systems.

1.2 Research Question

The question to be addressed by the dissertation is as follows: "To what extent can a thermal storage tank, as a supplement to a battery storage system, reduce the electrical component of cooking energy in PV systems?"

The motive of this research is to explore how typical storage water heater tanks can assist in storing PV energy for thermal energy applications. This could provide options to consider smaller batteries for renewable-based cooking systems, which partly contributes to addressing the challenges of clean-cooking access.

1.3 Research Objectives

The following objectives have been identified to address the research question:

(i) To identify a commonly consumed staple food item that can benefit from a cooking process using pre-heated water from the thermal storage tank, with an objective measurement method for evaluating the state of the food.

(ii) To develop and validate mathematical models of a storage water heater and a cooking appliance taking into account the thermal losses involved.

(iii) To examine the impact of reducing the additional electrical energy required for cooking with this topology using the developed models through case study scenarios.

1.4 Research Scope and Assumptions

The key assumptions made for the research are as follows:

(i) The PV system is designed to meet the power and energy requirements of cooking in individual households and does not include the energy demands of other household tasks.

(ii) The cooking system is not studied in a specific geographic location. The performance of system is explored under different solar irradiation and temperature levels.

(iii) The performance comparison focuses on the battery sizing between the electrical and hybrid systems. This is because the battery is the major cost of a PV system and will provide insight into the potential cost savings of the entire system.

1.5 Dissertation Guide

The research question, objectives, scope and assumptions have been outlined, the rest of the dissertation is structured as follows:

- *Chapter 2* provides the necessary **background** information by reviewing the challenges on existing PV systems for rural electrification. It examines the current thermal storage used in renewable-based systems and discusses the modelling techniques adopted for thermal systems. Moreover, it gives a survey of existing techniques used for analysing the readiness of a staple food item.

- *Chapter 3* outlines the **research approach**, providing a detailed description of the overall decisions and methods chosen in this research. The problems and opportunities of PV systems are explained and the hybrid cooking system topology is defined. The chapter also provides an overview of the experimental set-up for the cooking system, and an explanation of the texture measurement method for determining the state of the selected cooking medium. The modelling technique chosen to represent thermal systems is explained, and the selected experiments used for studying the influence of cooking with pre-heated water are discussed. Additionally, the cooking scenarios identified to explore the overall performance of the hybrid cooking system are defined.

- *Chapter 4* focuses on the **model development** for thermal systems, including the thermal storage tank and cooking appliance selected for the hybrid cooking system. The chapter uses a parameter identification method to determine the parameters of the developed models, and these models are validated using experimental results.

- *Chapter 5* presents the results of the **pre-heated water influence** on cooking. It discusses the amount of additional electrical energy required to cook rice to the desired state by starting with pre-heated water at different temperatures. The chapter also presents a derived relationship between the initial water temperature and the expected reduction in the additional electrical energy.

- *Chapter 6* evaluates the **hybrid cooking system performance** under three cooking scenarios that resembles household cooking patterns. The simulations use the models of the thermal systems developed in *Chapter 4* and apply the energy reduction relation derived in *Chapter 5*. The chapter examines the extent of battery reduction achieved by the hybrid cooking system compared to a pure electrical system in each scenario.

- *Chapter 7* gives a **discussion of the research** by summarising the key findings resulting from experiments and simulations. Additionally, a discussion on potential areas for further research is given.

- *Chapter 8* gives the **conclusion** of the research work by linking the key results to the research objectives and question.
- The appendices at the end of the document provide additional information to support the work presented in the main chapters. *Appendix A* contains additional background information, *Appendix B* includes the experimental work, *Appendix C* provides the model diagrams, pseudo-codes, and simulations used, and *Appendix D* provides additional results of the hybrid system performance.

Chapter 2

Background

According to the IEA [4], approximately 43% of the population in Africa, most in rural areas, lack access to electricity, and over 69% lack access to clean-cooking solutions. Solar energy stands out as the most abundant renewable energy source in Africa [14]. The continuous improvements in solar PV cell efficiencies and the rapid decrease in solar PV prices, due to the reduction in manufacturing costs, have contributed to their increase in popularity [15–17]. These points provide a good argument for considering off-grid clean-cooking solutions that are based on solar energy.

This chapter explains the limitations and challenges of small-scale PV systems that are used for rural electrification in *Section 2.1*, and discusses the topology of supplementing thermal storage in order to enhance their effectiveness for cooking purposes in *Section 2.2*. Previous clean-cooking systems related to the research are discussed in *Section 2.3*. Modelling techniques of thermal systems, specifically for storage water heater tanks and cooking appliances, which are an integral part of the research, are discussed in *Section 2.4*. Common staple foods in Africa and the measurement methods to objectively analyse the cooked state of a food item in the research are discussed in *Section 2.5*. The chapter is concluded in *Section 2.6*.

2.1 Rural Electrification with Solar PV Systems

In African rural areas, first-time access to electrification is typically done at the point of consumption to avoid the need for high-cost and extensive electrical distribution infrastructure. This has been made possible with isolated systems such as small-scale off-grid PV systems [4]. Because of the intermittent nature of renewable energy sources, energy storage are integrated into the systems to ensure reliable and consistent power supply. Batteries are typically used as energy storage because electrical energy can be stored and retrieved with less losses to power electrical loads during periods of scarce PV generation.

The small-scale PV systems with batteries are commonly used for low-demand applications such as lighting, charging, and television. In some cases, they are also used for intermittent refrigeration. However, these solutions do not meet the higher power and energy demands of cooking. Additionally, the capital cost of solar PVs with batteries sized to meet cooking requirements is not financial feasible for rural areas in Africa. As a result, traditional cooking methods using biomass sources remain prevalent in almost two-thirds of African households [4], and the adoption of solar PV systems for cooking is limited.

2.2 Supplementing Thermal Storage in Solar PV Systems

Thermal energy storage systems provide a promising and cost-effective alternative to battery storage systems, particularly for thermal energy applications [15, 18]. Instead of relying solely on batteries, integrating a thermal storage system can allow for energy to be stored as heat, which can be used directly for cooking. While this topology may not be applicable for most household energy tasks due to the absence of energy-efficient methods to convert heat back to electrical energy. It is considerable because cooking, including the processes of combining and mixing food, requires a significant fraction of household energy in the form of heat to execute.

The two common categories of thermal energy storage systems use sensible heat or latent heat storage materials. Sensible heat storage involve storing thermal energy by raising the temperature of a material without changing its phase. Solids such sand and concrete, or liquids

Table 2.1: Thermo-physical properties of common sensible heat storage materials [19, 20].

State	**Material**	**Specific heat capacity** [J/kg·°C]	**Density** [kg/m^3]	**Volumetric heat capacity** [kJ/m^3·°C]
Liquid	Water	4182	998	4174
	Molten salts	1570	1950	3062
	Transformer oil	2090	842	1760
Solid (non-metal)	Sand	1465	1587	2325
	Rocks	850	2600	2210
	Concrete	920	2300	2116
Solid (metal)	Iron	465	7850	3650
	Copper	419	8300	3478
	Aluminium	945	2700	2552

such as water and molten salt can be used as low-cost sensible heat storage materials [19, 20]. In contrast, latent heat storage (also known as Phase Change Material (PCM) storage) involve storing thermal energy through the phase change transition of a material at constant temperature. Storage materials for this category can be organic, such as paraffin and erythritol or inorganic, such as a sodium acetate trihydrate and potassium nitrate [19, 20]. However, according to [21, 22], access to latent heat storage materials is limited, and their cost per energy stored is typically greater compared to sensible heat storage materials.

The total energy stored using sensible heat storage materials is directly proportional to their specific heat capacity, density, and operating temperature. The thermo-physical properties of common and accessible sensible storage materials are given in *Table 2.1.* Notably, water has the highest volumetric heat capacity which benefits from its high specific heat capacity and relatively high density. This means water has the ability to store more energy and requires less volume in comparison to the listed materials. The usage of hot water at boiling point to cook staple foods is also considerable, which makes storage water heaters good candidates for thermal energy storage systems. These appliances are capable of heating and storing thermal energy for long periods of time if equipped with good thermal resistance, as demonstrated in [23–27].

The overview of how a thermal storage tank can be incorporated into a PV system with batteries for cooking is represented in *Figure 2.1.* This approach requires minimal modifications, as the PV system can sequentially charge the storage units using an automatic change-over switch and

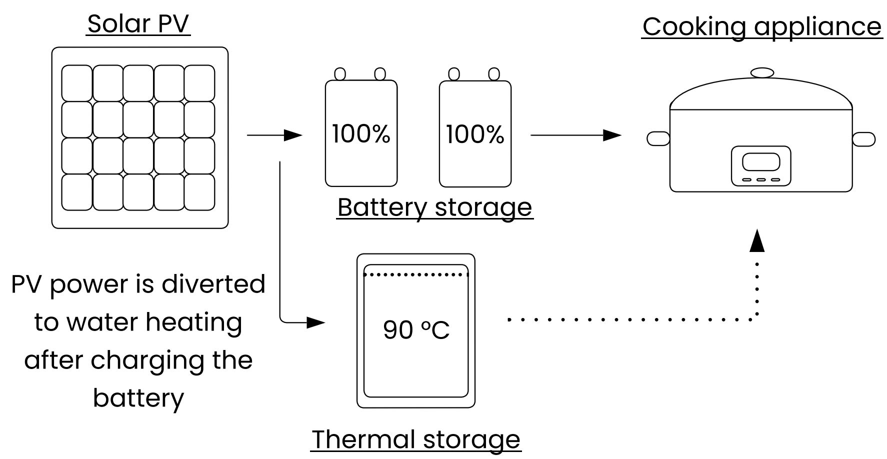

Figure 2.1: Representation of a PV cooking system with battery and thermal storage.

power the cooking appliance. The addition of a thermal storage tank, such as a storage water heater, allows for water to be heated and stored so that it is used directly during the cooking process. While pre-heated water alone may not complete the cooking process, the remaining steps can be accomplished using additional electrical energy. This topology could offer cooking options that are low-cost compared to standalone battery systems because thermal storage systems typically use cheap storage materials compared to electrochemical battery storage.

2.3 Existing Cooking Systems with Solar PV Energy

Converting renewable energy into heat and storing it in a thermal storage system for thermal applications can influence the overall electrical energy consumption of appliances in both off-grid and grid-connected households. Numerous research has been conducted to assess this impact [15, 28–31]. The literature reviewed in this section focuses on the use of renewable-based systems in the context of cooking.

Non-metal solids such as sand, rocks, and concrete are some of the most affordable and accessible storage materials. Authors in [28] have conducted experimental studies on using sand as a storage material, while the work done in [29] has developed a large-scale sand-based storage system to supply a community with thermal energy. In this system, resistive elements powered by solar panels heat up air which is then circulated in heat-transfer pipes to raise the temperature of the sand to 600 °C. Then heat-exchange pipes are used to provide the heat and hot water to households, with some of the heat converted to electricity. These systems have the potential to be used as thermal storage for cooking, but due to their charging and discharging complexity, the large volume requirements, and high inefficiencies of converting heat back to electrical energy, they may not be practical and cost-effective for small-scale systems especially compared to storage water heater tanks.

In [30] the authors developed a cooking system that stores solar energy in a PCM (erythritol) during the day to cook using high temperature after sunset. The developed system covers a cooking vessel with 2.5 kg of erythritol that is heated by a resistive element using a solar panel. When heated to 180 °C, the system can boil 1 ℓ of water in 5 minutes and 20 seconds. While the system is effective for storing thermal energy and cooking different foods, the key drawbacks are that erythritol thermally degrades after several months when cycled at high temperatures and that low temperatures are not effective to boil or cook food. Additionally, the thermal losses increase at high temperatures, which encourages immediate cooking after sunset. To complete the cooking process when temperatures are low, the authors powered the cooker using an AC to DC adaptor connected to the grid. This hybrid compensation is an essential aspect of this research where battery energy can be used to complete the cooking process after energy from the thermal storage tank has been applied.

The research conducted in [31] examines the use of PV systems to supply common household thermal appliances such as freezers, water heaters, and space heaters to reduce the grid electricity cost. Since cooking primarily depends on heat, it is more appropriate to consider heating storage devices for cooking purposes, while cooling storage devices are mostly relevant for food storage. The findings reveal that storage water heaters for bathing are the main power consumers and have the potential to significantly reduce grid energy cost when powered by PV during the day. This research focuses on using small-sized storage water heaters commonly found in the market to store part of the PV energy and reduce the battery size requirements for cooking using an electrical appliance.

In [15], a DC solar cooking system that automatically switches to grid power for backup was proposed. The system includes a storage water heater that uses solar power and has a 500 W limit for any cooking appliance used. To evaluate the system performance, rice was mixed with water heated to 95 °C by a solar panel and then cooked with electrical power from the grid. Compared to starting to cook rice with cold water, the results showed an 18% reduction in grid electrical energy consumption for a conventional pressure cooker and 30% reduction for an electrical pressure cooker. However, it is not always guaranteed to heat up water and maintain it at high temperature in off-grid PV systems, and the state of the cooked rice was not objectively evaluated in the study. This research evaluates the total amount of additional electrical energy required to cook a staple food item after adding pre-heated water from a storage tank supplied only by a PV system, considering different levels of solar irradiation. A measurement method for the texture of the staple food item, which is discussed in *Section 2.5*, is used to validate its readiness.

2.4 Systems Modelling Techniques

System models are required to simulate and analyse the extent to which the integration of a storage water heater reduces the required battery capacity under various cooking scenarios and different weather conditions. Thermal systems can be modelled using various approaches to characterize their behaviour. An effective model can accurately estimate the energy consumption of these systems and can provide insight into their internal dynamics under different operating conditions.

Authors in [32] proposed a grey-box thermal modelling technique based on a thermal-electrical analogy. It uses circuit analysis techniques to solve for thermal parameters. The technique considers several factors such as temperature change within the system, energy storage in the system, and the loss of energy to both the system components and the surrounding environment. The accuracy of models can be enhanced by increasing the number of temperature zones used, but this comes at the expense of increasing model complexity.

Different models have been developed for water heaters with varying levels of complexity [33–38]. References [34–36, 38] proposed water heater models using the thermal-electrical analogy, incorporating an on-off thermostat, and accounting for the effects of water draw and standing losses. The models simulate both power consumption and internal temperature, providing a valuable tool for investigating the performance of water heaters.

Simple models often rely on linear equations to calibrate the model parameters, while complex models require the use of parameter identification methods to optimize these parameters. Once the parameters have been determined, the simulated results of the model can be compared with experimental results to validate its accuracy.

2.5 Food State Analysis

In order to analyse the benefits of cooking with additional thermal energy in the form of hot water, an objective method of measuring the state of cooked food is required. The state of the food must be continuously monitored throughout the cooking process to accurately quantify when it becomes fully cooked.

According to [39], the common staple foods in Sub-Saharan Africa (SSA) include maize, millet, sorghum, wheat, and rice. Globally, rice serves as a staple for almost two-thirds of the population [40]. In SSA, rice consumption is increasing at a rate of 6% annually, faster than any other staple foods [41–44]. It has become the second most important staple food in several SSA countries, following maize, and has replaced other traditional staples [39]. Due to these points and the ease of cooking, rice is a suitable candidate as a cooking medium in this study.

Several studies have focused on the analysis of rice texture [40, 45], highlighting Moisture Content (MC) and hardness as the two main factors for determining the texture of rice. Hardness is defined as the maximum force of a single grain under compression, while MC refers to the amount of water absorbed by the rice. As rice softens and absorbs more water whilst cooking, these factors provide a quantifiable means of assessing its texture. To ensure accuracy, multiple measurements are taken using several grains.

References [15, 46, 47] perform the texture measurement of rice using a texture analyser on a single grain. The grain is compressed to a range of 75% and 85% deformation while the deformation force data is collected. The maximum value of the resulting force is taken as the hardness of the grain. In [3] the MC is determined by comparing the absorbed water to the initial dry grains, whereas [40] performs it by compressing out the absorbed water and comparing it to the drained grains. A wide range of MC of rice which gives a desirable state for consumption is determined.

2.6 Conclusion

Various methods have been proposed in previous studies to store thermal energy for cooking purposes, such as using small-grain storage materials and phase-change materials. However, these methods have limitations in small-scale off-grid cooking systems due to their high volume requirements, high energy losses and complex implementation. Based on the literature review, a storage water heater with thermal insulation is identified as good candidate for storing thermal energy in an off-grid cooking system, as it can heat and store hot water for an extended period. This research will explore the performance of the hybrid system topology using thermal modelling techniques and food state measurement methods from the literature.

Chapter 3

Research Approach

This chapter outlines the approach taken to address the research objectives. The approach includes the design choices, model decisions, experimental methods, and the cooking scenarios selected for validation. It begins with the problem statement covering the cooking system topology in *Section 3.1.* The experiment setup and procedures are discussed in *Section 3.2*. A discussion of the model strategies chosen for the subsystems is given in *Section 3.3*, which is followed by an explanation of the case study scenarios in *Section 3.4* to showcase the performance of the cooking topology. The chapter concludes in *Section 3.5*.

3.1 Problem Statement

This section discusses the reasons why a hybrid storage system supplied with PV could improve the lack of access to clean-cooking solutions in rural Africa. It begins with the problems and opportunities with storing PV energy in *Section 3.1.1.* This is followed by an explanation of the chosen hybrid cooking system in *Section 3.1.2* and a detailed discussion of the energy transfer mechanism of its subsystems in *Section 3.1.3*.

3.1.1 Energy Storage in PV Systems

The electrical energy harnessed from the sun by solar PVs can be used for a wide range of applications. As mentioned in *Chapter 2*, there has been some level of adoption of PV systems

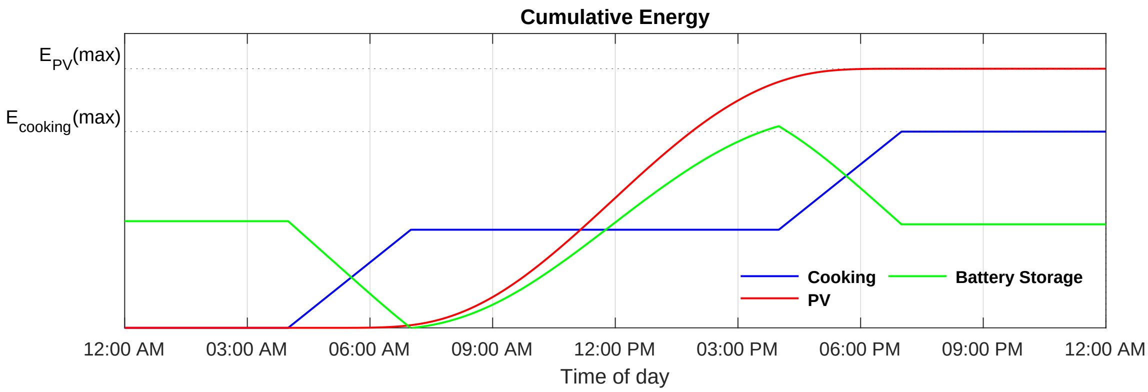

(a) Electrical cooking system.

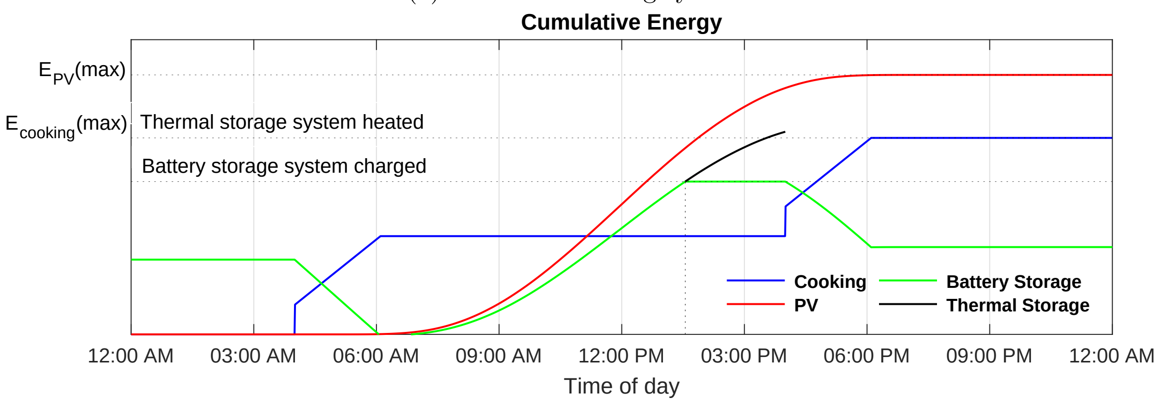

(b) Hybrid cooking system.

Figure 3.1: An illustration of a PV cooking system energy performance. (a) Electrical cooking system. (b) Hybrid cooking system.

with batteries for low-energy tasks such as lighting and charging applications in rural Africa. However, the core limitation of scaling these systems for high-energy tasks such as cooking is the requirements of large and costly batteries. An illustration of the energy performance of a PV cooking system with a battery (electrical cooking system), and the potential low-cost alternative with a battery and thermal storage system (hybrid cooking system) is presented in *Figure 3.1*. The results are based on a comprehensive sizing and performance analysis detailed in *Appendix A*, which focus on a PV system designed to cook two meals in the morning and afternoon.

In the electrical system, as the sun rises, the PV power exceeds the load and charges the battery which reaches full capacity before sunset. The cooking energy is then supplied from the electrical energy stored in the battery ($E(cooking) = E(battery)$). Battery storage systems provide long-term energy storage with minimal standby losses but come at an expensive cost.

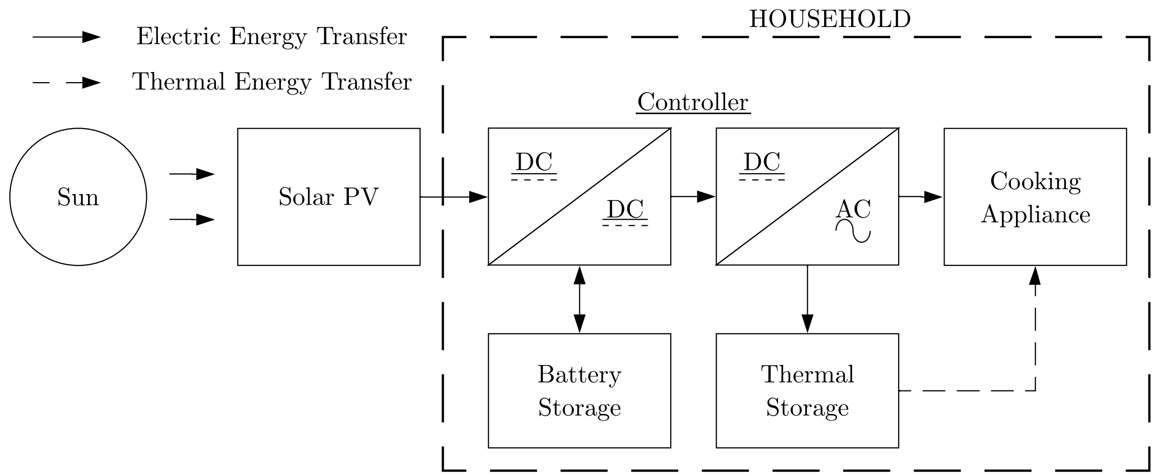

Figure 3.2: Topology of a PV cooking system with battery and thermal storage.

In the hybrid system, once the battery (that is sized smaller compared to the electrical system) reaches full capacity, the PV energy is diverted to the thermal storage system. The cooking energy is then supplied from a combination of electrical and thermal energy stored ($E(cooking) = E(battery) + E(thermal)$). This means the electrical component of cooking energy could be reduced by adding thermal energy. Thermal storage systems are typically cheaper storage systems that are well suitable for thermal loads such as cooking. However, they are likely to have high losses depending on their thermal insulation.

The hybrid system topology, as explained aims to reduce the requirements of large and expensive batteries. Therefore, this research explores the extent to which a thermal storage system, as a storage water heater, can reduce the electrical component of cooking energy stored in batteries. The following subsection discusses the hybrid storage cooking system in detail.

3.1.2 Hybrid Electrical-Thermal Cooking System

The hybrid energy storage cooking system that is proposed, is an off-grid PV solution with a battery and thermal storage tank aimed for individual households in rural areas of Africa and other high solar irradiation regions. The key functionality of the system is the thermal storage tank that heats up water using PV energy and stores it for the cooking process. The schematic topology of the off-grid cooking system is shown in *Figure 3.2*. It comprises of subsystems: solar PV, battery storage, thermal storage, controller, and a cooking appliance.

This research focuses solely on evaluating the energy performance of the hybrid system against the electrical system. The energy-based analysis considers both thermal and electrical energy losses involved to accurately assess the system performance. The following subsections provide a detailed discussion of each subsystem and how it is considered.

3.1.3 Subsystems of the Cooking System

The cooking appliance converts electrical energy to heat, which is used to prepare food in a vessel. The appliance has to operate at low power and effectively transfer the generated heat to cook with minimal heat losses to the environment. These are important factors considering the limited power and energy availability of typical small-scale PV systems. The cooking appliance is a load powered by the PV and battery through a DC to AC inverter.

The thermal storage tank heats up water and stores it to be used directly in the cooking process. The focus is on exploring a storage tank that is food-safe, not piped and does not require pressurization. A food-safe tank is important to store water that is suitable for preparing food without health risks. A tank that is not piped or pressured is ideal for areas that lack tap water in their households, because the stored hot water can be used without an immediate need to be refilled. The choice of the thermal storage tank and cooking appliance and their experimental setup are explained in *Section 3.2.1*.

The electrical energy generation is done using a solar PV only, and the energy is stored firstly in the battery. After the battery is charged, the controller redirects the power to the thermal storage tank before sunset. The solar PV energy output during the day is emulated and considered as a power source with a battery back-up to ensure that the cooking appliance operates at the rated constant power.

The hybrid system topology has been explained. The following sections describe the methods chosen to achieve the research objectives about the cooking topology as formulated in *Section 1.3*.

3.2 Experiment: Setup and Procedure

This section outlines the choice of experimental methods used in the research. The cooking setup of the selected thermal storage tank and cooking appliance are presented in *Section 3.2.1*. The choice of an objective method for measuring the state of a staple food is presented in *Section 3.2.2*, and the experimental method chosen to investigate the implication of starting to cook with pre-heated water is provided in *Section 3.2.3*. The diagrams and a detailed discussion of the components and methods used for the experimental work is presented in *Appendix B*.

3.2.1 Cooking Setup

In order to explore the performance of the hybrid cooking system, the thermal storage tank and cooking appliance have to be selected and sized for the cooking system. Storage water heater tanks are prevalent household appliances used to heat, store, and supply hot water for various tasks, including cooking. A commercial water urn has the ability to offer these functionalities. A 15 ℓ, 1.5 kW, stainless-steel urn in vertical orientation, as described in *Appendix B.4*, is modified to consume energy at 250 W of power using a variac and to store 5 ℓ of water. The maximum water temperature in the urn is selected to be approximately 90 °C to prevent it from boiling and turning into steam, which could cause gradual reduction in water volume and safety hazards.

A thermal blanket is wrapped around the tank to improve its thermal resistance by a factor of 4.55 (from 0.497 to 2.26 °C/W). This is a common and cost-effective method to reduce standing losses of storage water heater tanks such as geysers [23–27]. It is used in this study to ensure that the urn retains hot water for use the following day without reheating (refer to *Appendix B.4* for a further discussion on the applied thermal blanket). The power consumption of the urn is determined using RMS voltage and current measured. Three Resistance Temperature Detectors (RTDs), each with an accuracy of 0.5 °C, are used to measure the temperature profiles. Two of these RTDs are placed around the centre of the tank to measure the water temperature. It is assumed that the water in the urn, given its small varying volume, is uniformly heated. The third RTD measures the ambient temperature positioned at least 30 cm away from urn.

A variety of electrical appliances can be chosen for cooking using a PV system, including slow cookers, pressure cookers, and induction cookers. The focus is on slow cookers due to their low-power capabilities, automatic cooking process, and good thermal resistance. The considered slow cooker, as detained in *Appendix B.2*, has a cooking vessel capacity of $4\,\ell$ and a power rating of 200 W. The power consumption of the cooker is measured, including the temperature profiles using RTDs. One RTD measures the temperature of the food mixture, positioned approximately 5 mm above the bottom of the cooking vessel, while another RTD measures the ambient temperature positioned at least 30 cm away from the cooker. The measurements are logged every second.

The two subsystems are selected and modified considering a small-scale PV system with an AC continuous output power limit of 500 W and a system DC voltage of 12 V. While the two subsystems are unlikely to be used simultaneously, their combined power consumption is within the 500 W limit. The 200 W slow cooker is expected to require more time for cooking compared to high-powered cookers, but the additional heated water from the storage water heater tank before cooking is anticipated to shorten the duration. Moreover, the $5\,\ell$ water volume is chosen to meet the cooking requirements of a family of three to four members, as suggested in [15], guaranteeing that there is enough hot water for cooking.

3.2.2 Food State Measurement

The reasoning presented in *Section 2.5* is used to justify the selection of rice as a suitable cooking medium for this study. A single gene of rice is selected based on local availability to ensure consistency in the experiments. An objective measurement method is important to quantify the state of rice in each cooking experiment. This will provide insight into how the state of rice changes to reach a desirable state for consumption when the cooking process is started with water of different temperatures. Then the electrical energy component the cooker consumed to achieve this state in each case can be determined and compared. As discussed in *Section 2.5*, MC and hardness are the two main factors in determining the state of rice. While hardness can be determined using a texture analyser equipment, it is not available for this study, and therefore, MC is used as the main factor for measuring the readiness of rice. An additional assessment of the state of rice is done using a subjective taste method to support the results determined using the MC method. The procedure for selecting the state of rice on taste is summarised in *Table 3.1*.

To determine the MC of the rice on a wet basis (w.b) while cooking, the change in additional water content of the rice, over time, is measured. The computation of MC on a w.b is done through the following steps:

1. A sample of N dry and uncooked rice grains is taken, and its mass is measured.

2. The rice and water are added in the cooker, and the cooking process is started.

3. Every K minutes, a sample of N unburnt and unbroken rice grains is removed and its mass is measured.

4. The MC at each measurement point is calculated using *Equation (3.1)*.

$$MC = \frac{m_w - m_d}{m_w} \times 100\% \tag{3.1}$$

Where:

- m_d is the mass of dry rice grains [g]
- m_w is the mass of wet rice grains [g]

The rice grains are placed on a dry cloth to drain any excess water prior to measurements, and their mass is measured using a scale with a 1 mg resolution. In order to ensure accurate measurements, 50 grains and a time period of 30 minutes are selected as the values for N and K, respectively. With an average mass of 30 mg for a single grain, the selection of the N value results in a low-resolution error of less than 0.07%. Additionally, the measurements are repeated three times to increase accuracy (refer to *Appendix B.3.1* for detailed measurement steps, scale calibration, and a visual comparison of rice grains while cooking). The value of K is selected to ensure that there is minimal heat loss from opening the cooker lid multiple times during cooking, but enough time to collect few samples to observe the change in MC.

The state of rice is determined using two benchmark points of MC measurements, MC_{min}

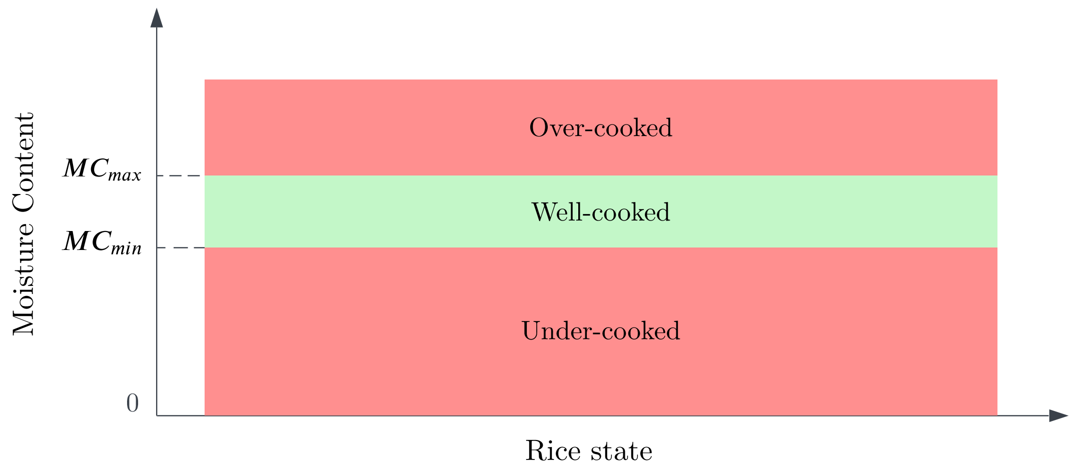

Figure 3.3: Moisture content method used to determine the state of rice during a cooking process.

Table 3.1: State evaluation of rice using a subjective taste test.

Taste classification	**Under-cooked**	**Well-cooked**	**Over-cooked**
Extremely hard	✓		
Hard	✓		
Medium hard		✓	
Soft		✓	
Extremely soft			✓

and MC_{max}. The values are selected as 58.5% and 60.5% using the procedure detailed in *Section 3.2.3* which factors in the results from the subjective tests. The method to determine the state of rice is presented in *Figure 3.3*. The rice is considered under-cooked if, $MC < MC_{min}$, which means the grains have not cooked long enough resulting in dry or hard rice. It is well-cooked if, $MC_{min} \leq MC \leq MC_{max}$, which means the grains have cooked to the desired state for consumption. It is over-cooked if, $MC > MC_{max}$, which means the grains have cooked for too long, often with an initial high water to rice ratio, resulting in an extremely soft state.

3.2.3 Pre-Heated Water Implication

The method chosen to investigate the impact of starting to cook rice with pre-heated water on the additional electrical energy consumption of the cooker is discussed. A range of experiments that show how the state of rice evolves throughout the cooking process are conducted. The experiments are performed in the same season under similar ambient temperature conditions to ensure consistency and comparability of the results.

Long grain parboiled rice, stored at room temperature, with the manufacture's recommended rice to water ratio of 1:2, is used as the subject of the experiments. Dry rice of 300 g ($1\frac{1}{2}$ cups) that results in three to four servings and 600 mℓ of water is considered in each experiment. Four experiments involving water temperatures starting at 25.0, 50.0, 75.0 and 97.6 °C respectively are conducted. The range of water temperatures are selected to cover possible temperature levels in a storage water heater tank ranging from room to boiling point temperatures.

Previous studies on cooking rice suggest that a well-cooked state can be achieved with less than 500 Wh of energy when the temperature of the rice-water mixture is above 65 °C [15, 48, 49]. In this study, after the addition of rice-water mixture, the slow cooker is adjusted to consume approximately this amount of electrical energy to ensure that the state of rice reaches or surpasses the well-cooked state. This is done by adjusting the cooking period to be three hours. The state of the rice is monitored every 30 minutes using the measurement methods defined in *Section 3.2.2*.

While ideally the cooking should stop when the well-cooked state is achieved, the experiments are cooked for same period to provide comparison points of how the rice state evolves. The benefit of initially using pre-heated water will be determined by comparing the additional electrical energy consumed by the cooker in every experiment to reach the well-cooked state. A successful analysis will involve deriving a mathematical relationship between the pre-heated water temperature (input) and the expected reduction in additional electrical energy consumption of the cooker (output). This will provide the basis understanding of the required battery capacity to complete the cooking process when the water temperature in the storage water heater tank is known. The experimental results and analysis are detailed in *Chapter 5*.

3.3 Modelling and Validation

This section describes the chosen modelling technique used for thermal systems in *Section 3.3.1* and the method for identifying parameters of complex models in *Section 3.3.2*. The models will be validated and used to examine the performance of the hybrid system topology under case studies to be specified in *Section 3.4*.

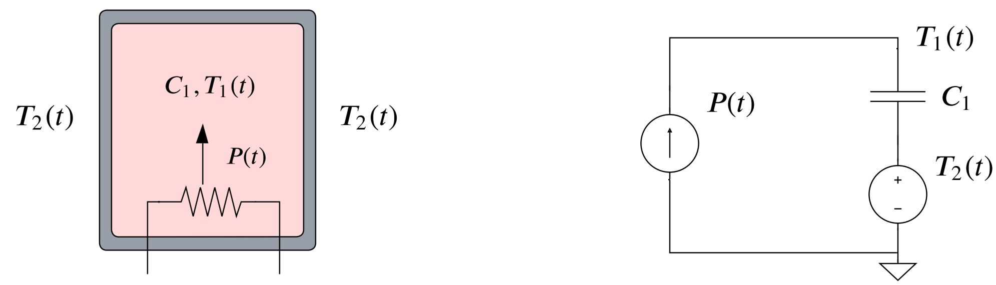

(a) Thermal system. (b) Analogous thermal circuit.

Figure 3.4: Analogous circuit of a thermal system with a homogeneous material. (a) Thermal system. (b) Analogous thermal circuit.

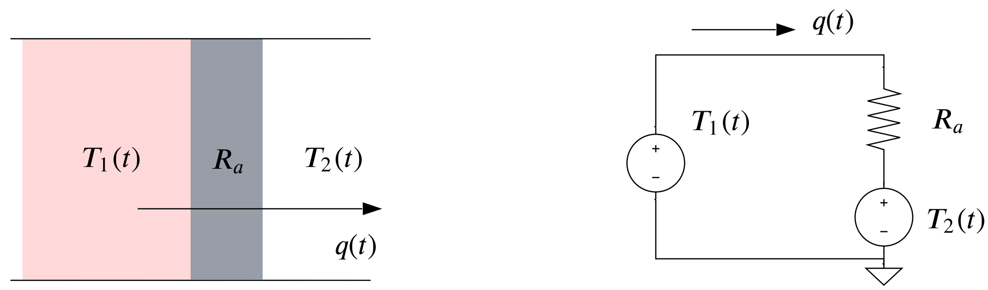

(a) Thermal system. (b) Analogous thermal circuit.

Figure 3.5: Analogous circuit of one-dimensional heat conduction in an object. (a) Thermal system. (b) Analogous thermal circuit.

3.3.1 Model Development

In literature, numerous techniques on modelling thermal systems using the thermal-electrical analogy are used [32, 34–36]. The objective is to establish an analogy between thermal systems that are driven by the flow of heat and electric circuits that are driven by the flow of current. This enables the creation of models for thermal systems using electric circuits to analyse using circuit principles. The models can describe the temperature evolution in the systems, amount of thermal energy storage, and the flow of heat.

Thermal systems have the ability to store and release heat by utilising the thermal mass of a material, as demonstrated in *Figure 3.4(a)*. When heat is applied to the material from a heat source, its temperature increases. Conversely, as heat flows out, the temperature of the material decreases [50, 51]. This phenomenon is necessary for understanding the amount of energy stored in a homogeneous material. Similar to the electrostatic equation of a capacitor when current is applied, demonstrated in *Figure 3.4(b)*, the heat flow into a material can be determined using *Equation (3.2)*.

$$P(t) = C_1 \frac{d}{dt} \left(T_1(t) - T_2(t) \right) \tag{3.2}$$

Where:

- $P(t)$ is the heat flow into the material [W]
- C_1 is the thermal capacity of the material [J/°C]
- $T_1(t),\ T_2(t)$ is the real-time temperature of the material and the surroundings [°C]

The thermal capacity is determined as the product of the mass of the material and its specific heat capacity. Therefore, increasing either the mass or specific heat will result in a higher thermal capacity and consequently, the ability to store more heat. As discussed in *Section 2.2*, water is identified as a suitable thermal storage material for the cooking system due to its high specific heat capacity, relatively high density, wide availability, and its common use in cooking.

A temperature difference across a medium promotes the flow of heat. This is illustrated in *Figure 3.5(a)*, where the medium is positioned between two heat sources and $T_1(t) > T_2(t)$. This principle is described by the one-dimensional Fourier's law of heat conduction, which shares a similar mathematical form to Ohm's law in electric circuits [50, 51]. Therefore, an analogous thermal circuit model can be derived as shown in *Figure 3.5(b)*. The equation describing the flow of heat is shown in *Equation (3.3)*.

$$q(t) = \frac{T_1(t) - T_2(t)}{R_a} \tag{3.3}$$

Where:

- $q(t)$ is the rate of heat transfer [W]
- R_a is the thermal resistance of the medium [°C/W]
- $T_1(t),\ T_2(t)$ is the real-time temperature of the heat sources [°C]

The thermal resistance R_a describes the difficulty for heat to flow through a medium. It is influenced by the dimensions of the medium and its thermal conductivity. A medium with higher thermal resistance will impede the flow of heat for the same temperature difference compared to one with lower thermal resistance. The chosen urn, as described in *Section 3.2.1*, is equipped with an improved thermal resistance of 4.55 times by wrapping a thermal blanket around it.

3.3.2 Model Parameter Identification

The parameters that describe the behaviour of the internal temperature variations of a thermal system must be determined to complete the models. Non-linear methods are primarily used to determine optimal solutions of the parameters due to the intrinsic nature of the system processes [52]. The Genetic Algorithm (GA) method detailed fully in [53–56] is adopted for parameter identification of models with a set of first-order differential equations. This algorithm is chosen because it can quickly search for parameters near optimal values with minimal error between the model and measured results [53]. To validate the models, it is necessary to show a close agreement between the temperature response of the simulated model and the measured system.

3.4 Case Study using Cooking Scenarios

The utilisation of PV energy for cooking is mainly limited by the mismatch of peak sun hours and cooking schedules. To determine the effectiveness of supplementing a thermal storage in PV-supplied systems, it is necessary to test the hybrid system under typical food consumption schedules and different cooking conditions. This includes preparing multiple meals in a day and starting most processes at off-peak sun hours. Additionally, the impact of weather conditions which alters the amount of solar energy generated to heat-up water is considered. By evaluating the use of the thermal storage tank under such scenarios, an understanding of how it impacts the electrical energy component of cooking energy can be made, and its potential to reduce the reliance on larger batteries.

This section describes the selected cooking scenarios in *Section 3.4.1*, and implication on battery

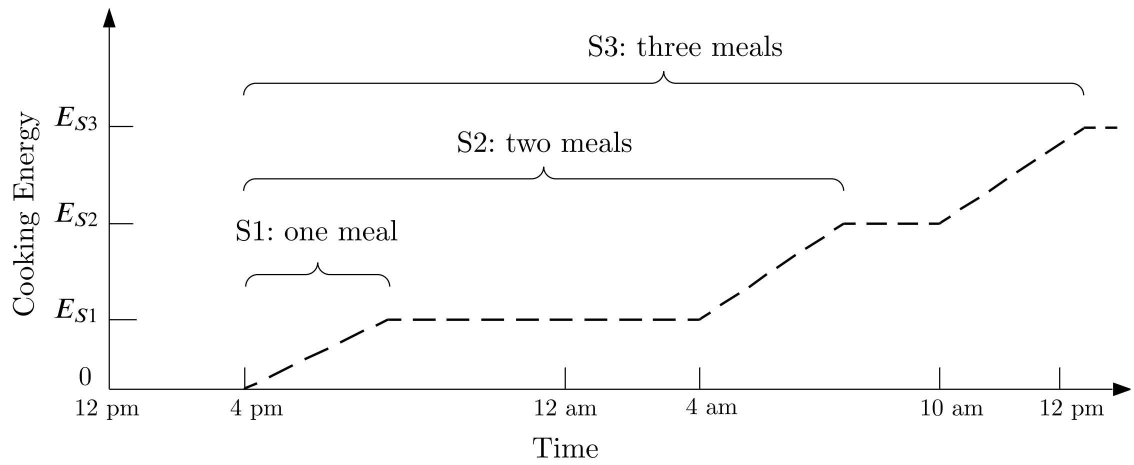

Figure 3.6: Cooking times of meals for three cooking scenarios.

sizing in *Section 3.4.2*.

3.4.1 Cooking Scenarios

Three different scenarios have been selected, each involving the cooking of one to three meals at different times of the day. The starting times for slow cooking have been chosen to reflect typical meal consumption times. It is assumed that the same rice meal, for three to four servings, is prepared three times per day. While this may not reflect usual household practice, it gives an idea of how the storage can participate in reducing the additional electrical energy for multiple meals cooked in a day. The cooking times for each meal are given in *Figure 3.6*, and the three selected scenarios are:

- Scenario $S1$: one meal a day (supper)
- Scenario $S2$: two meals a day (supper and breakfast)
- Scenario $S3$: three meals a day (supper, breakfast, and lunch)

In scenario $S1$, one meal is cooked in the afternoon as supper, starting at 04:00 pm for consumption at 07:00 pm. The heated water will be used to reduce the additional electrical energy required to complete the cooking process. The cooking system in this scenario will require the smallest battery capacity to complete the cooking of one meal.

In scenario $S2$, two meals are cooked, with the first meal as supper from $S1$. The second meal is cooked in the morning as breakfast starting at 04:00 am for consumption at 07:00 am. The system is expected to contain double the battery capacity compared to $S1$ because two meals are cooked during off-peak sun hours.

In scenario $S3$, three meals are cooked. The first two meals follow the same pattern as $S2$, and a third meal is cooked as lunch starting at 10:00 am for consumption at 01:00 pm. The scenario considers two options for battery sizing. In option 1, the battery is sized to accommodate all three meals. In option 2, the battery assists in cooking the first two meals during off-peak sun hours, while the third meal uses PV power since it is being cooked on-peak sun hours.

The scenarios have been chosen to cover a wide range of system sizes and to evaluate the performance of the hybrid topology under different conditions. The validated models developed in *Chapter 4* in conjunction with the equation of the water temperature to the additional electrical energy reduction determined in *Chapter 5* are applied to simulate the behavior of the hybrid system in *Chapter 6*. The results of a pure electrical system will be simulated and compared to the results of the hybrid system.

The three scenarios require different solar PV sizes because of the difference in the energy requirement in each scenario. The simulations consider the availability of solar energy required to heat-up water during high, medium, and low solar irradiation days (H_{high}, H_{medium} and H_{low}). In this context, a high solar irradiation day, H_{high}, is defined as a day that produces enough energy to heat the water to the temperature set-point of the storage water heater. On the other hand, H_{low} is considered as 50% of the energy in H_{high}, and H_{medium} is 75% of the energy produced on a H_{high} day. A constant ambient temperature of 22.5 °C is applied in the simulations to produce average results, and a sensitivity study is done to assess how a change in temperature affects the obtained results.

3.4.2 Battery Sizing

The important aspect of the research is to evaluate the impact of adding a thermal storage tank to the sizing of the battery storage system. By reducing the electrical energy component of the cooking process, it means less battery storage is necessary. The implication on battery capacity is determined using *Equation (3.4)* [57].

$$C_B = \frac{E_S}{\eta_{DC/AC} \times \eta_B \times V_B \times DOD} \tag{3.4}$$

Where:

- C_B is the required battery capacity [Ah]
- E_S is the total electrical cooking energy in each scenario [Wh]
- V_B is the battery voltage [V] (12.8 V)
- η_B is the battery efficiency (95%)
- $\eta_{DC/AC}$ is the charge controller and inverter efficiency (90%)
- DOD is the depth of discharge (80%)

In order to compare the battery capacity values, the selection of a battery technology is necessary. Lithium-ion and lead-acid batteries are commonly used in PV systems. The lithium-ion battery is preferred due to its superior performance characteristics, including higher efficiency, a greater number of cycles, and higher energy density compared to the lead-acid battery [58, 59]. The drawback is the initial high cost of lithium-ion battery, but it has been revealed that the initial and replacement costs for the lead-acid battery over the lifespan of the off-grid systems is sometimes higher than that of the lithium-ion battery. The selected values of η_B and DOD in *Equation (3.4)* are the typical values for the lithium-ion battery technology.

3.5 Conclusion

This chapter highlighted the approach taken to conduct the study for a PV-supplied hybrid storage system that incorporates both battery and thermal storage for a cooking application. The design choices of the hybrid storage topology are then explained with its subsystems. The chapter followed by explaining the reasoning for selecting the experimental methods, the modelling technique, and the cooking scenarios to evaluate the system performance. The decisions are made based on the three research objectives identified in the research introduction to effectively answer the research question.

Chapter 4

Model Development

This chapter covers the modelling and validation of the thermal storage tank and the cooking appliance subsystems of the hybrid cooking system. The method used to develop the models is described in *Section 4.1*. The model and validation of the thermal storage tank is presented in *Section 4.2*, followed by that of the cooking appliance in *Section 4.3*. The chapter is concluded in *Section 4.4*.

4.1 Model Development Method

The thermal-electrical analogy, as discussed in *Section 3.3*, is used to model the thermal systems. The modelling method involves the following steps:

1. In the system, the temperatures of the mediums to be modelled are selected, and a thermal capacitor is added for each medium at that temperature.

2. The thermal capacitors are connected to the selected temperatures and the other terminals are grounded. A thermal resistor is added between thermally connected capacitors to model the temperature drop between two mediums. When mediums have good thermal conduction, such as those connected through thermal paste, the thermal resistance is negligible.

3. The inputs to the system, such as heat sources and temperature disturbances, are modeled

using power sources.

4. The components are connected through their respective resistors to complete the model, and circuit principles are employed to derive the mathematical equations of the models.

The equation that describes the thermodynamics of the systems are characterised using the general first-order state *Equation (4.1)* and the output *Equation (4.2)*.

$$\dot{x}(t) = Ax(t) + Bu(t) \tag{4.1}$$

$$y(t) = Cx(t) \tag{4.2}$$

Where:

- $x(t)$ are the state variables
- $y(t)$ are the output variables
- $u(t)$ are the input variables
- A , B , C is the system, control, and output matrix

4.2 Thermal Energy Storage Tank

An urn is used as the storage water heater tank to heat, store and supply hot water for the cooking process. In this section, the energy flow mechanism, model and validated results of the urn are discussed.

4.2.1 Energy Flow of Storage Water Heater

The heat and water flow of the urn is illustrated in *Figure 4.1*. Small urns comprise a resistive heating element, a top lid for cold water insertion and a tap for hot water draw. The water inside the varying volume tank is assumed to be homogeneous and its temperature is regulated thermostatically on a set-point by turning on and off the element. Electrical energy is consumed by the element to raise and maintain the water temperature to the desired set point. This inherently compensates for thermal losses through the tank's wall.

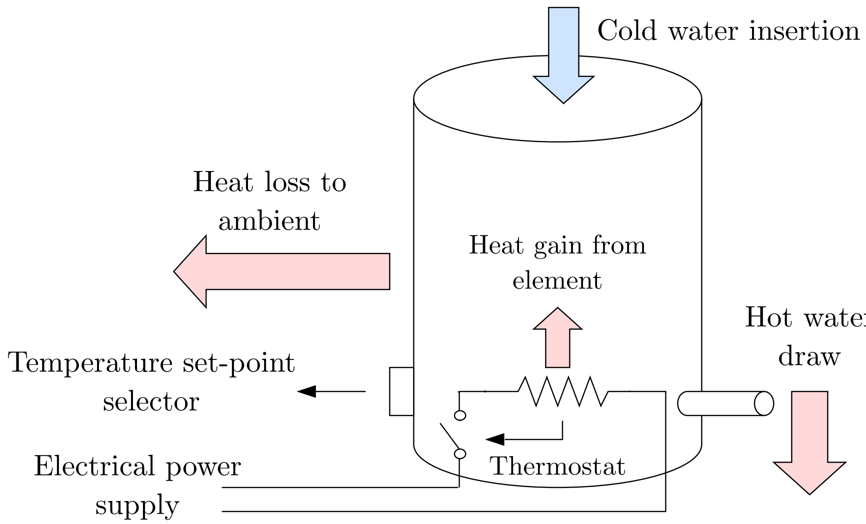

Figure 4.1: Heat and water flow diagram of a storage water heater.

4.2.2 Modelling of Storage Water Heater

The model of the urn is developed using the steps described in *Section 4.1*. The key temperature considered is the internal water temperature. The power produced by the heating element acts as an input to the system, while losses occur due to ambient temperature and system components. The water volume varies, decreases during water withdrawal, and increases during insertion. The analogous thermal circuit diagram that contains all components is illustrated in *Figure 4.2*.

The power of the heating element is represented by a heat source P, with a heat loss factor to the system components η. This is the main source that increases the temperature of water by storing heat energy in the thermal capacity, represented by C_{wh}. The water temperature is regulated by a thermostatic switch around a hysteresis set-point T_{sp} to prevent over- or under-heating. The total thermal capacity of water changes due to a draw or insertion event, modelled using a capacitor C_{in} and it is dependent on the internal temperature T_{in}. The thermal resistance R_a models the heat losses to ambient temperature T_{amb}, which affects the ability to keep water hot in the absence of a heat source. The first-order differential and output equation of the circuit is shown in *Equation (4.3)* and *Equation (4.4)* respectively.

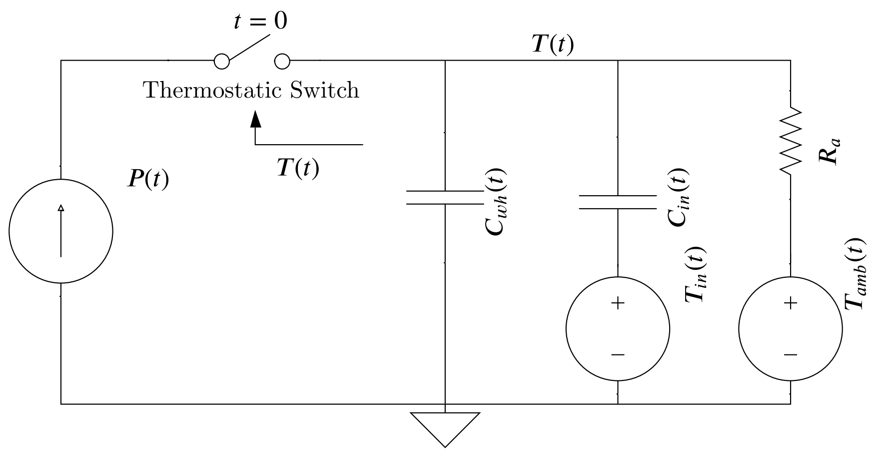

Figure 4.2: Analogous thermal circuit of a storage water heater.

$$\eta P(t) = C_{wh}(t)\frac{d}{dt}(T(t)) + C_{in}(t)\frac{d}{dt}(T(t) - T_{in}(t)) + \frac{1}{R_a}(T(t) - T_{amb}(t)) \tag{4.3}$$

$$y(t) = T(t) \tag{4.4}$$

The ambient temperature and input water temperature are time-dependent variables that vary based on weather conditions. In addition, the amount of water drawn or inserted is also time-dependent and varies during the day. The values for the components are defined using *Equation (4.5)*, *Equation (4.6)*, and *Equation (4.7)*.

$$C_{wh}(t) = \rho c V(t) \tag{4.5}$$

$$C_{in}(t) = \rho c \int Q(t)dt \tag{4.6}$$

$$R_a(t) = \frac{1}{UA(t)} \tag{4.7}$$

Where:

- ρ is the water density [kg/m^3]
- c is the water specific heat [J/kg·°C]
- $V(t)$ is the initial volume of water in the vessel [m^3]

- $Q(t)$ is the real-time water insertion or draw rate [m^3/s]
- $A(t)$ is the water contact surface area [m^2]
- U is the heat transfer coefficient [W/m^2·°C]

When there is no water withdrawal or insertion ($Q(t) = 0$) the value of $C_{in}(t) = 0$, indicating no thermal capacity change. The thermal resistance R_a fluctuates in response to changes in the contact surface area, which occur due to variations in water volume. The cooling trend of the internal water temperature, when there is no input power and water draw on the tank, is described by *Equation (4.8)*.

$$T(t) = T_{amb}(t) + (T(t_0) - T_{amb}(t))e^{-\frac{t-t_0}{R_a C_{wh}}} \tag{4.8}$$

The product of the thermal capacity of water and the thermal resistance of the tank $R_a C_{wh}$ is the time constant of the system, which defines the rate of temperature change. A large thermal resistance or thermal capacity leads to a larger time constant, which results in slower cooling trends.

4.2.3 Results and Model Validation

The models are validated using experiments of a 250 W, 5 ℓ water urn for two scenarios: without a water draw and with a water draw, on the setup explained in *Section 3.2*. The state-space *Equation (4.3)* and output *Equation (4.4)* has been developed in MATLAB Simulink to simulate the system performance and the diagram is provided in *Appendix C.2.1*. The thermal resistance R_a is calibrated using the cooling curves of the urn. The value of η, is tuned as 73.56% by comparing the energy required to raise the temperature of water to the set-point with the measured energy consumed by the urn. The detailed derived equations of R_a and η used are presented in *Appendix C.3.3*. The temperature set-point T_{sp} was adjusted to a value below 90 °C using the tank's selector, resulting in a measured average value of 86.34 °C and an average hysteresis of 2.201 °C during a steady-state test.

In both experiments, the heating power was supplied for the first three hours to emulate the

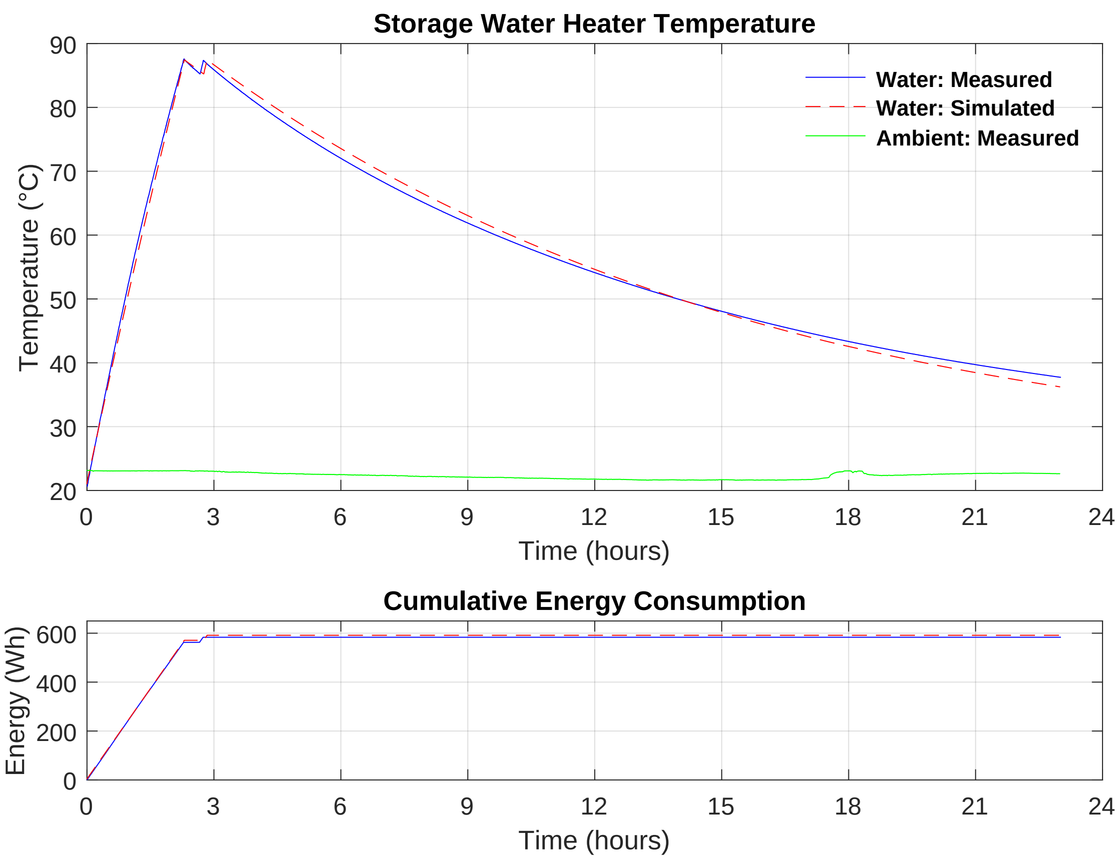

Figure 4.3: Measured and simulated results of a storage water heater without a water draw.

duration of available PV power, after which the tank was allowed to cool down over the course of a full day. In the experiment with a water draw, 600 mℓ of water (which is the volume selected to cook a rice meal) was drawn after four hours, which was simulated with a flow rate of 36 ℓ/hr. The flow rate was estimated from measuring the time it takes to draw a litre of water from the tank's tap.

The thermal resistance is tuned to be 2.259 °C/W from a cooling curve with 5 ℓ of water, and 2.355 °C/W with 4.4 ℓ. This is because reducing the water volume results in an increase in thermal resistance due to the reduction in water contact surface area. For the storage tank used, a 12% decrease in water volume or thermal capacity led to a 4.26% increase in thermal resistance. The change in thermal capacity and thermal resistance is included in the simulation with a water draw. The simulation parameters are summarised in *Table 4.1*. A visual comparison of the results without a water draw is presented in *Figure 4.3*, and with a

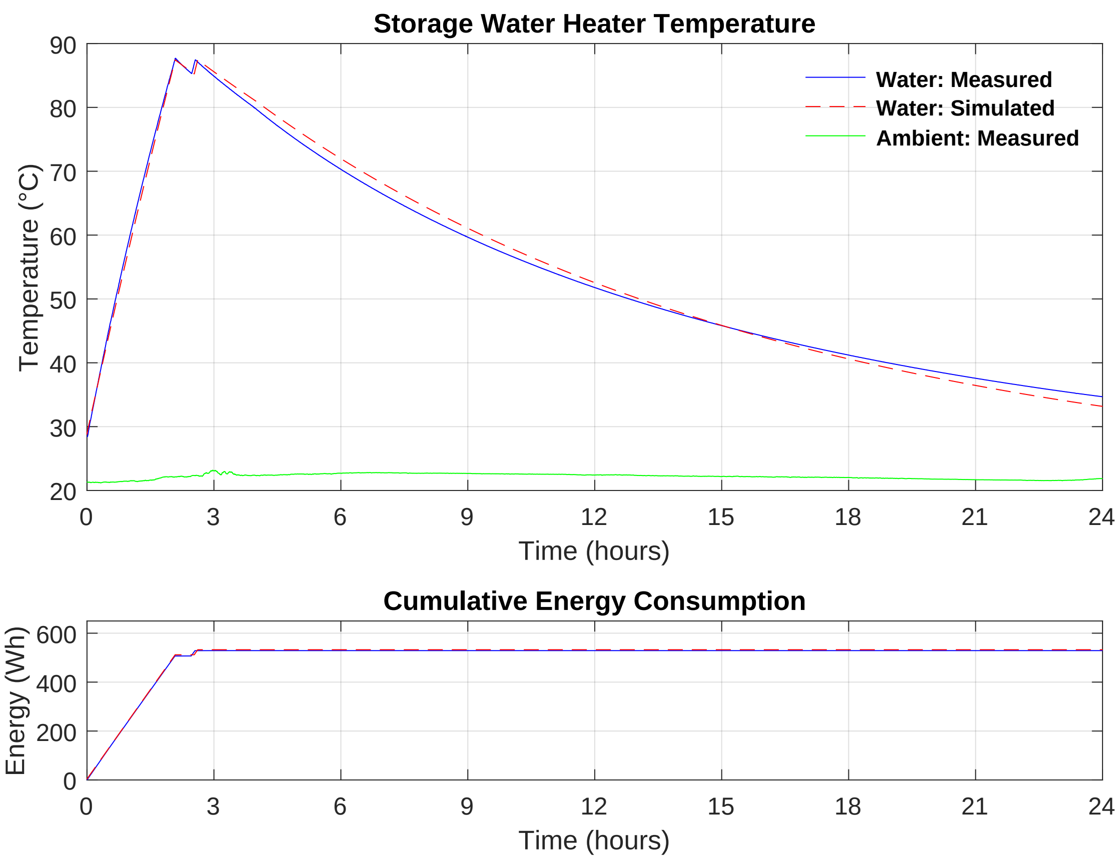

Figure 4.4: Measured and simulated results of a storage water heater with a water draw.

Table 4.1: Parameters of a storage water heater model.

Parameter	c	ρ	$V(t)$	$Q(t)$	R_a	P	η	T_{sp}
Experiment (no draw)	4181	998	5	0	2.259	246.3	73.56	86.34
Experiment (with a draw)	4181	998	5	36	2.355	246.3	73.56	86.34
Unit	J/kg·°C	kg/m^3	ℓ	ℓ/hr	°C/W	W	%	°C

Table 4.2: Storage water heater comparison: experiment vs simulation results from *Figure 4.3* and *Figure 4.4*.

Parameter	**Experiment**	**Simulation**	**Difference**
Heating energy [Wh]	562.64	571.01	1.49%
Steady-state energy [Wh]	20.80	20.51	1.39%
Temp. drop no draw (3 to 23 hours) [°C]	48.15	50.43	4.74%
Temp. drop with a draw (3 to 23 hours) [°C]	49.30	52.64	5.63%

water draw is presented in *Figure 4.4*.

The urn operation is classified into three stages: heating, steady-state, and cooling for comparison. By visual inspection, the simulated temperature profiles match the measured profiles

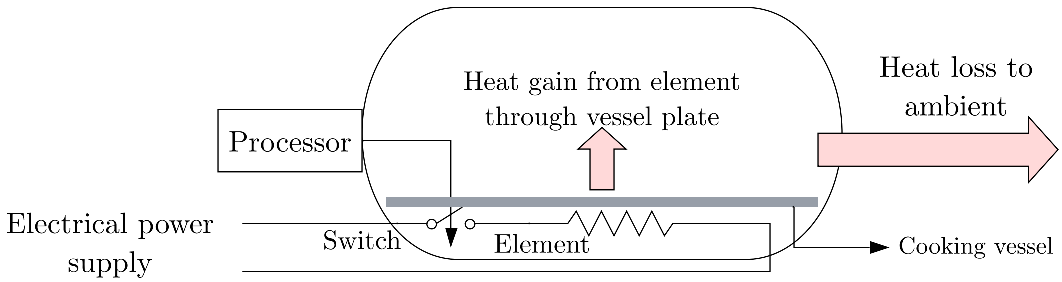

Figure 4.5: Heat flow diagram of a slow cooker.

on all stages. However, a slight discrepancy in the steady-state switching times exists due to the measured results not switching between the same temperature points as assumed in the simulation. This could also be due to the difference in temperature sensor placement, with the RTDs in the experiment setup directly measuring the water, whereas on the urn the sensor is placed beneath the bottom of the tank. The measurement tolerance of the RTDs, which is 0.5 °C, may also contribute to the observed difference. The energy consumed on each stage and the cooling temperatures are summarised in *Table 4.2*.

In *Table 4.2*, the initial heating energy of the simulation is overestimated by 1.49% compared to the experiment. However, the steady-state replacement energy is underestimated by only 1.39%. The cooling temperature drop from 3 to 23 hours is overestimated by 4.74% in the simulation without a water draw, and by 5.63% in the simulation with a water draw. A decrease in cooling temperature due to a decrease in water volume is matched closely by the simulation, with a difference of only 1.99%. These findings indicate that the simulation results match the measured results, demonstrating that the model can effectively simulate the energy and temperatures of the storage water heater.

4.3 Cooking Appliance

A slow cooker is used as the cooking appliance to heat food in its vessel. In this section, the energy flow, model and validated results of a slow cooker are discussed.

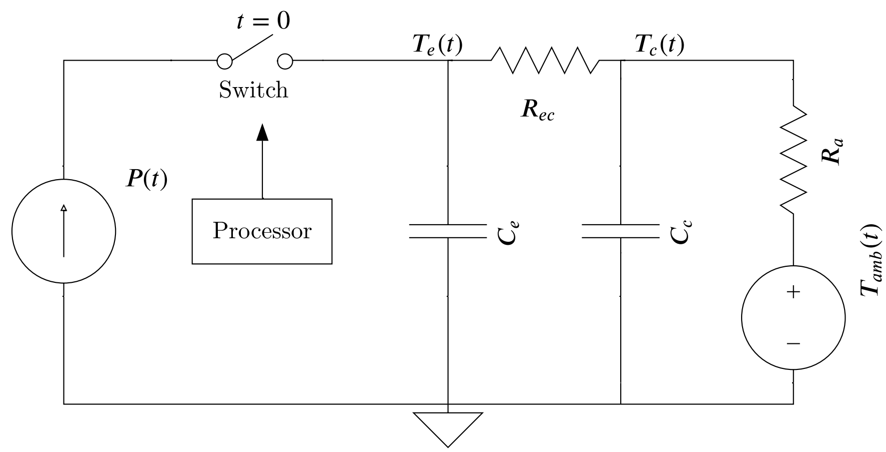

Figure 4.6: Analogous thermal circuit of a slow cooker.

4.3.1 Energy Flow of Cooking Appliance

The heat flow mechanism of a slow cooker is presented in *Figure 4.5*. Slow cookers consist of a cooking vessel which is heated by a resistive element, and a processor to regulate the average power drawn based on the chosen heat setting option. The slow cooker in this study offers three heat settings: low, high, and warm. Heat losses to the environment are experienced by the body of the cooker. This study focuses on cooking with constant power which is achieved by selecting the high heat setting option. Therefore, the modelling section considers only this process.

4.3.2 Modelling of Cooking Appliance

The temperature of the cooking vessel and food mixture are considered for modelling the slow cooker. The power drawn by the heating element is an input to the system and the energy losses occur due to the environment. The analogous thermal circuit diagram that contains all components is illustrated in *Figure 4.6*.

On the circuit diagram, the power input to the system P represents the heat source produced by the heating element. This power directly causes an increase in the temperature of the cooking vessel C_e, which then heats up the food mixture C_c, through the contact thermal resistor R_{ec}. The switch represents a relay which is energised by the processor to regulate the average power input. The entire system loses thermal energy to the ambient temperature through the resistor

R_a. By analysing the circuit, the state and output equations for the system are derived in *Equation (4.9)* and *Equation (4.10)* respectively.

$$\begin{bmatrix} \frac{dT_c(t)}{dt} \\ \frac{dT_e(t)}{dt} \end{bmatrix} = \begin{bmatrix} -\left(\frac{1}{R_{ec}C_e} + \frac{1}{R_a C_c}\right) & \frac{1}{R_{ec}C_e} \\ \frac{1}{R_{ec}C_e} & -\frac{1}{R_{ec}C_e} \end{bmatrix} \begin{bmatrix} T_c(t) \\ T_e(t) \end{bmatrix} + \begin{bmatrix} 0 & \frac{1}{R_a C_c} \\ \frac{1}{C_e} & 0 \end{bmatrix} \begin{bmatrix} P(t) \\ T_{amb}(t) \end{bmatrix} \tag{4.9}$$

$$y(t) = T_c(t) \tag{4.10}$$

Where:

- $P(t)$ is the element power [W]
- $C_e,\ C_c$ represent the thermal capacity of the cooking vessel and food mixture [J/°C]
- $T_e(t),\ T_c(t),\ T_{amb}(t)$ is the real-time cooker element temperature, food mixture temperature, and ambient temperature [°C]
- $R_{ec},\ R_a$ represent the thermal resistance between the cooking vessel and food mixture, and the thermal resistance between the cooker and surroundings [W/°C]

4.3.3 Parameter Identification

The slow cooker model consists of two first-order differential equations. The thermal capacitors (C_e and C_c) can be estimated using the specific heat capacity and mass of the cooking vessel and the food mixture. However, the thermal resistors (R_{ec} and R_a) are unknown and cannot be easily tuned from measured data. The GA introduced in *Section 3.3.2* is used to estimate the parameter values of complex models. The algorithm initially considers the estimated values of the parameters and their allowable range. It then uses the measured input power, internal and ambient temperatures to estimate the parameters. The GA implementation is depicted by the flowchart in *Figure 4.7*, and a detailed explanation of the implemented code is provided in *Appendix C.3.2*

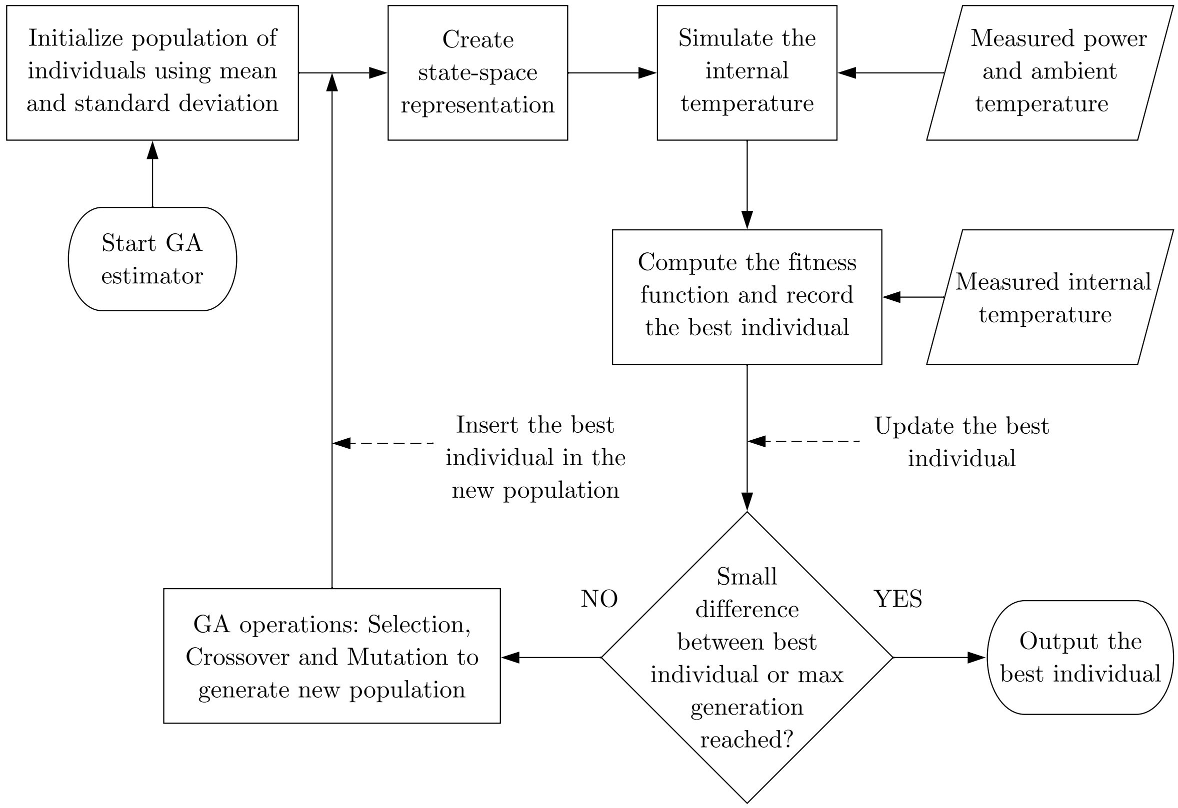

Figure 4.7: Flow chart of the GA estimator for parameter identification of a model.

Table 4.3: Parameters of a slow cooker model estimated using the GA.

Parameter	R_{ec}	C_e	R_a	C_c
Generated value	0.589	2881.7	0.420	3292.3
Unit	°C/W	J/°C	°C/W	J/°C

4.3.4 Model Validation

The slow cooker with specification of 200 W, 4 ℓ as discussed in *Section 3.2* is used for validation. The experiment used for validation is of cooking rice for 2.5 hours with water initially at ambient temperature. The model using the state and output description in *Equation (4.9)* and *Equation (4.10)* has been developed in MATLAB Simulink and the diagram is presented in *Appendix C.3.1*. The steps taken to determine the model parameters using the GA is given in *Appendix C.3.3* and the resulting values are summarised in *Table 4.3*. To test the validity of the model, the same power and ambient temperature profile recorded from the cooker's experiment were applied in the simulation. The energy and temperature profiles of the measured and the simulated results are presented in *Figure 4.8*.

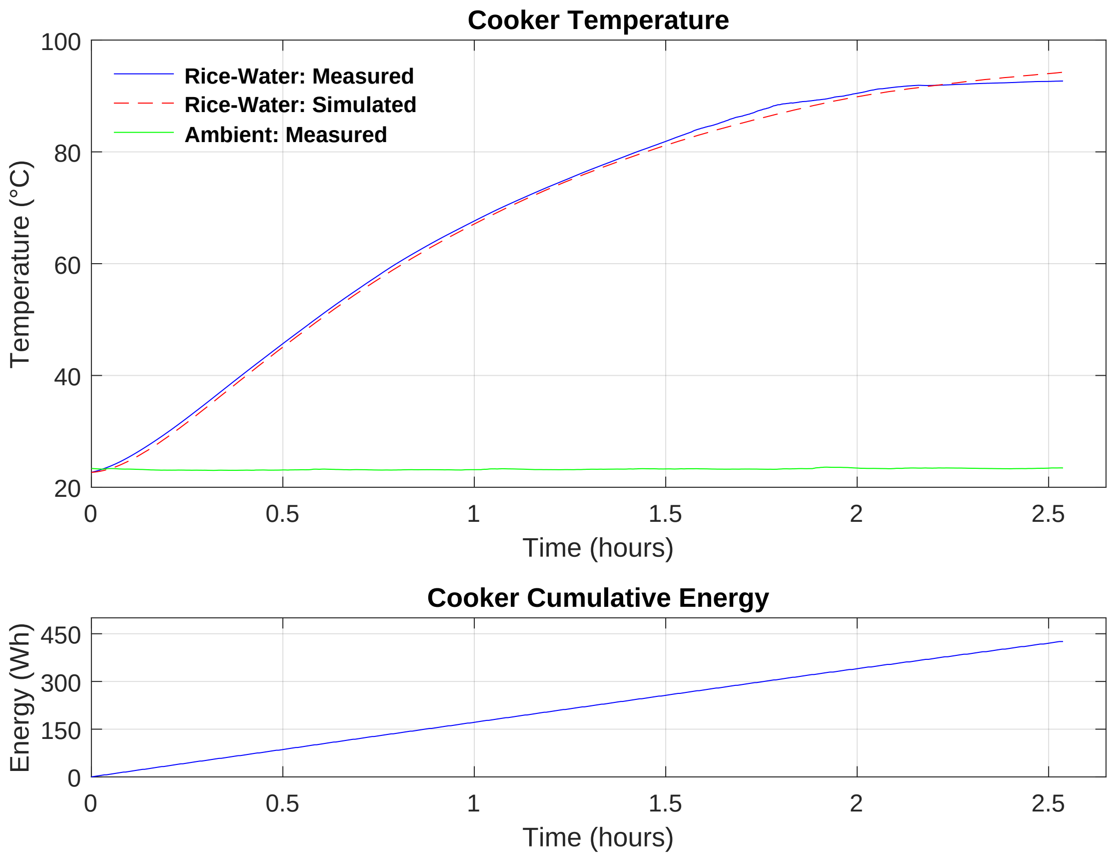

Figure 4.8: Experimental and simulated results of a slow cooker.

Table 4.4: Slow cooker comparison results: experiment vs simulation from *Figure 4.8*.

Cooking energy	**Experiment**	**Simulation**	**Difference**
Heating stage (22.7 - 50 °C) [Wh]	101.01	102.58	1.55%
Heating stage (22.7 - 75 °C) [Wh]	211.87	214.40	1.19 %
Heating stage (22.7 - 92.5 °C) [Wh]	409.90	385.09	6.05%

The temperatures observed in the experiment and simulation results exhibit a level of similarity with a mean absolute error of 0.72 °C. The energy consumed to reach the three temperature levels is presented in *Table 4.4*. The simulated energy at the end of the cooking period is underestimated by only 6%. This level of agreement provides evidence for the effectiveness of both the developed model and the parameter identification method, which suggests that they can be applied to simulate the performance of the slow cooker.

4.4 Conclusion

The models presented for the thermal storage tank and cooking appliance using the thermal-electrical analogy, provide a valuable tool for simulating their performance. These models have been calibrated and validated using experimental results and have been shown to accurately capture the energy flow and internal temperature behaviour of the subsystems. The ability to simulate the behaviour of these systems means the energy requirements of the hybrid cooking system can be explored under various cooking scenarios.

Chapter 5

Pre-Heated Water Influence

This chapter evaluates the impact of using pre-heated water at the start of the cooking process. The evaluation is explored using experiments of cooking rice starting at different temperature levels, where the cooking energy results of water temperatures above ambient are compared. The chapter is organised into three sections: the impact of cooking rice using pre-heated water is discussed in *Section 5.1*, the resulting reduction in additional electrical energy is detailed in *Section 5.2*, and the conclusion is provided in *Section 5.3*.

5.1 Effects of Cooking using Pre-Heated Water

The experimental setup and the parameters for exploring the influence of cooking with pre-heated water are discussed in *Section 3.2.3*. Rice was cooked for three hours (approximately 500 Wh of additional electrical energy) with water starting at 25.0 °C "the experiment baseline", and for the same period with pre-heated water at 50.0, 75.0 and 97.6 °C. The results from the experiments are demonstrated in *Figure 5.1*. The profiles show the absorbed MC of the rice, inside temperature dynamics, and the initial thermal energy added with the cumulative electrical energy consumption of the cooking process.

The profiles in *Figure 5.1* show that the rate of moisture absorption is quicker initially with pre-heated water, and that the rice-water mixture reaches steady-state temperatures quicker.

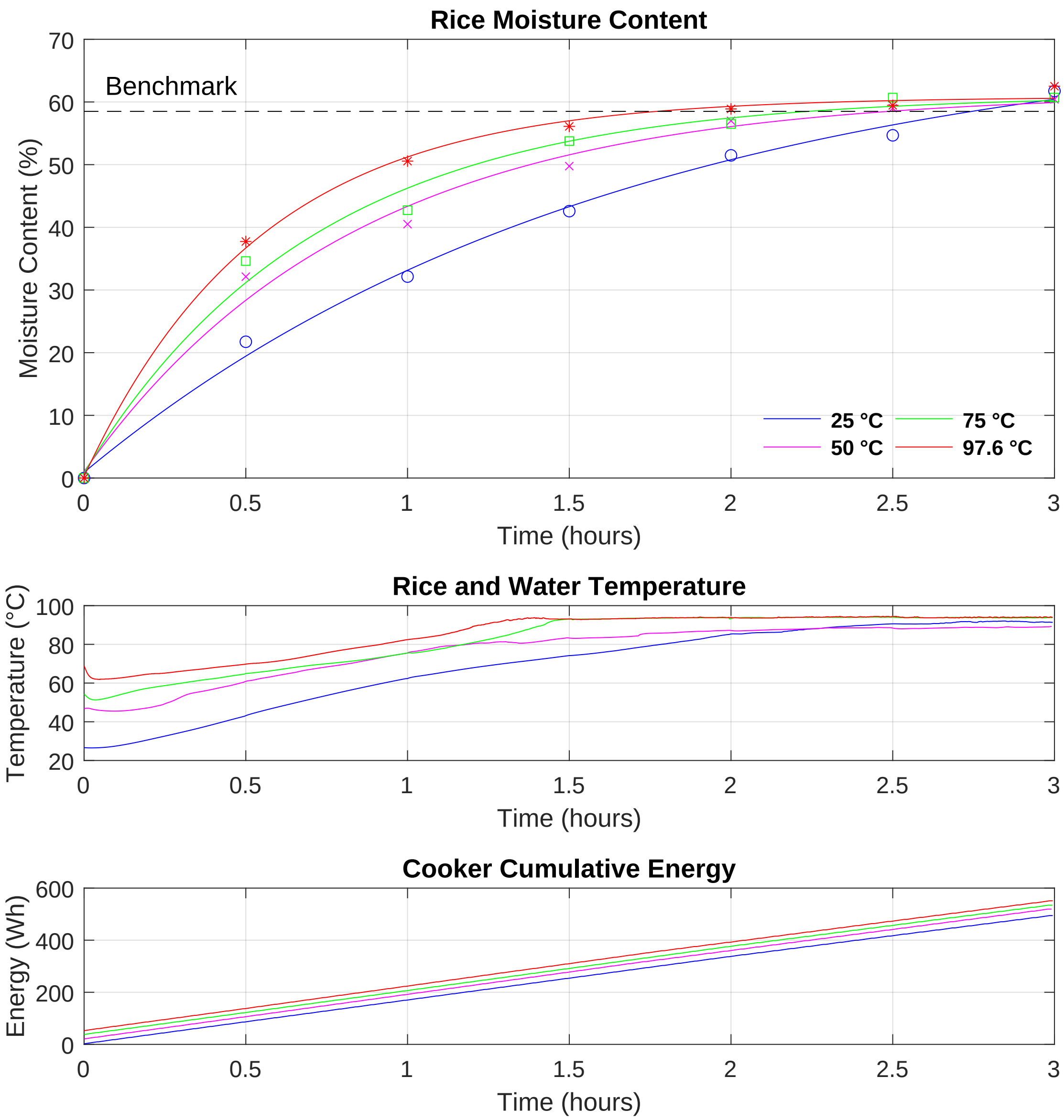

Figure 5.1: Resulting profiles of rice MC, rice-water temperature, and the added electrical energy combined with the initial thermal energy of water.

Between 1.0 and 2.0 hours, the moisture absorption rate slows down rapidly for the cooking processes that started with pre-heated water. From 2.0 to 2.5 hours, the MC increased by less than 2% indicating that the rice has absorbed almost all the available water in the cooking vessel. The scatter plots of the measured MC exhibit a strong exponential growth which are improved by fitting exponential trend lines as shown in *Figure 5.1*.

Table 5.1 shows the evaluated state of rice results from the subjective taste method starting after the first hour. The rice cooked the fastest with water initially at 97.6 °C in 2.0 hours,

Table 5.1: Evaluation of the state of rice using a subjective taste test.

Parameter	**25 °C**	**50 °C**	**75 °C**	**100 °C**
1.0 hours	Under-cooked	Under-cooked	Under-cooked	Under-cooked
1.5 hours	Under-cooked	Under-cooked	Under-cooked	Under-cooked
2.0 hours	Under-cooked	Under-cooked	Under-cooked	Well-cooked
2.5 hours	Under-cooked	Well-cooked	Well-cooked	Well-cooked
3.0 hours	Well-cooked	Well-cooked	Well-cooked	Well-cooked

Table 5.2: Results of cooking rice in a slow cooker with pre-heated water of different temperatures.

Parameter	**25 °C**	**50 °C**	**75 °C**	**100 °C**
Initial water temperature [°C]	26.00	52.00	77.00	97.60
Ambient temperature [°C]	22.86	22.14	22.56	22.07
Thermal energy of water added [Wh]	2.20	20.81	37.94	52.64
Electrical cooking energy [Wh]	453.36	417.86	376.37	304.03
Additional electrical energy reduction	0%	7.83%	16.98%	32.94%

followed by 75.0 °C and 50.0 °C, both in 2.5 hours. The experiment baseline, starting with water at 25 °C finished last in 3.0 hours. For the MC results, well-cooked rice is benchmarked between 58.5% and 60.5% MC. The minimum MC is determined from the taste tests and the maximum MC is the rice that has absorbed all water. The minimum MC line is drawn on the MC profiles to indicate the time and energy required for the rice to reach the well-cooked state.

5.2 Electrical Cooking Energy Reduction

From *Figure 5.1*, where the respective curves intersect the minimum MC line, the corresponding electrical cooking energy added after using water at 25.0, 50.0, 75.0 and 97.6 °C is 453 Wh (2.75 hours), 418 Wh (2.49 hours), 376 Wh (2.24 hours), and 304 Wh (1.77 hours), respectively. This means pre-heated water temperatures can potentially reduce the electrical component of cooking energy by a range of 7.83 to 32.9%, as presented in *Table 5.2*.

The experimental results have demonstrated the effectiveness of using pre-heated water initially to cook rice. In order to establish a mathematical relationship between the initial water temperature and the reduction in additional electrical energy, the results are plotted in *Figure 5.2*. Three different trend lines: linear, quadratic and exponential are fitted on the data points using *Equation (5.1)*, *Equation (5.2)*, and *Equation (5.3)*, respectively. The values of the coefficients

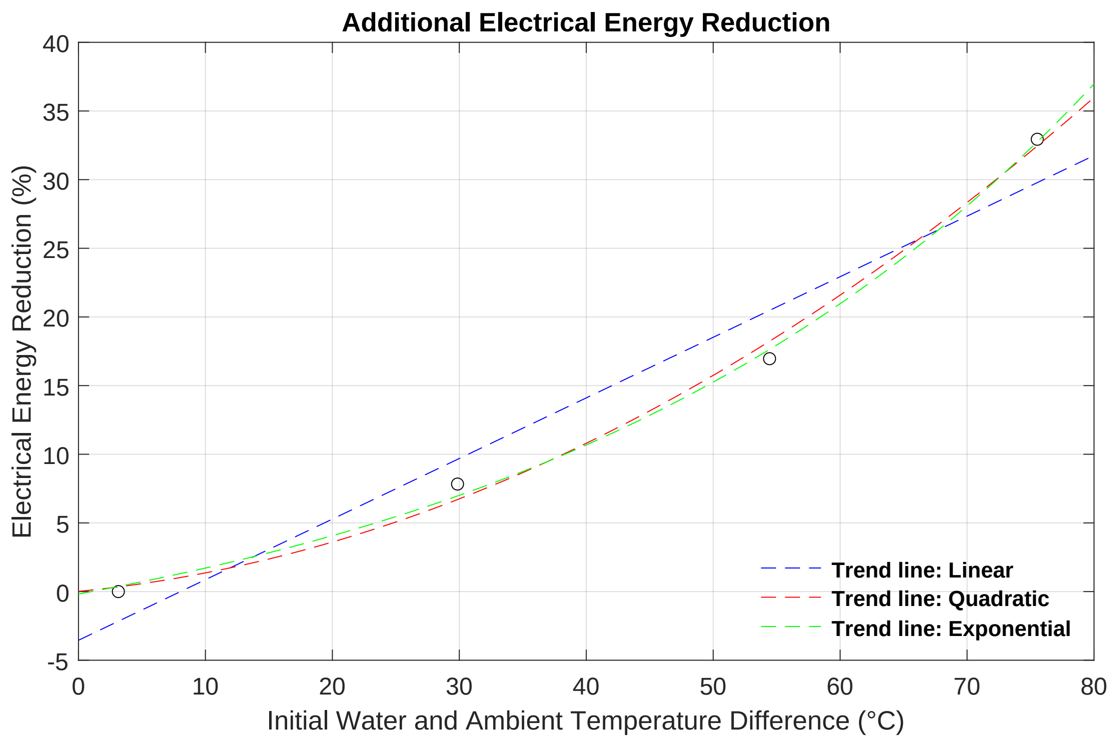

Figure 5.2: Fitted linear, quadratic and exponential trend lines for the additional electrical cooking energy reduction using pre-heated water.

of the three trend lines are summarised in *Table 5.3*.

$$R_E(\Delta T) = a\Delta T + b \tag{5.1}$$

$$R_E(\Delta T) = a\Delta T^2 + b\Delta T + c \tag{5.2}$$

$$R_E(\Delta T) = ae^{\frac{\Delta T}{b}} + c \tag{5.3}$$

Where:

- R_E is the additional electrical energy reduction of the cooker [%]
- ΔT is the temperature difference of pre-heated water and ambient [°C]
- a, b, c is the coefficient of the trend lines

By visual inspection, both the quadratic and exponential lines closely follow the trend of the data points. The coefficient of determination (R^2 where $R^2 \in [0\ 1]$) defined using *Equation (5.4)*,

Table 5.3: Coefficient of a linear, quadratic, exponential trend lines from *Figure 5.2.*

Parameter	**Linear**	**Quadratic**	**Exponential**
a	0.441	0.00450	7.632
b	-3.546	0.0896	45.214
c		0.0147	-7.807
R^2	0.950	0.995	0.998

is used to select the better fit line. The trend line with the highest value of R^2 means it is better at predicting the data points.

$$R^2 = 1 - \frac{\sum_{i=1}^{n}(R_{Ei} - \widehat{R_{Ei}})^2}{\sum_{i=0}^{n}(R_{Ei} - \overline{R_E})^2} \tag{5.4}$$

- Where R^2 is the coefficient of determination
- R_{Ei} is the energy reduction data points [%]
- $\overline{R_E}$ is the mean value of the energy reduction data points [%]
- $\widehat{R_{Ei}}$ is the energy reduction points from the trend line [%]

The R^2 values for each trend line are: 0.950 for linear, 0.995 for quadratic, and 0.998 for exponential, as presented in *Table 5.3.* The exponential trend line provides the better fit with the highest R^2 value that is closer to 1. Therefore, *Equation (5.3)* is selected to estimate the additional electrical energy that can be reduced when the temperature of the water and ambient are known. This means the required capacity of the battery that supplies the stored electrical energy can be reduced by the same factor based on *Equation (3.4).* Considering that it is an exponential growth, the electrical energy reduction from pre-heated water nearing boiling point will be significantly greater compared to water at temperatures closer to ambient.

5.3 Conclusion

A cooking experimental setup was used to study the impact of cooking rice with pre-heated water. It was showed from the experiments that rice absorbs water quicker, and the time to reach the desired state decreases drastically when hot water temperatures are initially used. This idea significantly decreases the additional electrical energy required to cook and the time to cook with a low-powered cooking appliance.

The experiments showed that pre-heated water at any temperature above ambient can reduce the electrical component of cooking energy by up to 33%, in the case of boiling water. This implied that the battery size required can be reduced by a similar range, which will carry through to a reduction in the financial cost of the storage unit in PV systems.

An exponential equation is derived from the trend of the initial water and ambient temperature difference against the additional electrical energy reduction of cooking rice. The following chapter implements the idea in PV systems by using simulations of a storage water heater and the slow cooker to determine its impact in everyday usage.

Chapter 6

Hybrid Cooking System Performance

This chapter covers the overall impact of supplementing a battery with a thermal storage tank by considering typical cooking scenarios. The scenarios selected enable analysis of the systems designed for cooking one to three meals throughout the day. This was done to evaluate the extent that the thermal storage tank could reduce the battery capacity requirements of PV-supplied cooking systems. The developed models of the subsystems in *Chapter 4*, and the derived equation of the reduction in electrical component of cooking energy using the difference between the water and ambient temperatures in *Chapter 5* are utilised. The energy performance of the electrical cooking systems is presented in *Section 6.1*, followed by a comparison with the hybrid cooking systems in *Section 6.2*. A detailed discussion on how the hybrid storage topology reduces the battery requirements is presented in *Section 6.3*, and the chapter is concluded in *Section 6.4*.

6.1 Electrical Cooking System

This section presents an analysis of the performance of the electrical cooking system, exploring the energy and battery capacity requirements for three cooking scenarios.

The three scenarios for cooking rice, as previously detailed in *Section 3.4.1*, are defined based on the number of meals being cooked. Scenario $S1$ involves cooking one meal, scenario $S2$ involves

Table 6.1: Electrical cooking energy and battery requirements in an electrical cooking system for preparing one to three meals.

Parameter	$\boldsymbol{S1}$	$\boldsymbol{S2}$	$\boldsymbol{S3}$
Electrical cooking energy [Wh]	454.15	908.31	1 362.46
Battery capacity [Ah]	51.87	103.74	155.62

cooking two meals, and scenario $S3$ involves cooking three meals. Since it is a pure electrical system with battery only, the cooking is started with water initially at ambient temperature of 22.5 °C for all meals. The rice is prepared in high heating mode and the cooker consumes 454.15 Wh of additional electrical energy in 2.75 hours based on *Equation (5.3)*.

The total additional electrical energy steps up by 454.15 Wh for each meal. In $S1$, the cooker consumes 454.15 Wh from 04:00 pm to 06:45 pm. In $S2$, the cooker operates for a second session from 04:00 am to 06:45 am and uses a total of 908.31 Wh. Finally in $S3$, the cooker operates for a third session from 10:00 am to 12:45 pm and uses a total electrical energy of 1 362.46 Wh. The battery capacity required to fulfil each cooking scenario is determined using *Equation (3.4)* and the results are summarised in *Table 6.1*. The battery capacity required is 51.87 Ah for one meal, 103.74 Ah for two meals, and 155.62 Ah for three meals. These results represent the foundation for exploring the energy and battery requirements in the hybrid cooking system, serving as a baseline for comparison in the following section.

6.2 Electrical-Thermal Cooking System

This section presents the results of the hybrid storage cooking system with battery and thermal storage for three cooking scenarios. A comparison at three different daily solar irradiation levels (H_{high}, H_{medium}, and H_{low}) is made with the results obtained from the electrical cooking system. The amount of PV energy used for water heating, the capability of the storage tank to store hot water, and its effect on the electrical cooking energy and the battery capacity requirements are discussed in the following subsections.

6.2.1 Scenario S1: One Meal a Day

The results in *Figure 6.1* show the profiles of the PV energy at different solar irradiation levels used by the storage water heater, the corresponding water temperature, the water volume in the tank, and the cumulative electrical energy of the cooker for preparing one meal in 24 hours. The results of both the hybrid and electrical cooking systems are shown.

In the case of a hybrid cooking system, the PV power is diverted to heat water once the battery is charged. As explained in *Section 3.4.1*, H_{high} is simulated as a condition that produces enough PV energy to heat-up water to the temperature set-point (similar to a fully charged storage system). H_{medium} is considered as 75% of the energy used in H_{high}, and H_{low} is 50% of the energy used in H_{high}. The results in *Figure 6.1* show that the diversion process is started from 01:44 pm for H_{high}, 02:18 pm for H_{medium}, and 02:52 pm for H_{low} until 04:00 pm. This results into PV energy consumption of 557.00 Wh, 417.80 Wh, and 278.54 Wh respectively by the thermal storage tank. At 04:00 pm, the water temperature is 87.43 °C (H_{high}), 72.23 °C (H_{medium}), and 56.37 °C (H_{low}), after which it begins to cool down. Due to the thermal resistance of the tank, the water does not cool down fast.

To cook the one meal in scenario $S1$, 600 mℓ of water is drawn at 04:00 pm, which drops the water volume from 5 to 4.4 ℓ in the tank. The implication of this volume change is discussed in detail with respect to scenarios where multiple meals are cooked in *Section 6.2.2* and *Section 6.2.3*.

The comparative results of the electrical and hybrid cooking systems for scenario $S1$ are presented in *Table 6.2*. The impact of using pre-heated water from the storage water heater is evident from the cumulative electrical energy profiles of the cooker in *Figure 6.1*, which show shorter cooking duration and lower electrical energy usage. In the electrical cooking system, where water starting from ambient temperature is used at 04:00 pm, 454.15 Wh of electrical energy is consumed to cook. However, in the hybrid cooking system, the difference between the water and ambient temperature before cooking the first meal ranges from 33.87 to 64.93 °C, depending on the level of solar irradiation. This results in an estimated 8.334 to 24.28% reduction in the additional electrical cooking energy, meaning 415.58 to 343.30 Wh is used.

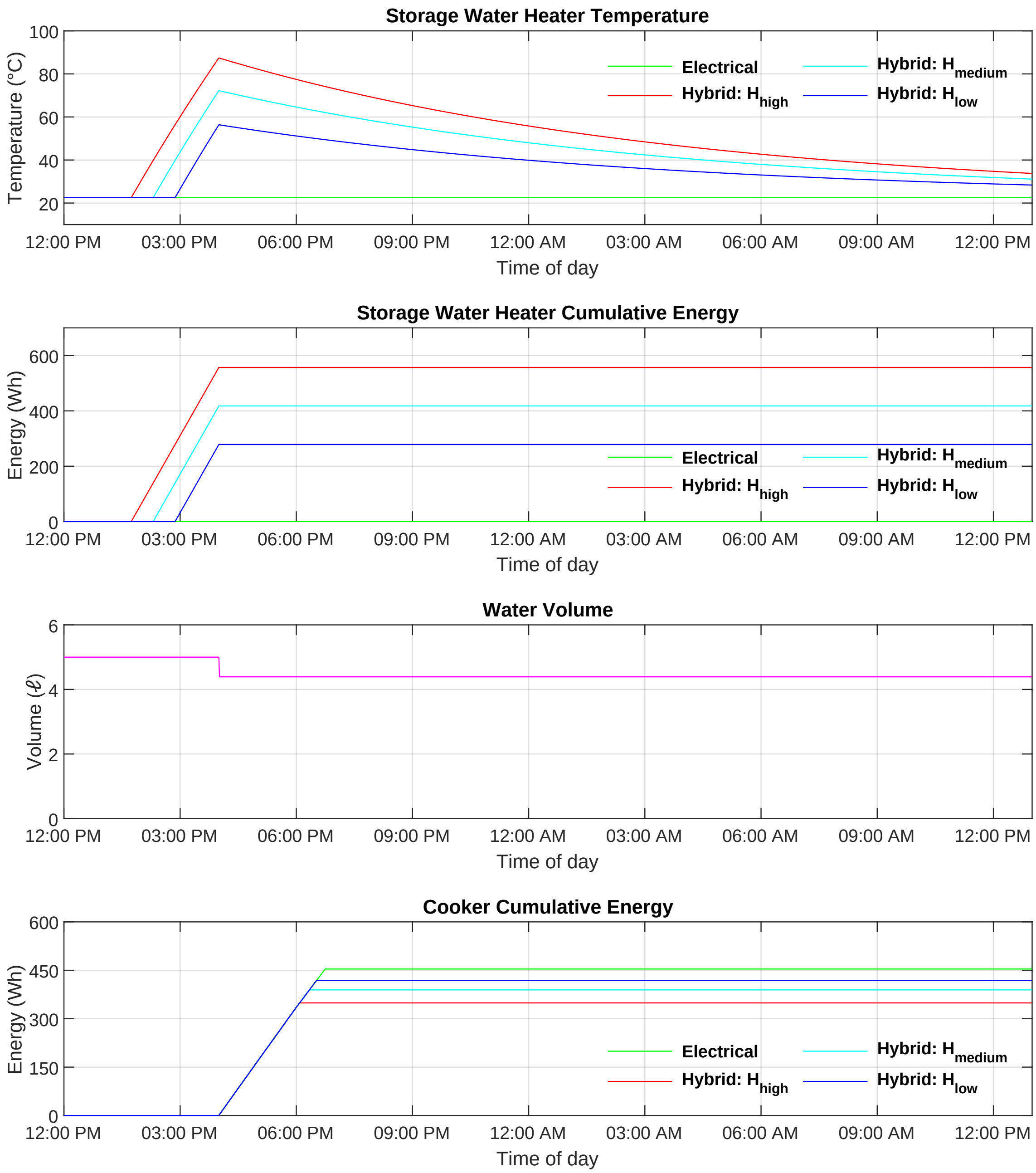

Figure 6.1: Results of cooking one meal with an electrical and hybrid system.

The implications on the battery capacity is determined using *Equation (3.4)*. From the pure electrical cooking system results, the system requires an estimated battery capacity of 51.87 Ah. However, with the addition of a storage water heater, approximately 4.40 to 12.66 Ah of battery capacity could be reduced (or utilised for other household tasks). The required battery capacity is estimated to be in the range of 39.21 to 47.47 Ah.

Table 6.2: Performance of cooking one meal using electrical and hybrid system.

Parameter	Electrical	Hybrid		
Daily PV energy level	**-**	**High**	**Medium**	**Low**
Water and ambient temp diff. (1st meal) [°C]	0	64.93	49.74	33.87
Electrical energy reduction [%]	0.0%	24.28%	15.12%	8.334%
Additional electrical cooking energy [Wh]	454.15	343.30	384.81	415.58
Battery capacity [Ah]	51.87	39.21	43.95	47.47

6.2.2 Scenario S2: Two Meals a Day

The profiles in *Figure 6.2* show the results of the hybrid and electrical cooking system when two meals are prepared. The water draw to cook the first meal at 04:00 pm decreased the water volume to 4.4 ℓ. As mentioned in *Section 4.2.3*, this decreases the water thermal capacity of water by 12.0% and increases the tank's thermal resistance by 4.26%. Consequently, the time constant, representing the product of thermal capacity and thermal resistance, decreases by only 8.25%. This means the cooling trend speeds up by 8.25% after the water draw.

The second meal is prepared at 04:00 am, precisely 12 hours after the first meal. During this period, the water temperature decreased to 34.94 °C for H_{low} , 40.77 °C for H_{medium}, and 46.35 °C for H_{high}. This indicates some level of heat retention by the tank even after a reduced water volume because the water remains hot enough to impact the cooking process of the second meal. The second water draw of 600 mℓ causes another volume drop from 4.4 to 3.8 ℓ. This volume drop affects the potential to reduce the additional electrical energy of cooking the third meal, as discussed in *Section 6.2.3*.

The comparative results of the hybrid and electrical cooking systems for scenario $S2$ are presented in *Table 6.3*. The electrical cooking system requires an additional 454.15 Wh of electrical energy (totalling to 908.31 Wh) to cook the second meal from at 04:00 am compared to scenario $S1$. In the hybrid cooking system, the difference between water and ambient temperatures ranges from 12.44 to 23.85 °C which results in 2.24 to 5.13% reduction in additional electrical energy. This is a lower range compared to the first meal prepared due to the first water draw and cooling that occurred. Overall, the combined electrical energy reduction for cooking two meals ranges from 5.29 to 14.70% which translates to a consumption of 773.42 to 858.77 Wh.

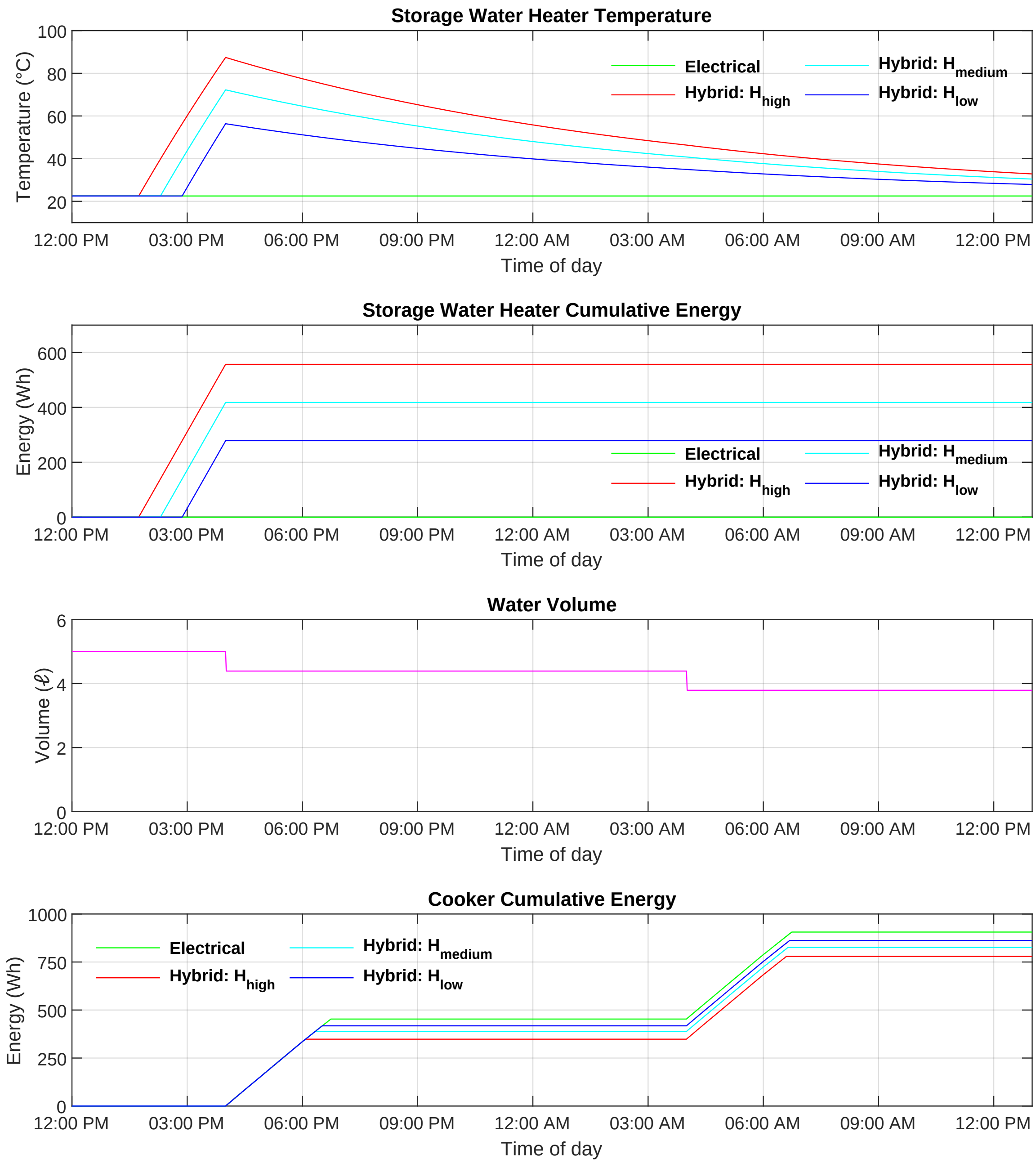

Figure 6.2: Results of cooking two meals with an electrical and hybrid system.

To cater for cooking two meals after sun-hours, the electrical cooking system has twice the battery capacity amounting to 103.74 Ah. However, when a storage water heater is supplemented, a capacity of 5.65 to 15.40 Ah can be reduced. This means a smaller battery size of 98.09 to 88.34 Ah can be used for completing two cooking processes.

Table 6.3: Performance of cooking two meals using electrical and hybrid system.

Parameter	**Electrical**	**Hybrid**		
Daily PV energy level	**-**	**High**	**Medium**	**Low**
Water and ambient temp diff. (1st meal) [°C]	0	64.93	49.74	33.87
Water and ambient temp diff. (2nd meal) [°C]	0	23.85	18.27	12.44
Additional electrical cooking energy [Wh]	908.31	773.42	821.72	856.77
Total electrical energy reduction [%]	0.0%	14.70%	9.373%	5.289%
Battery capacity [Ah]	103.74	88.34	93.86	98.09

6.2.3 Scenario S3: Three Meals a Day

The profiles in *Figure 6.3* show the results of the hybrid and electrical cooking system when three meals are prepared. The preparation of the third meal starts at 10:00 am. Between sunrise and the start of preparing the third meal, the PV energy is directed towards recharging the battery used for cooking the previous two meals and not for water heating.

The second water draw of 600 mℓ reduced the time constant by another 8.25%, leading to slightly faster cooling trends and relatively lower water temperatures of 29.63 °C for H_{low}, 32.97 °C for H_{medium}, and 36.17 °C for H_{high} at 10:00 am. The water temperatures are above ambient can still influence the cooking process to reduce the additional electrical energy to achieve a well-cooked rice. The third water draw of 600 mℓ causes the tank water volume to decrease to 3.2 ℓ and can be refilled afterward.

The comparative results of the electrical and hybrid cooking systems for scenario $S3$ are presented in *Table 6.4*. The electrical cooking system consumes an additional 454.15 Wh of electrical energy (totalling to 1 362.46 Wh) to cook the third meal compared to scenario $S2$. On the other hand, in the hybrid cooking system, the difference between water and ambient temperatures before cooking the third meal is in the range of 7.129 to 13.67 °C resulting in a 1.13 to 2.52% reduction in electrical energy usage. The combined electrical energy reduction range for all three meals becomes 3.90 to 10.6%, which means an energy consumption of 1 307.01 to 1 215.36 Wh.

The electrical system requires a battery capacity of 155.62 Ah to cook all three meals. However, by incorporating a storage water heater, it would be possible to reduce the required capacity by 6.34 to 16.81 Ah. This would allow for a 149.28 to 138.81 Ah battery to be used for completing

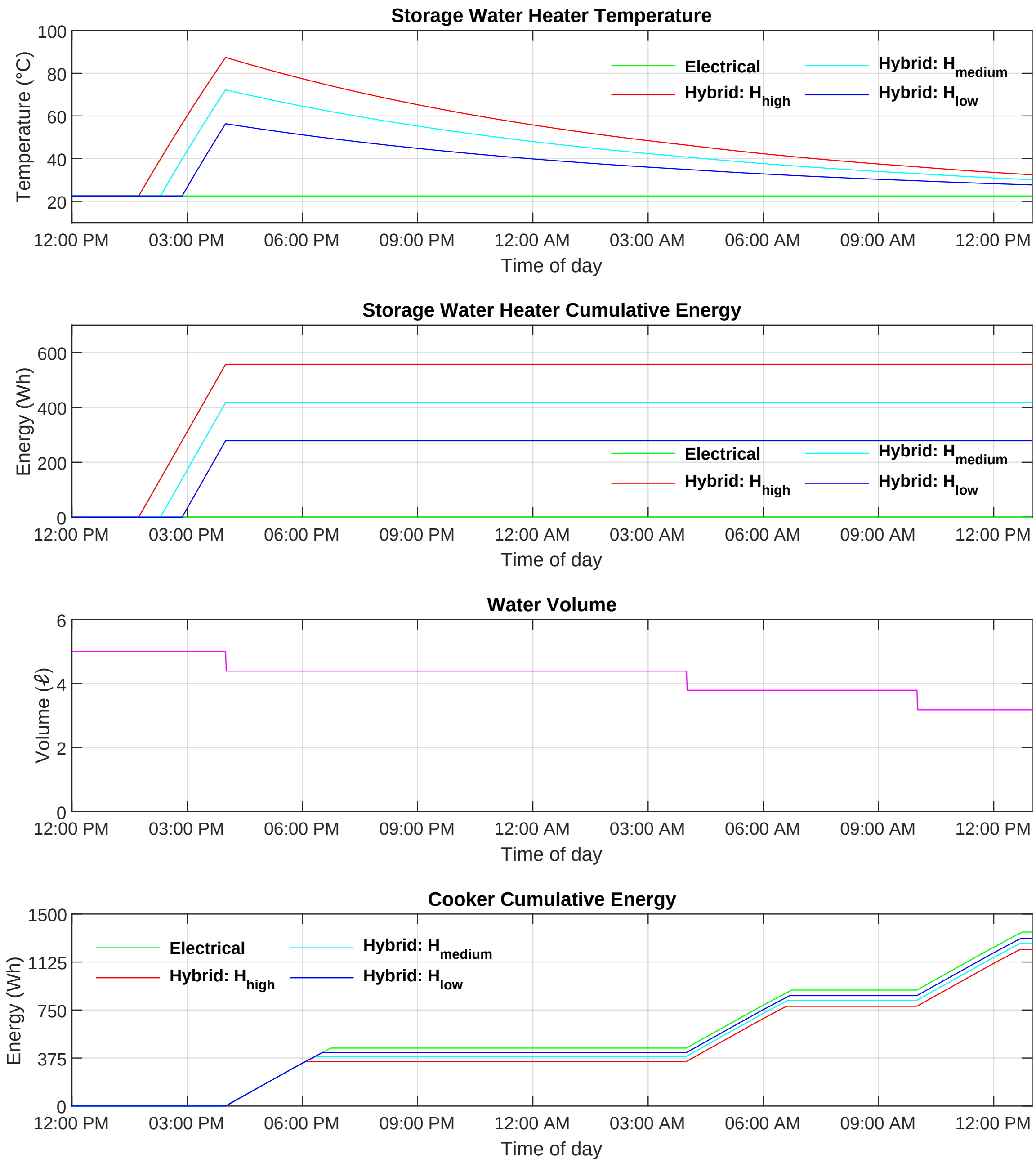

Figure 6.3: Results of cooking three meals with an electrical and hybrid system.

all three cooking processes.

In scenario $S3$, a second option is to size the battery for the first two meals that are prepared during off-peak sun hours. The third meal can be cooked mainly using PV power since it is prepared starting from 10:00 am during on-peak sun hours. However, cooking using PV power will increase the period required to fully charge the batteries. Nevertheless, the pre-heated

Table 6.4: Performance of cooking three meals using electrical and hybrid system.

Parameter	**Electrical**	**Hybrid**		
Daily PV energy level	**-**	**High**	**Medium**	**Low**
Water and ambient temp diff. (1st meal) [°C]	0	64.93	49.74	33.87
Water and ambient temp diff. (2nd meal) [°C]	0	23.85	18.27	12.44
Water and ambient temp diff. (3rd meal) [°C]	0	13.67	10.47	7.129
Additional electrical cooking energy [Wh]	1 362.46	1 215.36	1 266.87	1 307.01
Total electrical energy reduction [%]	0.0%	10.64%	6.853%	3.902%
Battery capacity [Ah] (option 1)	155.62	138.81	144.70	149.28
Battery capacity [Ah] (option 2)	103.74	88.34	93.86	98.09

water still reduces the cooking period, which allows for a much earlier diversion to heat water again. As a result, a reduced battery size similar to scenario $S2$ with a capacity of 98.09 to 88.34 Ah can be used for the hybrid system.

6.3 Discussion

The simulation performance of a hybrid, electrical-thermal energy storage cooking system in comparison to the electrical cooking system both supplied by solar PV has been analysed in *Section 6.2*. Three cooking scenarios representing the number of rice meals cooked at different times of the day within a 24-hour period were used. The first meal was prepared in the afternoon, the second in the morning, and the third in the evening. Each meal was designed to serve three to four individuals. The analysis focused on the ability of the hybrid system to use PV energy for water heating after charging the battery, the effectiveness of the thermal resistance of the tank, and a comparison of the electrical cooking energy and the battery capacity requirements in the hybrid and electrical systems. The reduction of the electrical cooking energy and the battery capacity requirements are summarised in *Table 6.1*, *Table 6.2*, *Table 6.3* and *Table 6.4*.

The battery size reduction plotted against the meal number cooked, and the battery requirements as a function of the total number of meals cooked are presented in *Figure 6.4*.

The electrical cooking system uses all energy stored in the battery to cook each meal with water starting from ambient temperature, and the results serve as a baseline for comparison. On the other hand, adding a storage water heater in the system reduces the battery size significantly,

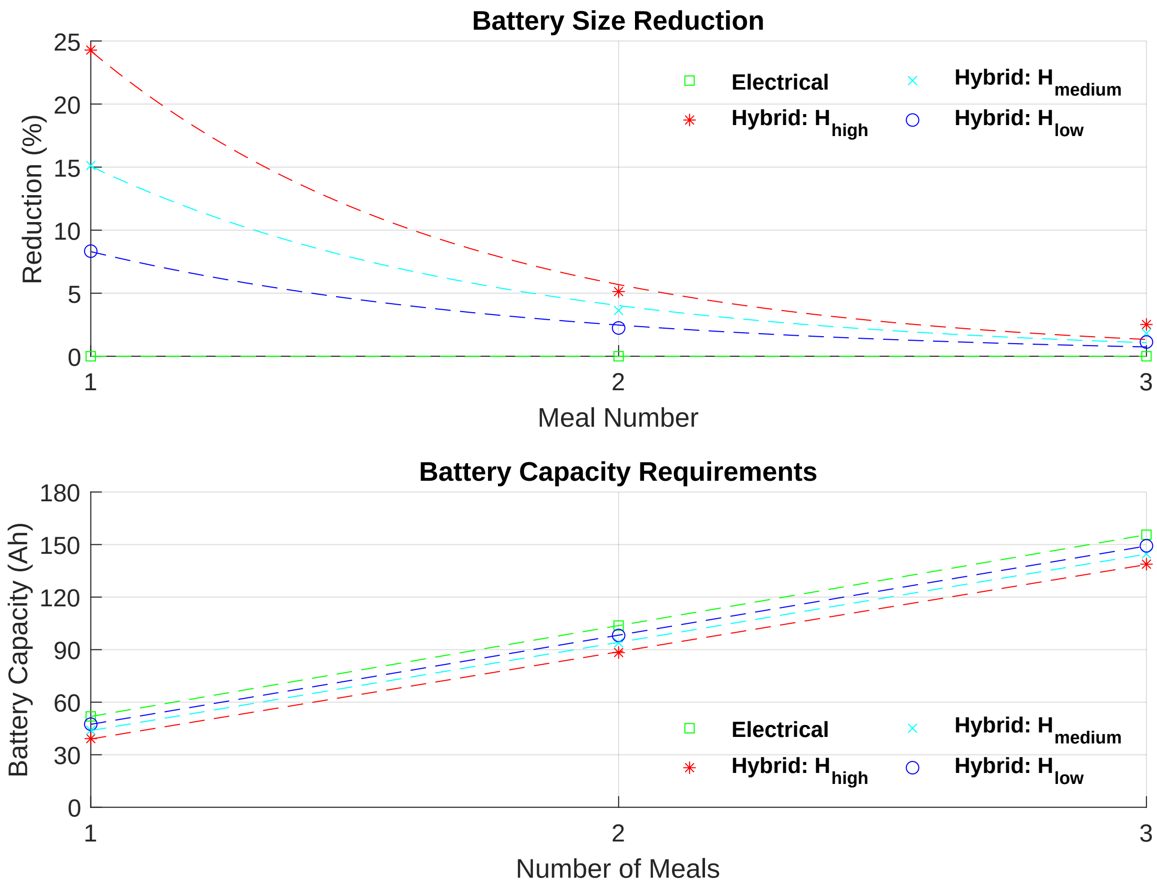

Figure 6.4: Battery requirements in an electrical and hybrid cooking system.

especially during high solar irradiation levels. However, the battery reduction values decrease for meals cooked after the first one, primarily due to heat losses. Since the systems are PV-supplied, the water is not re-heated due to the lack of PV energy after sunset until post midday the following day when the batteries have charged. The battery reduction follows the exponential decay trend of water cooling, as fitted on the scatter plots in *Figure 6.4*, with meals cooked after a long cooling period having the lowest battery reduction. This emphasizes the importance of good thermal resistance, as it can potentially maintain higher battery reduction for each meal cooked.

The relationship between the number of meals cooked and the required battery capacity exhibits a strong linear trend. The hybrid system has lower offsets than the electrical system, which indicates the reduced capacity requirements. The linear trend is represented using *Equation (6.1)*, enabling estimation of the battery capacity needed based on the number of meals

Table 6.5: Parameters of the battery capacity requirement to number of meals *Equation (6.1)*.

Parameter	**Electrical**		**Hybrid**	
Daily PV energy level	**-**	**High**	**Medium**	**Low**
a [Ah/meals]	51.88	49.80	50.37	50.91
b [Ah]	-0.01	-10.81	-6.58	-3.53

Table 6.6: Battery reduction in a hybrid cooking system compared to an electrical system.

Scenario	**Reduction**
Scenario $S1$	8.33 to 24.3%
Scenario $S2$	5.29 to 14.7%
Scenario $S3$	3.90 to 10.6%

cooked. The parameters of the equation for each case are presented in *Table 6.5*.

$$C_B(N_M) = aN_M + b \tag{6.1}$$

Where:

- C_B is the battery capacity required for the selected number of meals [Ah]
- N_M is the number of meals
- a is the linear best fit gradient [Ah/meals]
- b is the linear best fit offset [Ah]

The percentage reduction of the additional electrical cooking energy and the battery requirements are the same, as summarised in *Table 6.6*. The hybrid storage system can reduce the battery requirements for cooking by a range of 8.33 to 24.3% for one meal, 5.29 to 14.7% for two meals, and 3.90 to 10.6% for three meals.

6.4 Conclusion

This chapter has explored the performance of a PV-supplied cooking system with hybrid, electrical-thermal storage and compared it to the performance of an electrical cooking system. Three cooking scenarios representing meals cooked at different times of the day were used as case study. The use of PV energy by a storage water heater after charging the battery has led to significant reductions in the electrical component of cooking energy even at low solar irradiation levels. However, it was observed that water draws after sunset reduce the potential for higher electrical energy reduction for meals cooked later. The thermal resistance of the storage tank played a significant role in maintaining the water at a useful temperature, which influenced each of the three meals cooked before reheating again with PV energy.

In the three cooking scenarios considered, the storage water heater of the hybrid cooking system reduced the additional electrical energy to cook rice by up to 24.3% for one meal, 14.7% for two meals, and 10.6% for three meals in comparison to the electrical cooking system. These results translate to a similar battery capacity reduction, which demonstrate the potential for significant cost savings or the ability to allocate the saved battery capacity for other household tasks.

These results are subject to variation based on different cooking scenario designs, ambient temperatures, and thermal resistance of the thermal storage tank, as these factors significantly impact the performance of the system. The following chapter discusses the extent to which these variables and others could affect the key results and also discusses further research work.

Chapter 7

Discussion of the Research

This chapter presents the discussion of the key research results in terms of validity and reliability in *Section 7.1*. Limitations on areas of the research and potential directions for further research work are explored in *Section 7.2*. The conclusion is presented in *Section 7.3*.

7.1 Discussion of Results

The study has demonstrated, through experiments and simulations, the extent that a thermal storage tank can reduce the battery size requirements in PV cooking systems. This was the aim of the study, however, there are assumed variables that could impact the obtained results. The variables and their potential influence are discussed in the following subsections.

7.1.1 Varying and Fixed Volume Storage Tanks

The choice of a varying or fixed water volume storage water heater can affect the water cooling trends and, therefore, the amount of electrical energy required for cooking. In the study, an urn which is not piped and has a varying water volume was selected in order to analyse a system that is not limited to households with piped water. However, some rural areas have access to piped water, which makes a piped tank with fixed water volume (such as a small geyser or a wall mounted instant water boiler) more beneficial. The results of the three cooking scenarios for a fixed volume tank are presented in *Appendix D*, and the key findings in comparison to the

Table 7.1: Comparison of battery size reduction between a varying and fixed volume storage water heater.

Scenario	**Varying Volume**	**Fixed Volume**
Scenario $S1$	8.33 to 24.3%	8.33 to 24.3%
Scenario $S2$	5.29 to 14.7%	5.24 to 14.6%
Scenario $S3$	3.90 to 10.6%	3.84 to 10.5%

varying water volume tank are summarised in *Table 7.1*.

The fixed volume tank exhibits a lower battery reduction on scenarios $S2$ and $S3$ by approximately 0.1% because its cooling trend is slightly faster compared to the varying volume tank after draw events. This is because the replacement of water after a draw event mixes with colder water at ambient, which decreases the water temperature compared to reducing the volume of water (which also increases the thermal resistance by reducing the contact surface area). The difference in battery reductions is minimal, however, using a fixed volume tank eliminates the need to manually refill water after usage.

7.1.2 Environmental Conditions

Environmental conditions are one of the factors that affect the energy performance of PV systems. The simulations considered different solar irradiation levels, which produced variations in water temperatures of the storage water heater. The ambient temperature of 22.5 °C was chosen as the average room temperature across all seasons, which produced average results. The battery reduction results of low- and high-level ambient temperatures (a deviation of ±20% from the average temperature T_a) under the same cooking scenarios are presented in *Table 7.2*.

In instances of high ambient temperatures, heat losses to the surroundings are minimised due to a low difference between the internal water and ambient temperatures. Consequently, the battery reduction becomes exponentially low compared to cases with low ambient temperatures. As presented in *Table 7.2*, using +20% ambient temperature results in a decrease of up to 3.2%, while a -20% deviation increases the reduction by up to 2.4%. Therefore, if the PV system can be able to heat-up water across all seasons, high battery reductions are expected during winter seasons (where the average ambient temperatures is low), and low battery reductions during summer months (where the average ambient temperatures is high). However, it is worth noting

Table 7.2: Comparison of battery size reduction with different ambient temperature values.

Scenario	T_a	$0.8T_a$	$1.2T_a$
Scenario $S1$	8.33 to 24.3%	9.56 to 26.7%	7.19 to 21.1%
Scenario $S2$	5.29 to 14.7%	6.04 to 16.1%	4.58 to 12.9%
Scenario $S3$	3.90 to 10.6%	4.45 to 11.6%	3.39 to 9.35%

that cooking meals in lower ambient temperatures required more energy compared to higher ambient temperatures.

7.1.3 Cooking Times

The cooking scenarios of the study are based on the number of meals and the start time for cooking them. A change of when the meal is started could impact the results. It has been shown that meals cooked in the evening result in higher battery size reductions than meals cooked after an extended period of no PV energy. *Table 7.4* shows how the battery size reduction is affected when the cooking time is shifted by ±1 hour.

If the starting time is shifted by an hour earlier, the reduction decreases for scenario $S1$ by up to 14% because the storage water heater is still heating up and the initial water temperatures used are low. In the case of starting an hour later, the reduction only decreases by 3.1%. It is then recommended to schedule cooking meals during periods of high water temperature, such as in the afternoon and evening, in order to require less additional electrical energy and achieve higher battery reductions.

7.1.4 Thermal Resistance

The research has demonstrated that the cooling operation of the investigated thermal storage tank can retain 5 ℓ of water above 40 °C for 18 hours without re-heating. However, the low temperature level yields lower battery reduction based on the equation of the electrical energy reduction. To ensure that the water temperature inside the tank stays hot after 24 hours even in colder weather temperatures, the tank's thermal resistance R_a can be improved. *Table 7.4* shows how the battery size reduction is affected when using thermal resistance of $1.1R_a$, $10R_a$ and $100R_a$.

Table 7.3: Comparison of battery size reduction by shifting the cooking start times.

Scenario	0 hour	-1.0 hours	+1.0 hours
Scenario $S1$	8.33 to 24.3%	0.544 to 9.74%	7.51 to 21.2%
Scenario $S2$	5.29 to 14.7%	0.836 to 7.70%	4.78 to 12.9%
Scenario $S3$	3.90 to 10.6%	1.03 to 6.04%	3.53 to 9.39%

Table 7.4: Comparison of battery size reduction with different thermal resistance values.

Scenario	R_a	$1.1R_a$	$10R_a$	$100R_a$
Scenario $S1$	8.33 to 24.3%	8.38 to 24.3%	8.82 to 24.3%	8.87 to 24.3%
Scenario $S2$	5.29 to 14.7%	5.45 to 15.01%	8.22 to 22.2%	8.80 to 24.1%
Scenario $S3$	3.90 to 10.6%	4.08 to 11.01%	7.83 to 20.9%	8.76 to 23.9%

Improving the thermal resistance by a factor of 1.1 has a small change on the battery reduction, with the highest increase being 0.41%. However, improving the thermal resistance by a factor of 10 maintains the highest battery reduction at 20.9% or above, while a factor of 100 ensures that the highest reduction is 23.9% or more in all scenarios. A large thermal resistance could be achieved by using a similar small-sized storage tank such as a thermos that has vacuum between its double walls to prevent heat from transferring by convection.

7.1.5 Meal Size

The size of the rice meal considered is for three to four servings, and changing the meal size may not result in a proportional increase or decrease in electrical cooking energy. This is because the main factor influencing rice cooking is the internal temperature rather than the amount of heat supplied to the cooker. For example, cooking for two or six people may require roughly the same amount of electrical energy as cooking for four people. However, the water volume required from the storage water heater will vary based on the desired amount of rice using the same rice to water ratio of 1:2. *Table 7.5* shows how the battery reduction is affected when cooking rice for three and six servings.

Doubling the meal size does not affect the battery reduction in scenario $S1$ since the pre-heated water remains consistent in both cases. However, there is a slight decrease of up to 0.4% in battery reduction for scenarios $S2$ and $S3$. This is because drawing double the amount of water to cook rice for six servings compared to three servings cools down the water temperatures faster. Consequently, this reduces the potential for higher battery reduction.

Table 7.5: Comparison of battery size reduction with different meal sizes.

Scenario	**3 servings**	**6 servings**
Scenario $S1$	8.33 to 24.3%	8.33 to 24.3%
Scenario $S2$	5.29 to 14.7%	5.14 to 14.3%
Scenario $S3$	3.90 to 10.6%	3.68 to 10.1%

In applications of larger cooking systems that serve more than six people and require larger-sized PV and battery storage, the amount of electrical energy required for cooking would increase. However, when using the same rice to water ratio, the same battery reduction is expected.

7.2 Further Research Work

Having explored the extent to which adding a thermal storage tank to PV-supplied cooking systems reduces the battery size requirements, it is important to note the limitations of this research and potential directions for future work. The following subsections will outline these areas for further exploration.

7.2.1 Food and State Measurement

The state of rice is determined using an objective method for moisture content and a subjective taste method. It is suggested that integrating with an objective method for hardness could improve the accuracy of the food state results. A method to compress the rice grains and measure the force deformation data can be used. Additionally, the work could expand to include other staple foods commonly consumed in Africa, such as maize, millet, and wheat, to gain more comprehensive understanding of how the thermal storage tank can reduce the battery size requirements.

7.2.2 Cooking Appliance Technology

To adapt the cooking system topology, it would be beneficial to consider an easier cooking process. The selected slow cooker does not have the ability to determine when to stop cooking based on the readiness of the internal food mixture. Therefore, it is recommended to consider automated cookers with similar specifications that can detect when the food is well-cooked and turn off automatically. For instance, some basic rice cookers monitor the temperature of the food mixture and automatically switch off the heat once it surpasses the boiling point of water, indicating that the rice has fully absorbed the available water.

7.2.3 Large Scale Application

Scaling the idea for micro-grid PV systems could offer significant benefits to rural communities powered by PV systems. One of the challenges faced by micro-grids is also the inability to store and make use of PV energy at low-cost. Larger water volumes have the advantage of a slower cooling curve because of larger thermal capacity. With this advantage, hot water can be supplied to individual households using insulated tubes. Similar concepts have been proven to work with other thermal storage technologies to provide hot water and heating for households, as discussed in *Section 2.2*.

7.3 Conclusion

The variables that could impact the key results obtained throughout the study have been identified and discussed. In addition, the factors that could potentially limit the adoption of the hybrid cooking system topology have been identified, and further research was provided to address these limitations and optimise the design and performance of the system.

Chapter 8

Conclusion Remarks

The high energy requirements of cooking and the intermittent nature of renewables present a significant challenge in providing clean, cheap and sustainable cooking alternatives. This dissertation has addressed this challenge by exploring the performance of a hybrid energy storage system with a battery and a thermal storage tank for PV-supplied cooking systems. The thermal storage tank acts as a secondary storage system that heats up after the battery reached maximum capacity. In this way, the PV energy is stored in a combined cost-effective storage unit because thermal storage systems usually use cheaper storage materials than electrochemical batteries. This study aimed to explore the performance of the hybrid storage topology, and to achieve this goal, a research question and three research objectives were formulated. The following sections outline the outcomes of the research work presented in the preceding chapters and the conclusions made to answer the research question.

8.1 Summary of Research Work

In *Chapter 2*, a food-safe storage water heater with good thermal insulation is identified as a promising candidate for storing thermal energy in PV cooking systems. This type of storage system is commonly found in households and can directly influence the cooking process. Although the literature investigates various thermal storage methods in renewable-based systems, the methods were found to be inadequate and too complex for small-scale cooking applications.

Thermal modelling techniques that translate thermal systems to electrical elements were identified as suitable methods to simulate the performance of the hybrid system under various cooking scenarios. Moisture content and hardness measurement methods are necessary to objectively determine the readiness of staple foods such as rice.

The research approach in *Chapter 3* demonstrated the idea that PV energy for cooking could be stored in two separate storage units instead of a single high-cost battery. The hybrid storage cooking system, which supplements a thermal storage tank with a battery was explained with its subsystems. The thermal storage tank was chosen as a storage water heater designed to heat up water when the batteries have charged, and a slow cooker was chosen as the cooking appliance. The thermal-electrical analogy was chosen to model the storage water heater and the slow cooker. Rice was chosen as the cooking medium because it is the widely consumed staple food and the fastest growing in Africa that also benefits from initially cooking it with pre-heated water. The chosen measurement method of the readiness of rice uses moisture content and a subjective taste evaluation technique. The experiments and cooking scenarios selected to explore the performance of the hybrid system topology were also discussed in detail.

The models of the storage water heater and the cooking appliance were presented in *Chapter 4*. The models were built using the thermal-electrical analogy, which allowed simulations that captures the power and temperature performance. The storage water heater model was designed to have a varying thermal capacitor as water, which resulted in a single first-order differential equation that was simple to calibrate its parameters using measured results. The cooking appliance model was designed to have two thermal capacitors as the cooking vessel and food mixture, which resulted into two first-order differential equations. The model required an identification model to calibrate some of its parameters using measured results. Both models were validated against physical tests, where their internal temperature and energy consumption performance demonstrated a close similarity.

The results of the cooking experiments, which studied the effect of cooking rice for three to four servings with pre-heated water were presented in *Chapter 5*. The findings showed that when the temperature of the initial water used for cooking is increased, rice absorbs water more quickly, softens faster and reaches a well-cooked state sooner. In addition, as the rice continues to cook, the moisture absorption rate decreases drastically and reaches steady-state indicating that it has absorbed all the water. The results demonstrated that using pre-heated water between 50 to 97.6 °C can reduce the additional electrical energy to cook rice by a range of 7.8 to 32.9%. Interestingly, the points of the temperature difference between the initial water and ambient plotted against the electrical energy reduction revealed a strong exponential relationship. An equation was derived from the two variables to estimate the expected electrical energy reduction based on the initial water and ambient temperature difference.

The overall benefits of the hybrid storage system topology in PV-supplied cooking systems is investigated in *Chapter 6* using the models from *Chapter 4*, and the electrical energy reduction equation from *Chapter 5*. Three cooking scenarios were considered within a 24-hour period where each meal is designed for three to four servings, and the energy performance of hybrid cooking systems were compared against pure electrical systems. In the hybrid system, PV energy was used to heat the water from midday to afternoon, which cools after sunset. The thermal resistance of the storage tank played a crucial role in keeping the water hot enough to influence each meal before the water reheats again the following day. In scenarios where more than one meal was cooked, the hot water draws resulted in a faster water cooling trend. This reduction decreased the potential for having a higher electrical energy reduction for meals cooked afterward. The values of the reduced electrical energy were then translated into reduced battery capacities, which provides an option for a lower battery cost system or a saved-up battery capacity for other household tasks. The findings from the cooking scenarios are that the thermal storage tank reduces the electrical component of cooking energy by up to 24.3% for one meal (51.87 to 39.21 Ah battery reduction), 14.7% for two meals (103.74 to 88.34 Ah battery reduction), and 10.6% for three meals (155.62 to 138.81 Ah battery reduction).

The assumed factors that could impact the obtained results are discussed in *Chapter 7*, along with recommendations for further research. The key factors identified are the time to start to cook meals and the thermal resistance of the storage tank. The discussion suggested that the afternoon and evening periods be used for cooking in order to achieve higher battery reductions due to hotter water temperatures from the tank. In addition, if the thermal resistance of the selected storage tank is improved by at least ten times the tank keeps the water hot enough to reduce the battery size requirements in all cooking scenarios by more than 20.8%. The future research is proposed to focus on considering other staple foods commonly consumed in Africa, the use of automated cookers, and consideration of large scale applications.

8.2 Conclusion

In conclusion, the research objectives and how they were achieved are discussed, and the findings are linked to the research question.

The first objective was to identify a commonly consumed staple food item that can benefit from a cooking process using pre-heated water from the thermal storage tank, with an objective measurement method for evaluating the state of the food. Rice was used as the cooking food medium throughout the research and it was evaluated that starting to cook it with pre-heated water had a positive impact on its readiness. A moisture content measurement method was developed to measure the state of the rice at regular intervals during the cooking process, which successfully provided observable results on how the state of the rice changes when different water temperatures are initially used. Additionally, a subjective taste method was used to determine the state of rice and assisted in selecting the benchmark points for well-cooked state in the moisture content method. These methods were effective in determining when the rice becomes well-cooked and allowed for a reliable evaluation of the effects of hot water addition on the cooking of rice. The future work can enhance the measurements by incorporating an objective method to measure the hardness of rice to better analyse its state closer to the benchmark points.

The second objective was to develop and validate mathematical models of a storage water heater and a cooking appliance taking into account the thermal losses involved. The models of the subsystems were based on the thermal-electrical analogy and validated against measured results. The storage water heater model captured the heating, steady-state, and cooling stage operations, along with changes in water volume and thermal resistance when hot water is drawn. Simulation results of a tank with and without a water draw showed good agreement to the measured water temperature, element switching times, and energy consumption results.

The cooking appliance model captured the heating stage operation and produced an internal temperature response of rice that closely matched the measured results. The successful development of the validated models allowed for exploration of the performance of the hybrid cooking system topology under varying cooking conditions.

The third objective was to examine the impact of reducing the additional electrical energy required for cooking with this topology using the developed models through case study scenarios. This was achieved by conducting experiments and simulations on the hybrid cooking system. The experiments with four different water temperatures ranging from 25.0 to 97.6 °C achieved a reduction in electrical energy required to cook rice to a range of 7.8 to 32.9%. An exponential equation was derived from the results to estimate the electrical cooking energy reduction based on the pre-heated water and ambient temperature difference. The simulation results of three realistic cooking scenarios showed a significant electrical cooking energy reduction in the hybrid system when compared to a pure electrical system. The thermal storage tank reduced the electrical cooking energy by a range of 8.33 to 24.3% for one meal, 5.29 to 14.7% for two meals, and 3.90 to 10.6% for three meals prepared in a day under different solar irradiation conditions. The obtained results are subject to potential improvements if a storage tank with a thermal resistance of at least ten times is used.

The research objectives were derived from the main research question: "To what extent can a thermal storage tank, as a supplement to a battery storage system, reduce the electrical component of cooking energy in PV systems?" The findings indicated that the use of a storage water heater as a thermal storage tank, with an initial water volume of 5 ℓ and thermal resistance of 2.26 °C/W, reduces the electrical cooking energy by up to 24.3% for one meal, 14.7% for two meals, and 10.6% for three meals. This reduction led to a corresponding reduction in the required battery capacity for the PV systems.

Therefore, the findings from this study offer a significant contribution to enhancing access to clean-cooking solutions in rural Africa. By including a thermal storage system using small commercial storage water heaters with good thermal resistance in PV cooking systems, the size of a high cost battery required initially could be reduced. This hybrid topology increases the financial affordability of off-grid cooking systems which improves access to clean-cooking solutions.

References

[1] International Energy Agency. *Energy access outlook 2017: From poverty to prosperity.* Available: `https://www.iea.org/reports/energy-access-outlook-2017`, 2017.

[2] Kamil Kaygusuz. "Energy for sustainable development: A case of developing countries". In: *Renewable and Sustainable Energy Reviews* 16.2 (2012), pp. 1116–1126.

[3] Francesco Lombardi, Fabio Riva, Marco Sacchi, and Emanuela Colombo. "Enabling combined access to electricity and clean cooking with PV-microgrids: new evidences from a high-resolution model of cooking loads". In: *Energy for sustainable development* 49 (2019), pp. 78–88.

[4] International Energy Agency. *Africa energy outlook 2022.* Available: `https://www.iea.org/reports/africa-energy-outlook-2022`, 2022.

[5] Mahlodi Esther Masekela and Khomotso Semenya. "Factors influencing the use of firewood post-electrification in rural South Africa: The case of Ga-Malahlela village". In: *Journal of Energy in Southern Africa* 32.3 (2021), pp. 24–40.

[6] Kaniki J Mulumba, Kristy E Langerman, and Annlizé L Marnewick. "Determining the optimal energy use mix in a low-income household". In: *2019 International Conference on the Domestic Use of Energy (DUE).* IEEE. 2019, pp. 25–33.

[7] Simon Batchelor, Ed Brown, Nigel Scott, and Jon Leary. "Two birds, one stone—reframing cooking energy policies in Africa and Asia". In: *Energies* 12.9 (2019), p. 1591.

[8] S Batchelor. "Is it time for Solar electric cooking for Africa". In: *Gamos Concept Note, May, Reading, United Kingdom* (2013).

[9] M Leach and R Oduro. "Preliminary design and analysis of a proposed solar and battery electric cooking concept: costs and pricing". In: *Evidence on Demand, UK* (2015).

[10] Simon Batchelor. "Solar Electric Cooking in Africa in 2020: A synthesis of the possibilities". In: *London: Evidence on Demand/DFID, DOI* 10 (2015), p. 12774.

[11] Matthew Brandt, Jason Woods, and Paulo Cesar Tabares-Velasco. "An analytical method for identifying synergies between behind-the-meter battery and thermal energy storage". In: *Journal of Energy Storage* 50 (2022), p. 104216.

[12] Mohammed Guezgouz, Jakub Jurasz, Bennaissa Bekkouche, Tao Ma, Muhammad Shahzad Javed, and Alexander Kies. "Optimal hybrid pumped hydro-battery storage scheme for off-grid renewable energy systems". In: *Energy Conversion and Management* 199 (2019), p. 112046.

[13] Yi He, Su Guo, Peixin Dong, Chen Wang, Jing Huang, and Jianxu Zhou. "Techno-economic comparison of different hybrid energy storage systems for off-grid renewable energy applications based on a novel probabilistic reliability index". In: *Applied Energy* 328 (2022), p. 120225.

[14] Ademola A Adenle. "Assessment of solar energy technologies in Africa-opportunities and challenges in meeting the 2030 agenda and sustainable development goals". In: *Energy Policy* 137 (2020), p. 111180.

[15] M Rezwan Khan and Intekhab Alam. "A Solar PV-Based Inverter-Less Grid-Integrated Cooking Solution for Low-Cost Clean Cooking". In: *Energies* 13.20 (2020), p. 5507.

[16] Xiaojing Sun. "Solar technology got cheaper and better in the 2010s. Now what?" In: *Green Tech Media, December* 17 (2019).

[17] Dean Holland Clift and Harry Suehrcke. "Control optimization of PV powered electric storage and heat pump water heaters". In: *Solar Energy* 226 (2021), pp. 489–500.

[18] Henrik Lund, Poul Alberg Østergaard, David Connolly, Iva Ridjan, Brian Vad Mathiesen, Frede Hvelplund, Jakob Zinck Thellufsen, and Peter Sorknæs. "Energy storage and smart energy systems". In: *International Journal of Sustainable Energy Planning and Management* 11 (2016), pp. 3–14.

[19] Bingchen Zhao, Yannan Zhang, and Ruzhu Wang. *Materials for Thermal Energy Storage: Classification, Selection and Characterization*. Elsevier, 2022.

[20] Akshansh Aggarwal, Naman Goyal, and Anil Kumar. "Thermal characteristics of sensible heat storage materials applicable for concentrated solar power systems". In: *Materials Today: Proceedings* 47 (2021), pp. 5812–5817.

[21] Alberto Rossi Espagnet. *Techno-economic assessment of thermal energy storage integration into low temperature district heating networks*. 2016.

[22] Muhammad Tawalbeh, Hafsah A Khan, Amani Al-Othman, Fares Almomani, and Saniha Ajith. "A comprehensive review on the recent advances in materials for thermal energy storage applications". In: *International Journal of Thermofluids* (2023), p. 100326.

[23] A Harris, M Kilfoil, and E Uken. *Domestic energy savings with geyser blankets*. Cape Peninsula University of Technology, 2007.

[24] Philip Johannes Cornelis Nel. "Rethinking electrical water heaters". PhD thesis. Stellenbosch: Stellenbosch University, 2015.

[25] Stephen Tangwe, Michael Simon, and Edson Meyer. "Impact of standby losses and potential reduction by installation of isotherm blanket on the hot water cylinders". In: *2017 International Conference on the Domestic Use of Energy (DUE)*. IEEE. 2017, pp. 101–109.

[26] IE Bosman, LJ Grobler, and AZ Dalgleish. "Determination of the impact on the standing losses of installing blankets to electric hot water heaters in South Africa". In: *Journal of Energy in Southern Africa* 17.2 (2006), pp. 57–64.

[27] Quinton Catherine, Jacques Wheeler, Richardt Wilkinson, and Gerhard de Jager. "Hot water usage profiling to improve geyser efficiency". In: *Journal of energy in Southern Africa* 23.1 (2012), pp. 39–45.

[28] D Schlipf, P Schicktanz, H Maier, and G Schneider. "Using sand and other small grained materials as heat storage medium in a packed bed HTTESS". In: *Energy Procedia* 69 (2015), pp. 1029–1038.

[29] Polar Night Energy. *Store Wind and Solar Power as Heat in Sand*. Available at: `https://polarnightenergy.fi/sand-battery`, Last Accessed 06 Dec. 2022.

[30] Martin Osei, Owen Staveland, Sean McGowan, Justin Brett Unger, Nathan Robert Christler, Matthew Weeman, Marcus Edward Strutz, Matthew Walker, Megan Belle Maun, Nicolas C Dunning, et al. "Phase change thermal storage: Cooking with more power and versatility". In: *Solar Energy* 220 (2021), pp. 1065–1073.

[31] Tobias Häring, Argo Rosin, and Helmuth Biechl. "Using common household thermal storages to support the PV-and battery system in nearly zero energy buildings in off-grid mode". In: *Sustainable Energy Technologies and Assessments* 35 (2019), pp. 12–24.

[32] Edgar Ramírez-Laboreo, Carlos Sagüés, and Sergio Llorente. "Thermal modeling, analysis and control using an electrical analogy". In: *22nd Mediterranean Conference on Control and Automation*. IEEE. 2014, pp. 505–510.

[33] Yu-Chieh Jessie Yen. "Demand modelling of horizontal electric water heaters". PhD thesis. University of the Witwatersrand, Johannesburg, 2021.

[34] A. Shabani, D. Dhamo, D. Panxhi, and O. Zavalani. "Modelling and simulation of home appliances using electric circuit analogy: Albanian case study". In: *2019 IEEE PES Innovative Smart Grid Technologies Europe (ISGT-Europe)*. IEEE. 2019, pp. 1–5.

[35] A Kerim Kar and Ümit Kar. "Optimum design and selection of residential storage-type electric water heaters for energy conservation". In: *Energy conversion and management* 37.9 (1996), pp. 1445–1452.

[36] Zhaojing Yin, Yanbo Che, Dezhi Li, Huanan Liu, and Dongmin Yu. "Optimal scheduling strategy for domestic electric water heaters based on the temperature state priority list". In: *Energies* 10.9 (Sept. 2017), p. 1425.

[37] LL Leeuwner, NH Naude, M Roux, and Marthinus J Booysen. "Evaluation of the energy model of a horizontally-mounted electric water heater through internal temperature measurement". In: *2017 IEEE Innovative Smart Grid Technologies-Asia (ISGT-Asia)*. IEEE. 2017, pp. 1–7.

[38] PJC Nel, Marthinus J Booysen, and Brink Van Der Merwe. "Electric water heater energy consumption determination using outlet temperature and volumetric estimation". In: *2015 IEEE Symposium Series on Computational Intelligence*. IEEE. 2015, pp. 665–672.

[39] Getachew Nigatu, James Hansen, Nathan Childs, and Ralph Seeley. *Sub-Saharan Africa Is Projected To Be the Leader in Global Rice Imports*. [online]. Available: `https://www.ers.usda.gov/amber-waves/2017/october/sub-saharan-africa-is-projected-to-be-the-leader-in-global-rice-imports/`. Last Accessed 06 Dec. 2023.

[40] Roy Poritosh, Daisuke Nei, Takahiro Orikasa, Hiroshi Okadome, Manasikan Thammawong, Nobutaka Nakamura, Takeo Shiina, et al. "Cooking properties of different forms of rice cooked with an automatic induction heating system rice cooker." In: *Asian Journal of Food and Agro-Industry* 3.4 (2010), pp. 373–388.

[41] Food and Agriculture Organization of the United Nations. *RICE – A SECTOR OF OPPORTUNITY: Boosting rural livelihoods and strengthening institutional capacities*. [online]. Available: `https://www.fao.org/3/cc1960en/online/ssc-sub-saharan-africa-2022/chapter-3.html`. Last Accessed 06 Dec. 2023.

[42] Aminou Arouna, Irene Akoko Fatognon, Kazuki Saito, and Koichi Futakuchi. "Moving toward rice self-sufficiency in sub-Saharan Africa by 2030: Lessons learned from 10 years of the Coalition for African Rice Development". In: *World Development Perspectives* 21 (2021), p. 100291.

[43] Jonne Rodenburg and Kazuki Saito. "Towards sustainable productivity enhancement of rice-based farming systems in sub-Saharan Africa". In: *Field Crops Research* 287 (2022), p. 108670.

[44] Kossi Lorimpo Adjah, Maxwell Darko Asante, Aboubacar Toure, Mawuli Aziadekey, Francis Osei Amoako-Andoh, Michael Frei, Yacouba Diallo, and Komi Agboka. "Improvement of rice production under drought conditions in West Africa: application of QTLs in breeding for drought resistance". In: *Rice Science* 29.6 (2022), pp. 512–521.

[45] C. Chen. "Evaluation of air oven moisture content determination methods for rough rice". In: *Biosystems engineering* 3.4 (2003), pp. 447–457.

[46] Orrawan Rewthong, Somchart Soponronnarit, Chaiyong Taechapairoj, Patcharee Tungtrakul, and Somkiat Prachayawarakorn. "Effects of cooking, drying and pretreatment

methods on texture and starch digestibility of instant rice". In: *Journal of Food Engineering* 103.3 (2011), pp. 258–264.

[47] P Abhilasha, US Pal, MK Panda, G Sahoo, R Nayak, K Rayaguru, and NR Sahoo. "Standardisation of cooking and conditioning methods for preparation of quick cooking germinated brown rice". In: *Journal of the Indian Chemical Society* 98.8 (2021), p. 100093.

[48] Batchelor Simon. "Africa cooking with electricity (ACE)". In: *Reading. Gamos Working Paper (Draft as at August 2015)* (2015).

[49] Sayedus Salehin and A.K.M. Sadrul Islam. "Performance Test of Wonder Bag: A Pathway to Reduce Cooking Energy Consumption and CO2 Emission". In: *energypedia* (July 2014).

[50] Theodore L Bergman, Theodore L Bergman, Frank P Incropera, David P Dewitt, and Adrienne S Lavine. *Fundamentals of heat and mass transfer*. 6th ed. John Wiley & Sons, 2011. Chap. 1, pp. 1–41.

[51] Roland S Burns. *Advanced control engineering*. Elsevier, 2001. Chap. 2, pp. 25–26.

[52] Lennart Ljung and Torkel Glad. "On global identifiability for arbitrary model parametrizations". In: *Automatica* 30.2 (1994), pp. 265–276.

[53] Shengwei Wang and Xinhua Xu. "Parameter estimation of internal thermal mass of building dynamic models using genetic algorithm". In: *Energy conversion and management* 47.13-14 (2006), pp. 1927–1941.

[54] William Devia, Alben Cardenas, Kodjo Agbossou, and Karine Lavigne. "Simplified Thermal Parameters Estimation in Residential Buildings Using Genetic Algorithms". In: *IECON 2019-45th Annual Conference of the IEEE Industrial Electronics Society*. Vol. 1. IEEE. 2019, pp. 2566–2571.

[55] David L Carroll. "Chemical laser modeling with genetic algorithms". In: *AIAA journal* 34.2 (1996), pp. 338–346.

[56] Za'er Abo-Hammour, Othman Alsmadi, Shaher Momani, and Omar Abu Arqub. "A genetic algorithm approach for prediction of linear dynamical systems". In: *Mathematical Problems in Engineering* 2013 (2013).

[57] G. M. Masters. *Renewable and efficient electric power systems*. New Jersey: John Wiley & Sons, 2004. Chap. 9, pp. 568–572.

[58] Abhishek Jaiswal. "Lithium-ion battery based renewable energy solution for off-grid electricity: A techno-economic analysis". In: *Renewable and Sustainable Energy Reviews* 72 (2017), pp. 922–934.

[59] Ghassan Zubi, Rajendra S Adhikari, Nazly E Sánchez, and Wilber Acuña-Bravo. "Lithium-ion battery-packs for solar home systems: Layout, cost and implementation perspectives". In: *Journal of Energy Storage* 32 (2020), p. 101985.

Appendix A

Additional Background Information

A.1 Introduction

This appendix provides information on the sizing of a PV based electrical cooking system and explores the potential opportunity to reduce the battery requirements through the addition of a thermal storage system. It includes the modelling of the cooking load profile, the sizing of the PV panel, and the analysis of both the electrical (with battery only) and hybrid (with battery and thermal storage) cooking systems.

A.2 Cooking Load Profile and Battery Storage System

A load profile for cooking in a rural household is simulated to analyse the power and energy behaviour of the PV systems throughout the day. The load focuses on the cooking of two rice meals for breakfast and supper. As discussed in *Section 3.2.3*, previous studies on cooking rice suggest that it can be cooked with electrical energy of less than 500 Wh. For the initial analysis, this energy is allocated for each meal and assumed that it will fully prepare the rice. The actual energy required to prepare well-cooked rice will be determined using the experimental work given in *Appendix B*. An electrical cooking appliance (with an average power of 166.67 W at high-heat level setting) is used to prepare the meal. Based on the power specifications, a meal takes three hours to be prepared. For breakfast, the cooking duration is selected to start from 04:00 to 07:00 am, while for supper it starts 04:00 pm to 07:00 pm. These times are chosen so that the meals are ready by the typical eating times of breakfast (before 08:00 am) and supper (before 08:00 pm). The resulting load profile of cooking these meals is presented in *Figure A.2(a)*.

The simulated energy of the cooker occurs in the morning and afternoon and has no consumption during the day. This motivates the necessity of a battery system in an electrical system to capture and use the energy of the sun during off-peak sun hours. The cooking energy in a day for the two meals amounts to 1.0 kWh. The battery in the electrical cooking system is sized to match this daily energy demand and serves to charge with the difference between the PV and load power.

A.3 Solar PV System

The solar PV system is sized and simulated to assess the power generation from the PV panel throughout the day. The irradiance and the temperature data measured every minute for five years (2018 to 2022) in Pretoria, South Africa were obtained from the Southern African Universities Radiometric Network (SAURAN) website to size and model the daily power variability of the panel [1]. The average daily solar irradiance, and three approximation methods: peak-sun hours, triangular, and sinusoidal are shown in *Figure A.1*. The solar irradiation values of the approximation method are summarised in *Table A.1*.

The sinusoidal approximation, which assumes a solar day of 11 hours, has a close similarly to the measured average irradiance and has a lowest error for the daily solar irradiation. The sinusoidal approximation using *Equation (A.1)*, is then chosen to determine the size of the PV panel. The equation considers energy losses of subsystems using *Equation (A.2)*. Based on the daily energy consumption of cooking, as computed in *Section A.2*, the panel size was calculated to be 245.02 W and a 250 W panel is chosen as the next available single panel size.

$$P_{pv} = \frac{E_L}{\eta_s \frac{G_p}{G_0} \int_{t_1}^{t_2} cos\left(\frac{\pi(t-12)}{\Delta T}\right) dt} \tag{A.1}$$

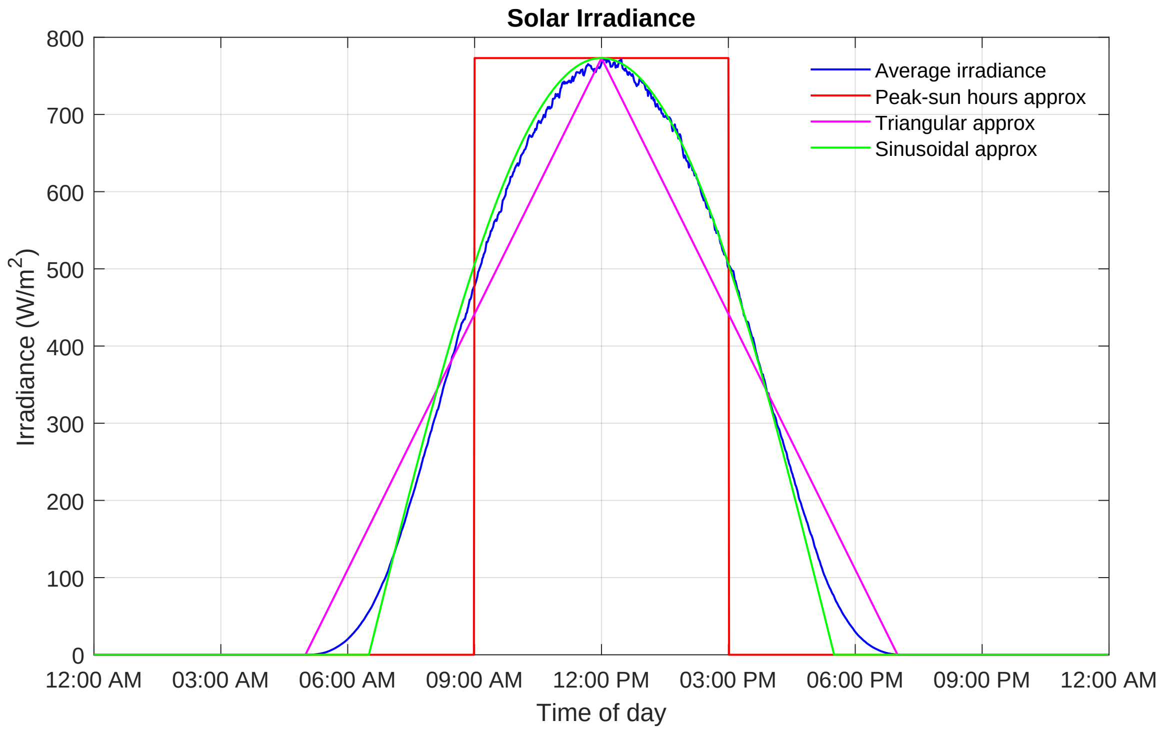

Figure A.1: Daily averaged irradiance with different approximation methods.

Table A.1: Daily solar irradiation of the average irradiance and the approximation methods.

Parameter	**Solar day**	**Irradiation**	**Difference**
Average irradiance	05:14 am to 06:56 pm	5 435.65	-
Peak-sun hours approximation	09:00 am to 03:00 pm	4 651.38	14.43
Triangular approximation	05:00 am to 07:00 pm	5 411.58	0.4428
Sinusoidal approximation	06:30 am to 05:30 pm	5 413.74	0.4031
Unit		Wh/m^2	%

$$\eta_s = \eta_{dc/ac} \times \eta_{dc/dc} \times \eta_{wire} \times \eta_b \tag{A.2}$$

Where:

- P_{pv} is the rated power of the PV array [W]
- E_L is the daily load energy consumption [Wh] (1.0 kWh)
- η_s is the system total efficiency (75%)
- $\eta_{dc/ac}$, $\eta_{dc/dc}$, η_{wire}, and η_b is the inverter subsystem efficiency (90%), the charge controller efficiency (90%), is the wire efficiency (97%), and the battery efficiency (95%), respectively.
- G_p, G_0 is the average daily peak solar irradiance (773.08 W/m^2), and the irradiance under

testing condition (1000 W/m^2) [W/m^2]

- t_1, t_2 is the sunrise (6.5 hours) and sunset times (17.5 hours) [hours]
- ΔT is the solar day period [hours] (11 hours)

The power produced from a PV is simulated using a single-diode and series-resistor model presented in [2, 3] shown using the voltage and current as in *Equation (A.3)*. The substitution *Equation (A.4)*, *Equation (A.5)*, *Equation (A.6)*, *Equation (A.7)*, and *Equation (A.8)* are also defined. This model is chosen because it considers constant parameters obtained from the panel datasheet of the manufacturer, as well as varying weather parameters such as solar irradiance and cell temperature.

$$V = V_{oc}(G,T) + V_T(T)ln\left(1 - \frac{I}{I_{sc}(G,T)}\right) - R_s I \tag{A.3}$$

$$V_{oc}(G,T) = V_{oc0}\left(1 + \beta(T - T_0)\right) + V_{T0}ln\left(\frac{G}{G_0}\right) \tag{A.4}$$

$$I_{sc}(G,T) = I_{sc0}\frac{G}{G_0}\left(1 + \alpha(T - T_0)\right) \tag{A.5}$$

$$R_s = \frac{V_{mp0}}{I_{mp0}} - \frac{2V_{mp0} - V_{oc0}}{I_{mp0} + (I_{sc0} - I_{mp0})ln\left(1 - \frac{I_{mp0}}{I_{sc0}}\right)} \tag{A.6}$$

$$V_T(T) = V_{T0}\frac{T}{T_0} \tag{A.7}$$

$$V_{T0} = \frac{(2V_{mp0} - V_{oc0})(I_{sc0} - I_{mp0})}{I_{mp0} + (I_{sc0} - I_{mp0})ln\left(1 - \frac{I_{mp0}}{I_{sc0}}\right)} \tag{A.8}$$

Where:

- $V,\ I$ is the panel voltage and current [V], [A]
- $G,\ T$ is the irradiance and temperature values [W/m^2], [°C]

Table A.2: Parameter values of a solar PV from the datasheet of the manufacture under standard test conditions [4].

Parameter	V_{oc0}	I_{sc0}	V_{mp0}	I_{mp0}	G_0	T_0	β	α
Value	37.8	8.7	31.5	7.94	1000	25	-0.34	0.06
Unit	V	A	V	A	W/m^2	°C	%/°C	%/°C

Algorithm 1 Solar PV power output using maximum power point (MPPT) tracking method

Initialize values of V_{oc0}, I_{sc0}, V_{mp0} I_{mp0}, G_0, T_0, β and α from the PV datasheet
Compute the initial values of R_s and V_{T0} using *Equation (A.6)* and *Equation (A.8)*
Initialize the solar irradiace and temperature data values: G and T with size N
Compute the values of $V_{oc}(G,T)$, $I_{sc}(G,T)$, and $V_T(T)$ using *Equation (A.4)*, *Equation (A.5)* and *Equation (A.7)* respectively
Initialize the MPPT container, $P_{PV}(MPPT)$ with size N
for j in range 1:N **do**
    Define new I values [0:0.001:$I_{sc}(j)$]
    Compute the corresponding V values using *Equation (A.3)*
    Search for the maximum product value $V \times I$ and insert value in $P_{PV}(MPPT)$
end for

- G_0, T_0 is the irradiance and temperature for standard testing conditions (STC) [W/m^2], [°C]
- $V_{oc}(G,T)$, $I_{sc}(G,T)$ is the open circuit voltage and short circuit current at G and T [V], [A]
- $V_T(T)$ is the thermal voltage at T value [V]
- R_s is the constant series resistance [Ω]
- β, α is temperature coefficient of V_{oc} and I_{sc} [%/°C]
- V_{oc0}, I_{sc0} is the open circuit voltage and short circuit current under STC [V], [A]
- V_{mo0}, I_{mp0} is the voltage and current at maximum power under STC [V], [A]

The parameters of the chosen panel are presented in *Table A.2*. The PV is operated at its maximum power by using the implemented *Algorithm 1*, which searches for the combination of voltage and current from the VI results using *Equation (A.3)* to obtain maximum power in every irrandiance and temperature point. The expected PV power output using the irradiance and temperature data is shown in *Figure A.2(a)*.

Algorithm 2 Energy performance of an electrical cooking system

1: Initialize the energy of the PV, load and battery containers: E_{PV}, E_L, E_B with size N
2: Find the time interval Δt of the data points
3: **for** j in range 1:N **do**
4: Compute the energy of the load: $E_L(j) += P_L(j) \times \Delta t$
5: Compute the energy supplied by the PV: $E_{PV}(j) += P_{PV}(MPPT)(j) \times \Delta t$
6: Compute the energy behaviour of the battery: $E_B(j) += E_{PV}(j) \times \eta_{dc/dc} \times \eta_{wire} \times \eta_b - E_L(j) \div \eta_{dc/ac}$
7: **end for**

A.4 Electrical Cooking System

The cumulative energy of the PV system, the energy consumed by the load, and the usable energy behaviour of the battery system are determined using *Algorithm 2* and the results are illustrated in *Figure A.2(b)*. The simulation is started from 12:00 am for a full day, and the battery begins at half of its usable energy (charged from the previous day) to supply the cooker for the breakfast.

In the case of an electrical system, the battery discharges at 04:00 am to supply the cooker for the first meal and around 06:15 am to 07:00 am some level of PV energy is supplemented. The battery starts recharging after the cooking ends at 07:00 am achieving full capacity before 04:00 pm. After this, the cooking of the second meal begins and the V power output is below the load, which means the battery discharges to supplement the PV. This process continues daily depending on the panel generation and load behaviour.

A PV cooking system designed in this manner would require a battery size of around 1.45 kWh (1.17 kWh of usable energy), which is unlikely to be affordable in rural Africa. This is primarily because the average cost of lithium-ion batteries cost is approximately 139 USD/kWh, while about 85% of Africans live under 5.50 USD/day [5, 6]. This means the cost of the battery is more than what most Africans use in a month. Therefore, there is a need for a storage unit that is cost-effective.

A.5 Hybrid Cooking System

It is hypothesised that using a hybrid cooking system, which combines a battery with a thermal storage system could offer a reduced cost price. This stems from the assumption that thermal

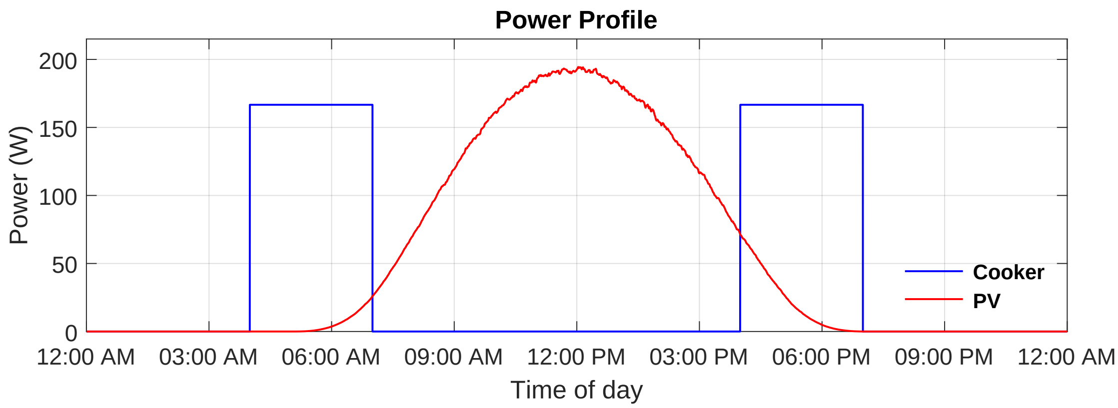

(a) PV and electrical cooker profiles

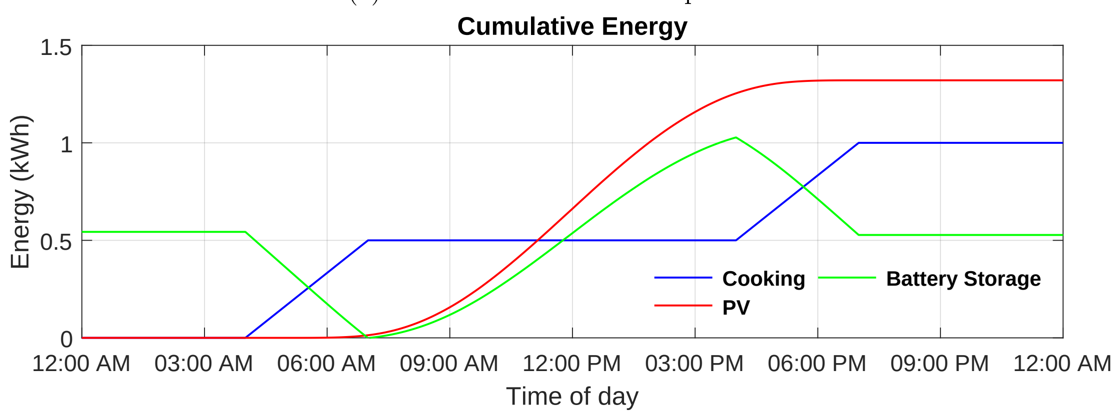

(b) Electrical cooking system.

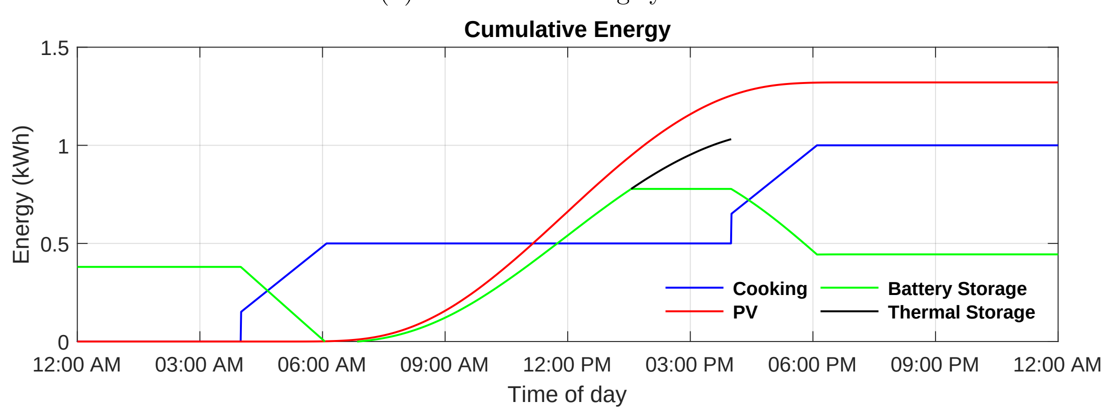

(c) Hybrid cooking system.

Figure A.2: Simulation results of a PV cooking system. (a) PV and electrical cooker profiles. (b) Electrical cooking system. (c) Hybrid cooking system.

storage systems typically use low-cost storage materials compared to electrochemical batteries. In this study, a storage water heater is considered, where heat is stored in the form of hot water, which is advantageous because people usually live where there is access to water.

From an energy perspective, cooking energy is now split into two components: electrical and thermal ($E(cooking) = E(battery) + E(thermal)$). To illustrate this concept, the total cooking energy obtained in *Section A.2* is divided as 75% electrical and 25% thermal energy, and the energy results of the hybrid system are illustrated in *Figure A.2(c)*. The terminology is that thermal energy (hot water) is used initially, followed by electrical energy to complete the process. This means the reduced battery would reach full capacity by 01:33 pm, with the remaining PV energy (approximately 253 Wh, as shown by the black plot) is directed towards water heating.

While the hybrid cooking system topology, as explained, appears promising, the important factors to consider in the system are:

- A cooking process relies on the temperature of the food mixture rather than the amount of energy supplied to the food. The readiness of the food has to be monitored after the addition of thermal energy to determine the actual amount of electrical energy required to complete the cooking process.
- A thermal storage system is likely to experience high energy losses compared to the battery on stand-by, which requires good resistance to store heat for long periods. A lossy storage system would require a slightly larger panel size to compensate for the energy losses, which is still likely to be cheaper than considering a larger battery.

A.6 Conclusion

This appendix focused on the sizing of a PV system with a battery for a simulated cooking load, and highlighted the potential to store part of the PV energy generated into a thermal storage system in order to have a reduced battery size.

References

[1] SAURAN. *Southern African Universities Radiometric Network, Solar radiometric data for the public*. [online]. Available: `https://www.sauran.ac.za/`, Last Accessed 14 Sept. 2023.

[2] L. Cristaldi, M. Faifer, M. Rossi, and S. Toscani. "A simplified model of photovoltaic panel". In: *2012 IEEE International Instrumentation and Measurement Technology Conference Proceedings*. IEEE. May 2012, pp. 431–436.

[3] A. Bellini, S. Bifaretti, V. Iacovone, and C. Cornaro. "Simplified model of a photovoltaic module". In: *2009 Applied Electronics*. IEEE. Sept. 2009, pp. 47–51.

[4] CENTSYS. *250W Solar panel specifications*. [online]. Available: `https://www.centsys.co.za/`, Last Accessed 14 Sept. 2023.

[5] Statista. *Lithium-ion battery price worldwide from 2013 to 2023*. [online]. Available: `https://www.statista.com/statistics/883118/global-lithium-ion-battery-pack-costs/`, Last Accessed 06 Dec. 2023.

[6] R. Andress Castaneda Aguilar, Dean Mitchell Jolliffe, Tony Fujs, Christoph Lakner, and Espen Beer Prydz. *85% of Africans live on less than $5.50 per day*. Wolrd Bank. [online]. Available: `https://blogs.worldbank.org/opendata/85-africans-live-less-550-day`, Last Accessed 06 Dec. 2023., 2019.

Appendix B

Cooking System Experimentation

B.1 Introduction

This appendix serves as a detailed lab report outlining the materials and experimental methods used during the research in the Goldfields Laboratory at the University of the Witwatersrand (Wits), Johannesburg. It covers the cooking experimental setup, thermal storage tank setup and the moisture content measurement equipment used.

B.2 Cooking Experiment Setup

The cooking experimental setup with a slow cooker is shown in *Figure B.1.* The slow cooker model is a SC-6004S and it has a measured peak power of 200 W and its cooking vessel has a volume of $4\,\ell$. The power flow to the slow cooker is measured using a measurement box which stepped-down voltages and currents and a data logger recorded the data every second. The temperature profiles were measured using two RTDs (PT100s); one sensor was placed approximately 5 mm above the bottom of the cooking vessel to measure the temperature of the food mixture (and not of the vessel which is at higher temperature), while the other measured the ambient temperature and was positioned at least 30 cm away from the cooker.

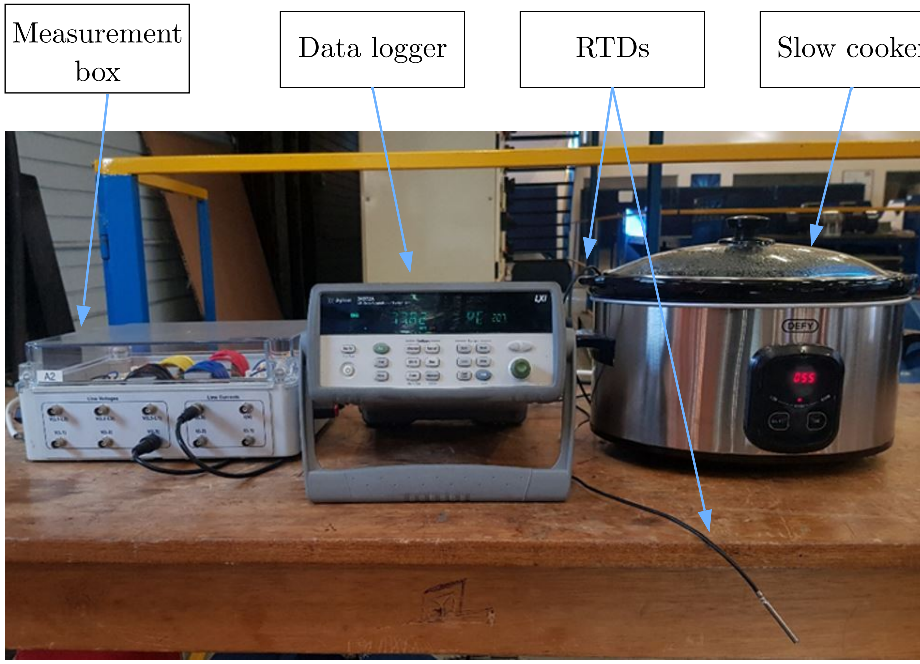

Figure B.1: Experiment setup of cooking with a slow cooker.

B.3 Measurement of Moisture Content

The high resolution scale allows for mass measurement of rice grains in order to determine the moisture content of rice. The scale has a resolution of 1 mg, which when compared to average mass of single grain (30 mg), the scale gives accurate measurements. Moreover, 50 grains were sampled each time, reducing the maximum error to less than 0.07%. To ensure comparable measurements, the scale is initially calibrated using a calibration weight of 20 g. The scale used in the experiments is shown in *Figure B.2*.

The initial investigation of how the moisture content of rice changes without heating it is done using the cooking set-up described in *Section B.2*. The rice was submerged in water (at a ratio of 1:2) for eight hours at ambient temperature of 25 °C without adding heat from the cooker. *Figure B.3* shows the rice-water temperature and the moisture content measurements taken every 30 minutes. During the first hour, the moisture content steadily increased and reached steady state after 1.5 hours. At the end of the 8-hour period, a significant amount of water remained in the cooker, and upon taste evaluation, the rice was still hard for consumption (but softer than the initial dry rice). The moisture content changed from 0 to 40.5% which falls

Figure B.2: Measurement of rice weight using a weight scale

well below the lowest threshold value for well-cooked rice. This highlights that rice cannot be well-cooked without the addition of heat to raise its temperature.

The moisture content trend exhibits an exponential growth which is represented by fitting an exponential trend line given by *Equation (B.1)*.

$$MC = -ae^{-bt} + c \tag{B.1}$$

Where:

- MC is the moisture content [%]
- t is the soaking period [s]
- a, b and c are the coefficients of the equation ($a = 39.59\%$, $b = 1.618$ s^{-1} and $c = 39.51\%$)

B.3.1 Rice Cooking Samples

The images in *Figure B.4* show rice samples that were cooked using two different methods: starting with water at room temperature (25 °C) and starting with pre-heated water (97.6 °C), with samples taken every 30 minutes over a 3-hour cooking period. The images demonstrate

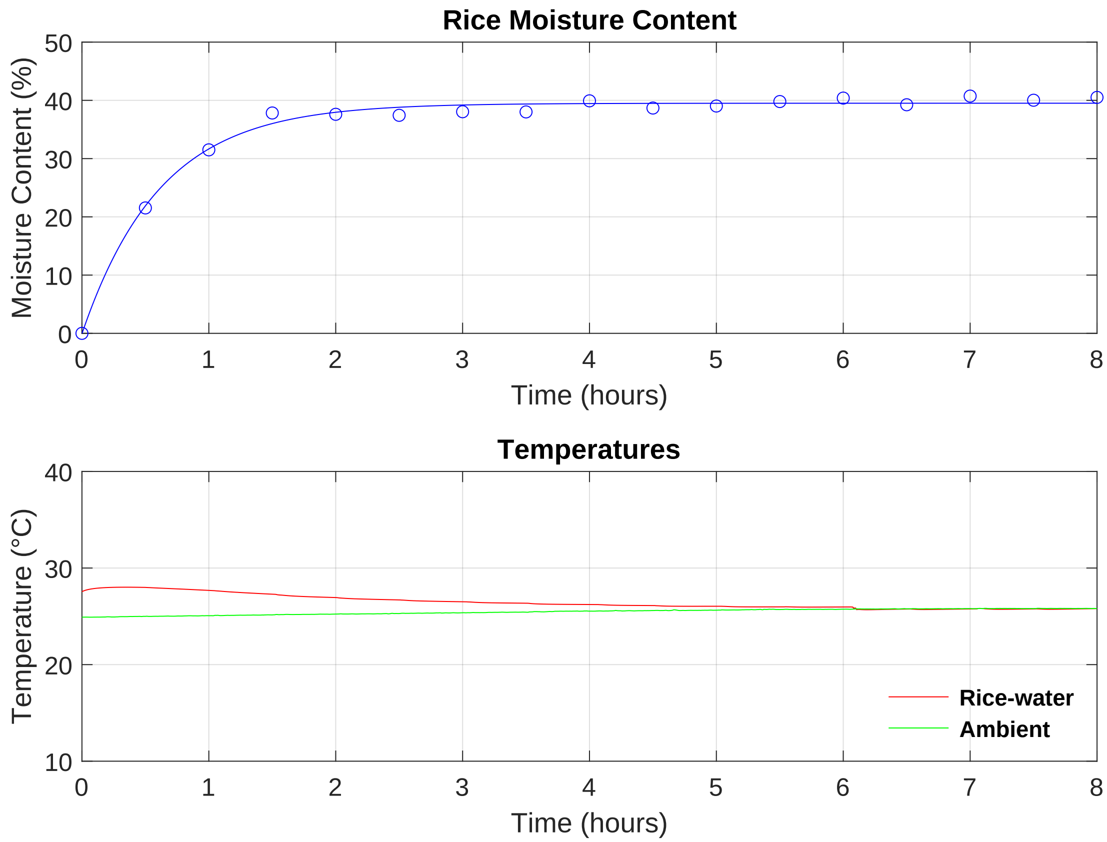

Figure B.3: Resulting rice moisture content, rice-water and ambient temperatures of soaking rice.

that the rice grains cooked with pre-heated water became less brown faster than those cooked with water at room temperature (sample 1 and 2). This indicates that the grains started to cook faster with pre-heated water.

Furthermore, the images show that by the end of the 3-hour cooking period, the whiteness of rice grains in sample 7 with water starting at room temperature was similar to sample 5 of water starting at boiling point. This suggests that using pre-heated water can result in a similar degree of cooking within a shorter duration, as the rice grains cooked with pre-heated water had already achieved a comparable state of cooking after two hours. These samples provide similar evidence as the moisture content that using pre-heated water results in faster cooking times for rice grains.

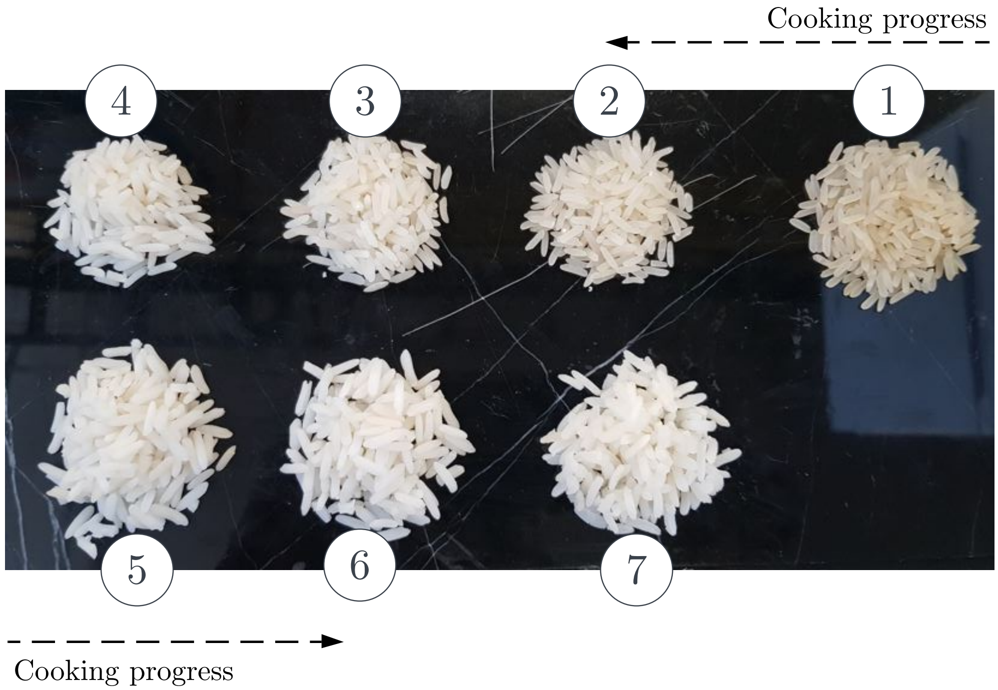

(a) Initial water temperature of 25 °C.

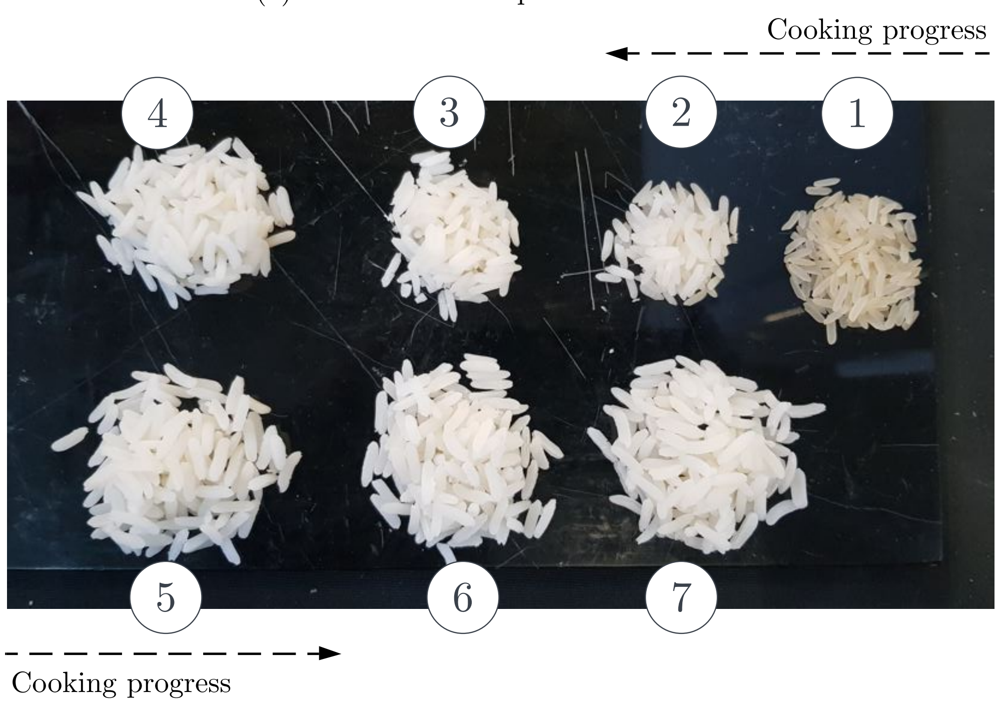

(b) Initial water temperature of 97.6 °C.

Figure B.4: Rice samples of two cooking processes. (a) Initial water temperature of 25 °C. (b) Initial water temperature of 97.6 °C.

B.4 Thermal Energy Storage System Setup

The thermal storage is done with a storage water heater. The storage water heater under test is a portable stainless-steel water urn with a maximum water volume of 15 ℓ and power rating of 1.5 kW designed to operate in a vertical orientation. The use of gravity for water pressure to exit and the top lid for water insertion are the primary design considerations. Unlike domestic water heaters, the urn does not need to be pressurized and or have a fixed water volume. The obtained water urn is shown in *Figure B.5 (a)*.

B.4.1 Thermal Blanket

To increase the heat retention of the urn, a thermal blanket was wrapped around the tank, as shown in *Figure B.5 (b)*. The thermal blanket increased the thermal resistance of the tank by 4.55 times (from 0.497 to 2.26 °C/W), resulting in longer cooling times. From experimental test, the water in the urn after applying a thermal blanket cools down from 87.6 to 40 °C over a period of 17.9 hours (additional of 13 hours without it) with the ambient temperature remaining approximately stable at 22.3 °C. Considering the availability of PV energy to maintain the water in the urn at 87.5 °C until 04:00 pm, the urn will cool down to 40 °C at 09:56 am the following day allowing for cooking in the morning. In general, the thermal blanket gives the urn good heat retention capabilities, allowing it to store hot water for longer periods.

B.4.2 Power Consumption

The cooking system was sized for a small-scale PV system below 500 W of AC output including the cooking appliance. To reduce power consumption of the urn from 1.5 kW to 250 W, modifications were made to the urn. The method for reducing power consumption at 230 V was accomplished using a variac to lower the voltage to the urn, as shown in *Figure B.6*. The secondary voltage of the variac, V_s, is selected using *Equation (B.2)*.

$$V_s = \sqrt{P_s \frac{V_{rated}^2}{P_{rated}}} = 94\ V \tag{B.2}$$

Where:

(a) Without a thermal blanket. (b) With a thermal blanket.

Figure B.5: Water urn under test. (a) Without a thermal blanket. (b) With a thermal blanket.

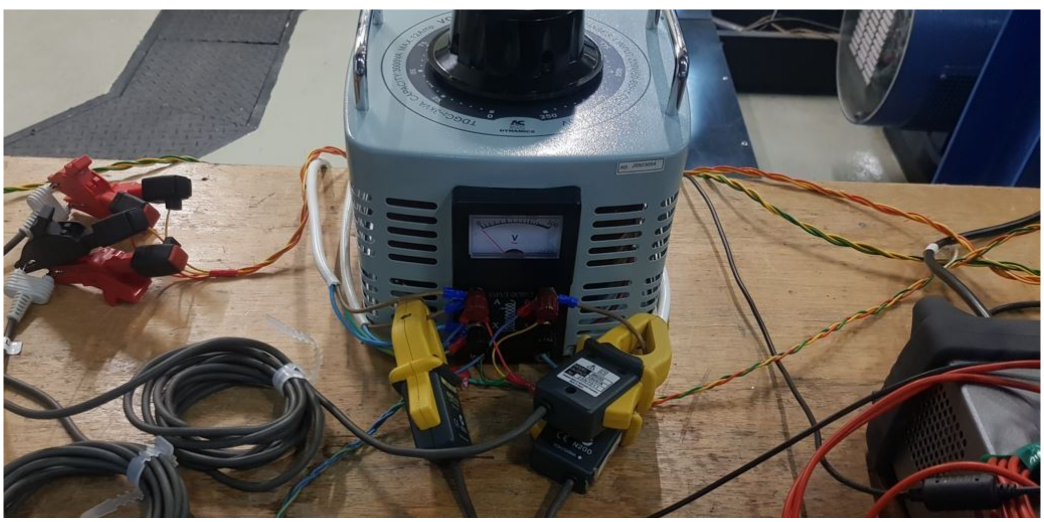

Figure B.6: Variac with current sensors on input and output.

- V_{rated} is the rated operation voltage [V] (230 V)
- P_{rated} is the rated power [W] (1.5 kW)
- P_s is the selected secondary power flow [W] (250 W)

Figure B.7: Experiment setup of a thermal storage tank using a water urn.

B.4.3 Measurement Equipment

The volume of water in the urn is limited to 5 ℓ, which is enough to cook three meals and to be used for other cooking-related tasks within 24-hour period before refiling. The volume of water inserted and drawn was measured using a scale with a resolution of 1 ml. Two RTDs were used for water temperature measurement around the centre of the tank. The RTDs are connected to a Data Acquisition System (model: DAQ970A) and logged every second. Two split-core current transformers were used to measure the current drawn by the heating element of the urn on the input and output of the variac. The voltage measurements were taken directly at the secondary terminal of the variac. A secondary voltage and current measurement system was installed to ensure the accuracy of the measured values by the DAQ. The period selected for water heating (three hours) is controlled using a PLC system. The thermal storage experimental setup is shown in *Figure B.7*.

B.4.4 Water Safety

Since the stored water is used for cooking, it is important to consider the safety of water. The Legionella bacteria thrives in stationary water between temperatures of 20 to 45 °C, with the optimal temperature being 32 to 37 °C [1]. Therefore, the low temperature set-point on the thermostat cannot be below 40 °C. The water temperature should be maintained above 40 °C. Since the appliance is portable, the 5 ℓ water can be replaced after it has been stored below

40 °C for days.

B.5 Conclusion

The experimental work on both the cooking and thermal storage tank setups was presented. The cooking setup involved the use of a slow cooker and measured the power consumption, internal temperature, and moisture content of rice throughout the cooking process. On the other hand, the thermal storage tank setup used a water urn with improved heat retention and measured the internal water temperature, power consumption, water insertion, and draw.

References

[1] Quinton Catherine, Jacques Wheeler, Richardt Wilkinson, and Gerhard de Jager. "Hot water usage profiling to improve geyser efficiency". In: *Journal of energy in Southern Africa* 23.1 (2012), pp. 39–45.

Appendix C

Model Simulation Code

C.1 Introduction

This appendix provides additional model designs for the storage water heater and the cooking appliance. The methods used to calibrate the parameters for each model and the simulation diagrams developed on MATLAB Simulink are provided.

C.2 Storage Water Heater

In this section, the simulation diagrams of the storage water heater, along with the equations used for parameter tuning are given. The schematics and equations are based on the state and output equations of the model discussed in the main document.

C.2.1 Simulation Model

The storage water heater models developed on MATLAB Simulink are illustrated in *Figure C.1*, including the varying volume tank in *Figure C.1* (a) and the fixed volume tank in *Figure C.1* (b). The varying volume tank is the one preferred in the main body, while the fixed volume tank is used for performance comparison. The key difference between the two diagrams is that the varying volume tank reduces the thermal capacitance of water during a draw event, while the fixed volume tank maintains a constant thermal capacitance by immediately replacing the drawn hot water with colder water.

C.2.2 Parameter Estimation Equations

The equations for estimating the unknown parameters, R_a and η, are derived. The first-order differential equation describing the circuit model is given by *Equation (C.1)*.

$$\eta P(t) = C_{wh}(t)\frac{d}{dt}\left(T(t)\right) + C_{in}(t)\frac{d}{dt}\left(T(t) - T_{in}(t)\right) + \frac{1}{R_a}\left(T(t) - T_{amb}(t)\right) \tag{C.1}$$

The parameters are found using a no water draw or insertion experiment, $C_{in}(t) = 0$, meaning constant total water capacity, $C_{wh}(t) = C_{wh}$. The general solution of the internal water temperature using Laplace Transforms is presented in *Equation (C.2)*.

$$T(t) = \eta P(t)R_a + T_{amb}(t) + (T(t_0) - (\eta P(t)R_a + T_{amb}(t)))e^{-\frac{t-t_0}{C_{wh}R_a}} \tag{C.2}$$

The value of the thermal resistance, R_a, is tuned using the cooling curve from the highest to the lowest temperature when, $P(t) = 0$, which is given in *Equation (C.3)*. R_a values are computed at each measurement point, and the average value is taken.

$$R_a = -\frac{t - t_0}{C_{wh}ln\left(\frac{T(t)-T_{amb}(t)}{T(t_0)-T_{amb}(t)}\right)} \tag{C.3}$$

The value of the efficiency, η, is tuned using the heating curve from the lowest to the highest water temperature. The resulting equation, including the heat loss is presented in *Equation (C.4)*.

$$\eta = \frac{T(t) - T_{amb}(t) - \left(T(t_0) - T_{amb}(t)\right)e^{-\frac{t-t_0}{C_{wh}R_a}}}{P(t)R_a\left(1 - e^{-\frac{t-t_0}{C_{wh}R_a}}\right)} \tag{C.4}$$

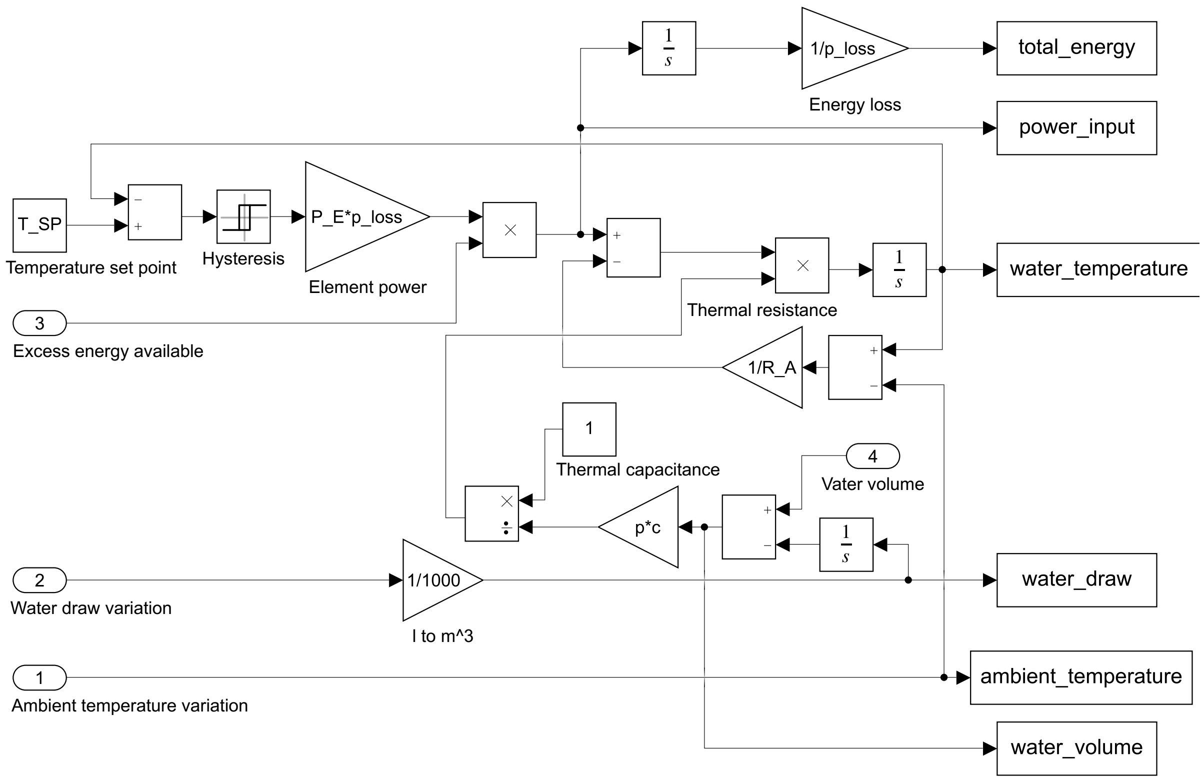

(a) Varying water volume.

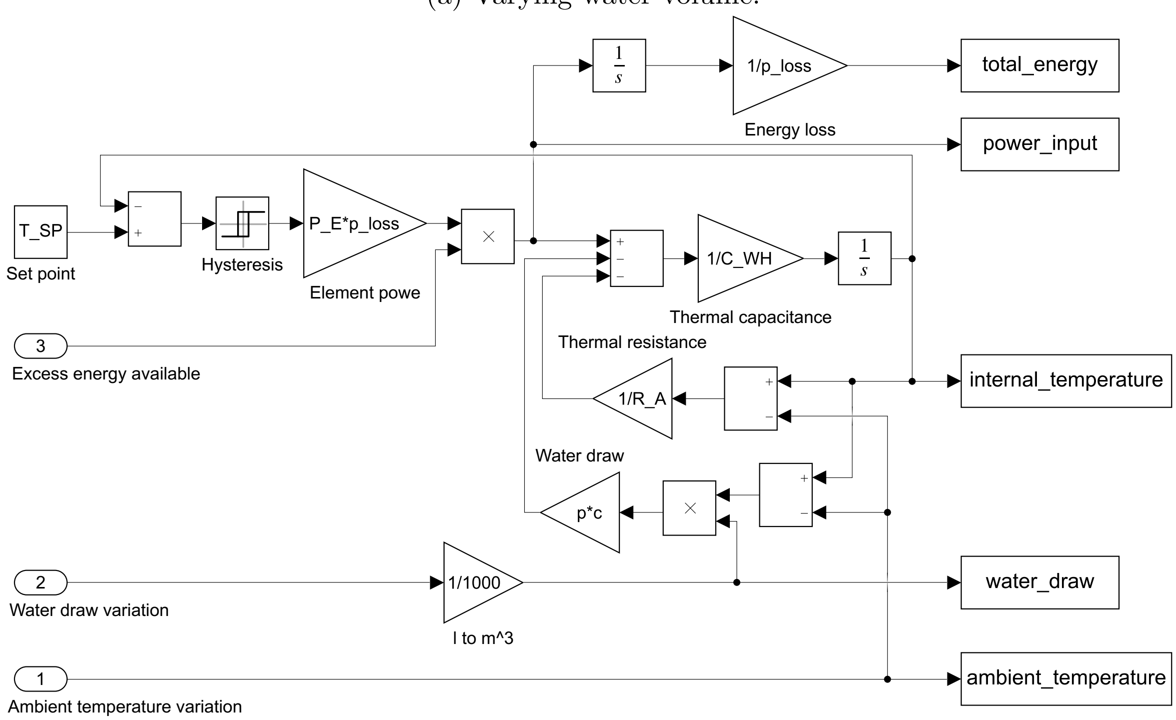

(b) Fixed water volume.

Figure C.1: Simulation model of a storage water heater. (a) Varying water volume. (b) Fixed water volume.

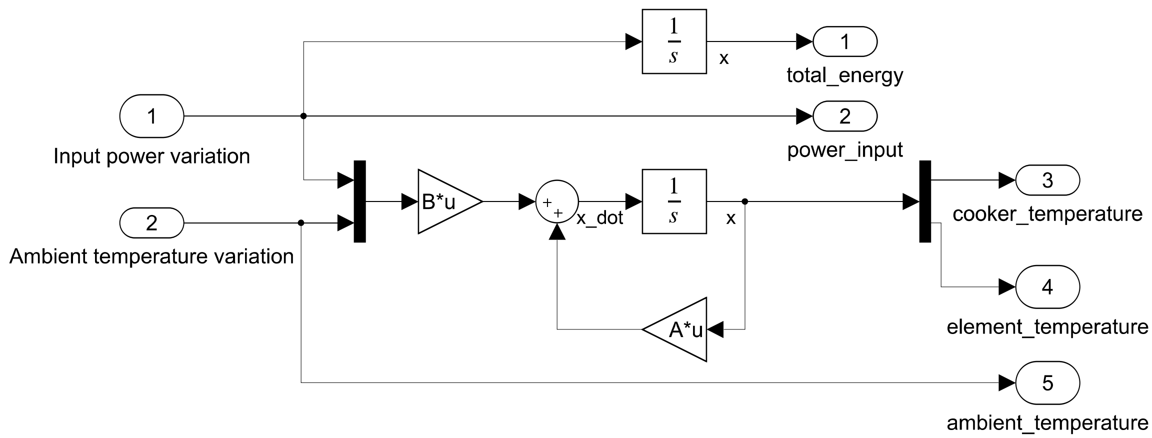

Figure C.2: Simulation model of a slow cooker.

C.3 Cooking Appliance

In this section the MATLAB Simulink schematic is provided, illustrating the implementation of the slow cooker model for simulation. The GA used for estimating the unknown parameters is described in detail. The steps involved in using the GA along with the obtained estimated parameters are also given.

C.3.1 Simulation Model

The MATLAB Simulink model of the cooking appliance is presented in *Figure C.2*. The model is constructed using matrix terms obtained from the state-space *Equation (C.5)*, which is derived in the main document. The GA developed to estimate the parameters of the matrix entries is explained in the following section.

$$\begin{bmatrix} \frac{dT_c(t)}{dt} \\ \frac{dT_e(t)}{dt} \end{bmatrix} = \begin{bmatrix} -\left(\frac{1}{R_{ec}C_e} + \frac{1}{R_aC_c}\right) & \frac{1}{R_{ec}C_e} \\ \frac{1}{R_{ec}C_e} & -\frac{1}{R_{ec}C_e} \end{bmatrix} \begin{bmatrix} T_c(t) \\ T_e(t) \end{bmatrix} + \begin{bmatrix} 0 & \frac{1}{R_aC_c} \\ \frac{1}{C_e} & 0 \end{bmatrix} \begin{bmatrix} P(t) \\ T_{amb}(t) \end{bmatrix} \quad \text{(C.5)}$$

C.3.2 Genetic Algorithm

The pseudo-code in *Algorithm 3* (implemented on MATLAB) summarizes the developed GA for the cooker. The algorithm determines the thermal resistor and capacitor parameters of the cooking appliance, and the thermal resistor of the thermal energy storage system.

1. *Initialization*: Firstly, a population that contains a set of individuals is created. Each individual contains genes with possible parameter values. The parameters are generated using normal random distribution, with an estimated mean and standard deviation values. The steps taken to estimate the mean values is explained in *Section C.3.3*.

2. *Evaluation*: A fitness function is used to evaluate the best generated individual (i.e. the one with the highest fitness value). This function is defined using *Equation (C.6)*.

$$f(i_n) = \frac{1}{RMS}; \text{ where } RMS = \sqrt{\frac{1}{K}\sum_{i=1}^{K}(T_{c(model)}[i] - T_{c(experiment)}[i])^2} \tag{C.6}$$

   The root mean square (RMS) is obtained using the modelled internal temperature and the experiment temperature with the experiment sample size, K. The next points, 3-5, define the genetic operations applied to the initial population to produce a population of new individuals.

3. *Selection*: The aim of this operation is to select the best individuals such that a new population can be created. The method considers a small tournament of randomly selected individuals from the population. New fitness values are calculated, and the best is inserted in a selection container. The size of the selection container is the same as the initial population. This operation is shown in *Algorithm 4*.

4. *Crossover*: The selection container is split into half to create two containers. The individuals in each container are used to generate two new individuals using the arithmetic crossover method, with a randomly selected crossover value. This is shown in *Algorithm 5*.

5. *Mutation*: This operation is applied to mutate 20% of the randomly selected crossover population. It adds a mutation factor (between 0 and 0.01) to each selected individual.

Algorithm 3 Genetic Algorithm to obtain the parameters of a cooking appliance

Define N, G, τ, ϵ
Obtain measured data: internal temperature, input power and ambient temperature
Initialize GA population, $P_N[C_e, R_{ec}, C_c, R_a]$, use randomly selected within mean and standard deviation range
Initialize $g = 0$, the iteration of the GA
while g < G **do**
    for each individual $i_n \in P_N$ **do**
        Create the state-space parameters: A, B, C and D; and input u
        Simulate the cooking material temperature: $T_c(t)$
        Calculate the fitness value using the measured food mixture temperature
    end for
    Record the best individual: maximum fitness value
    procedure GENERATIC OPERATIONS(P_N)
        Selection: Obtain new container, V_{sel}
        Crossover: Create new population from the selected container, $P_{N(new)}$
        Mutation: Mutate a randomly selected percentage of, $P_{N(new)}$
    end procedure
    Insert the recorded best individual in $P_{N(new)}$
    Replace content of P_N by $P_N(new)$
    g++
end while
Output the best individual

Algorithm 4 Selection

Initialize the selection container, $V_{sel}[C_e, R_{ec}, C_c, R_a]$, of size N
for each entry in V_{sel} **do**
    Define new tournament, Γ_τ, by randomly selecting τ individuals in P_N
    for each individual $i_n \in \Gamma_\tau$ **do**
        Create the state-space parameters: A, B, C and D; and input u
        Simulate the cooking material temperature: $T_c(t)$
        Calculate the fitness value using the measured food mixture temperature
    end for
    Insert the best individual in V_{sel}
end for

The algorithm is shown in *Algorithm 6*.

6. *Termination*: The initial population is replaced with the new population generated through the genetic operations and the algorithm repeats again. The process stops when the absolute difference between the previous maximum fitness value and the new maximum fitness value is less than 0.0001, or when the maximum number of alterations is reached.

C.3.3 Parameter Estimation

An experiment of a slow cooker with 300 mg of rice and 600 mℓ of water (initial value 25 °C) was conducted to obtain the parameters equivalent circuit model and to validate it. The internal

Algorithm 5 Crossover

Equally split V_{sel} into V_{sel1} and V_{sel2}
for each i_{sel1} and i_{sel2}: Where $i_{sel1} \in V_{sel1}$ and $i_{sel2} \in V_{sel2}$ **do**
  Generate a random number $\beta \in \mathbb{R}$ [0, 1]
  Create first child crossover: $i_{cross1} = i_{sel1} \cdot \beta + i_{sel2} \cdot (1 - \beta)$
  Create second child crossover: $i_{cross2} = i_{sel2} \cdot \beta + i_{sel1} \cdot (1 - \beta)$
  Insert i_{cross1} and i_{cross2} into P_{new}
end for

Algorithm 6 Mutation

Define mutation pool, V_{mut}, by randomly selecting ε individuals in $P_{N(new)}$
for every entry $i_n \in V_{sel}$ **do**
  Randomly select number of mutations: $n_{mut} \in \mathbb{Z}$ [1, n_{par}]
  for i in range 1:n_{mut} **do**
    Select a parameter index randomly $i_p \in \mathbb{Z}$ [0, n_{par}-1]
    Generate a random noise value $\eta \in \mathbb{R}$ [0, 0.1]
    Mutate the selected parameter: $i_n[i_p] \cdot= (1 + \eta)$
  end for
  Update the mutated individual i_n in V_{mut}
end for
Replace the mutated pool V_{mut} back to $P_{N(new)}$

temperature, the input power consumption, and the ambient temperature were measured during a 2.5-hour cooking period.

The slow cooker model incorporates two thermal capacitors, namely C_e and C_c, which are essential parameters for running the GA. C_e represents the thermal mass of the heating element and it is estimated by considering the mass of a ceramic material and its specific heat. On the other hand, C_c, represents the thermal mass of the food mixture, which is estimated by summing up the product of the mass of water and its specific heat with the mass of rice and its specific heat. The estimated values are summarised in *Table C.1*.

Given the limited information available to estimate the initial values of the thermal resistors, R_{ec} and R_a, the GA was employed to derive these parameters with a large sample range. The initial value of R_{ec} has been set to 2.000, while the value of R_a has been set to 0.250. To account for potential variability in these estimates, a large standard deviation of 25% has been applied for R_{ec}, and 45% for R_a. The values of the constants for the GA are $N = 1000$, $K = 3010$, $G = 100$, and $\tau = 5$. The resulting values obtained after running the GA are presented in *Table C.2*.

Table C.1: Initial value estimation of thermal capacitors of a slow cooker model.

Parameter	**m**	**c**	**Value**
C_e	3.484	850	2961.4
C_c	2.0	4182	8364
Unit	kg	J/kg·°C	J/°C

Table C.2: Parameter values of a slow cooker model using the GA.

Parameter	$R_{ec} : \mu(\sigma)$	$C_e : \mu(\sigma)$	$R_a : \mu(\sigma)$	$C_c : \mu(\sigma)$
Initial value	2.00(25%)	2961.4(10%)	0.25(45%)	8364 (15%)
Generated value	0.589	2881.7	0.420	3292.3
Unit	°C/W	J/°C	°C/W	J/°C

C.4 Conclusion

The MATLAB Simulink model of the storage water heater, as well as the corresponding equations for calibrating the unknown parameters using experimental data, have been presented in this appendix. Additionally, the Simulink model for the slow cooker, along with the Genetic Algorithm (GA) employed for tuning the values of the unknown parameters using experimental results are also demonstrated.

Appendix D

Hybrid Cooking System Performance: Fixed Volume Tank Analysis

D.1 Introduction

This appendix delves into the performance evaluation of the hybrid storage cooking system using a fixed volume storage water heater (piped tank). It examines three different cooking scenarios and compares the energy performance against the baseline electrical cooking system. The key findings are then compared to those obtained from a storage water heater with varying volume (non-piped tank) presented in the main body of the document.

D.2 Scenario S1: One Meal a Day

The performance of an electrical and a hybrid cooking system with a piped storage water heater is shown for the preparation of one meal in *Figure D.1.* A summary of the energy and battery sizing results for both systems is presented in *Table D.1.* For scenario $S1$, where one meal is cooked, 600 mℓ of hot water is drawn at a constant flow rate of 36 ℓ/hr at 04:00 pm. Due to the piped tank, the water is replaced immediately with water at ambient temperature, causing the water temperature to drop. The pre-heated water and ambient temperature difference before

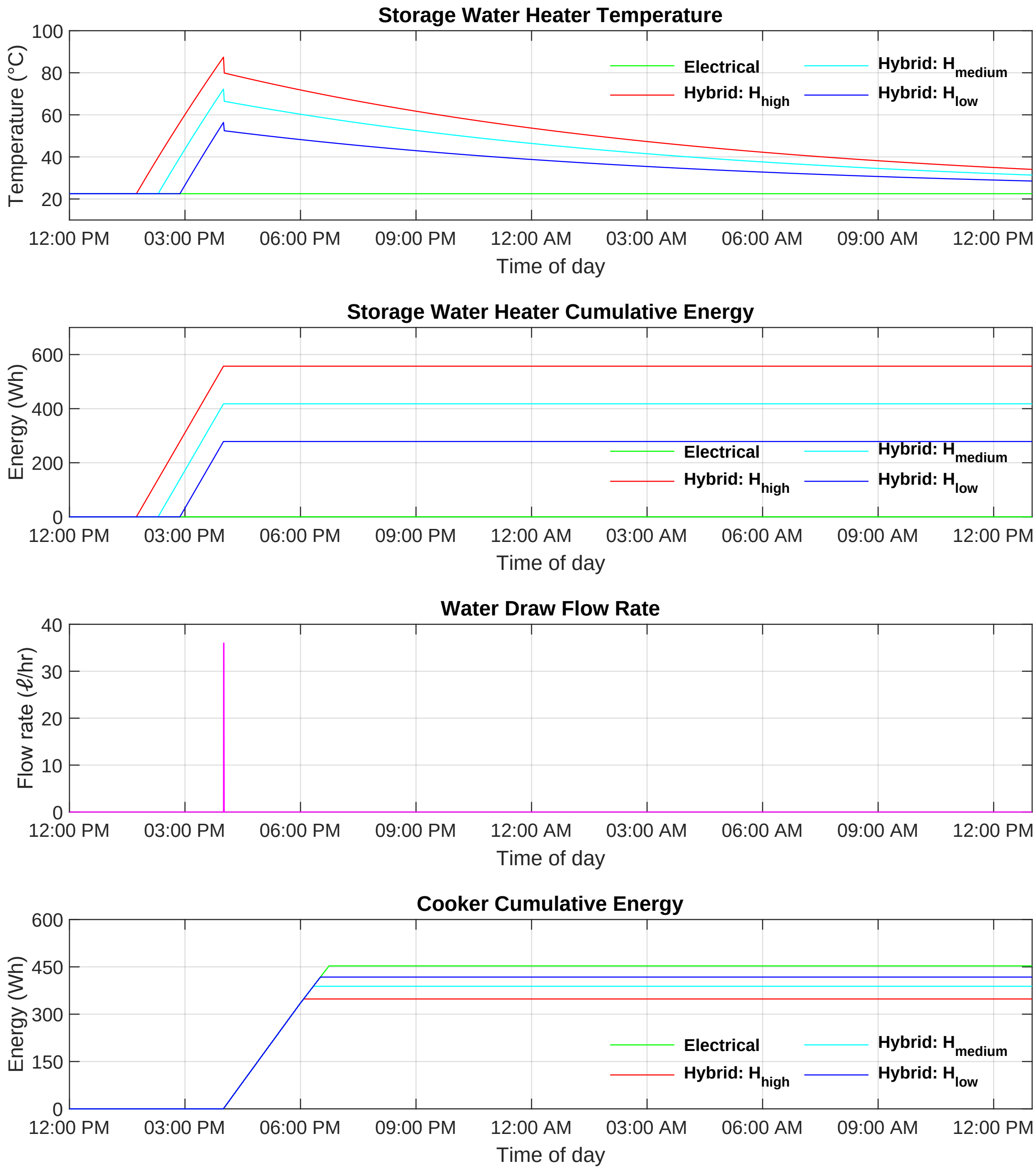

Figure D.1: Results of cooking one meal using an electrical and hybrid system with a piped storage water heater.

cooking is 64.93 °C for H_{high}, 49.74 °C for H_{medium}, and 33.87 °C for H_{low} which translated to an energy reduction of 24.3%, 15.1% and 8.33% respectively. By using the hybrid system, the battery capacity size of the electrical system can be reduced from 51.87 Ah to a capacity of 47.47 to 39.21 Ah. It is noted that scenario $S1$ produced the same results for the piped and non-piped storage water heater (results discussed in *Section 6.2.1*) since both cases the systems

Table D.1: Performance of cooking one meal using electrical and hybrid system with a fixed volume storage water heater.

Parameter	**Electrical**	**Hybrid**		
Daily PV energy level	**-**	**High**	**Medium**	**Low**
Water and ambient temp diff. (1st meal) [°C]	0	64.93	49.74	33.87
Electrical energy reduction [%]	0.0%	24.28%	15.12%	8.334%
Additional electrical cooking energy [Wh]	454.15	343.30	384.81	415.58
Battery capacity [Ah]	51.87	39.21	43.95	47.47

had not experienced any other water draw and cooling after heating from the PV energy.

D.3 Scenario S2: Two Meals a Day

The performance of an electrical cooking system and a hybrid cooking system with a piped storage water heater is shown for the preparation of two meals in *Figure D.2*. A summary of the energy and battery sizing results for both systems is presented in *Table D.2*. In scenario $S2$, the first water draw and replacement at 04:00 pm resulted in a temperature decrease that accelerated the cooling trend. The second meal was cooked 12 hours after the first meal at 04:00 am. During the 12-hour period, the water and ambient temperature difference dropped to 22.98 °C for H_{high}, 17.60 °C for H_{medium}, and 11.99 °C for H_{low} which translated to an energy reduction of 4.88%, 3.47%, 2.14% respectively. Overall, the energy reduction for cooking two meals amounts to a range of 5.24 to 14.6%. Therefore, the battery capacity of 103.74 Ah can be replaced with a smaller battery of 98.14 to 88.47 Ah for completing two cooking processes in the hybrid system. In scenario $S2$, the piped tank produced a slightly lower reduction by 0.12% than the non-piped tank (results discussed in *Section 6.2.2*). This is because the replacement of water after a draw event mixes with colder water at ambient which cools down faster compared to reducing the volume of water (which also increases the thermal resistance by reducing the contact surface area).

D.4 Scenario S3: Three Meals a Day

The performance of an electrical cooking system and a hybrid cooking system with a piped storage water heater is shown for the preparation of three meals in *Figure D.3*. A summary of

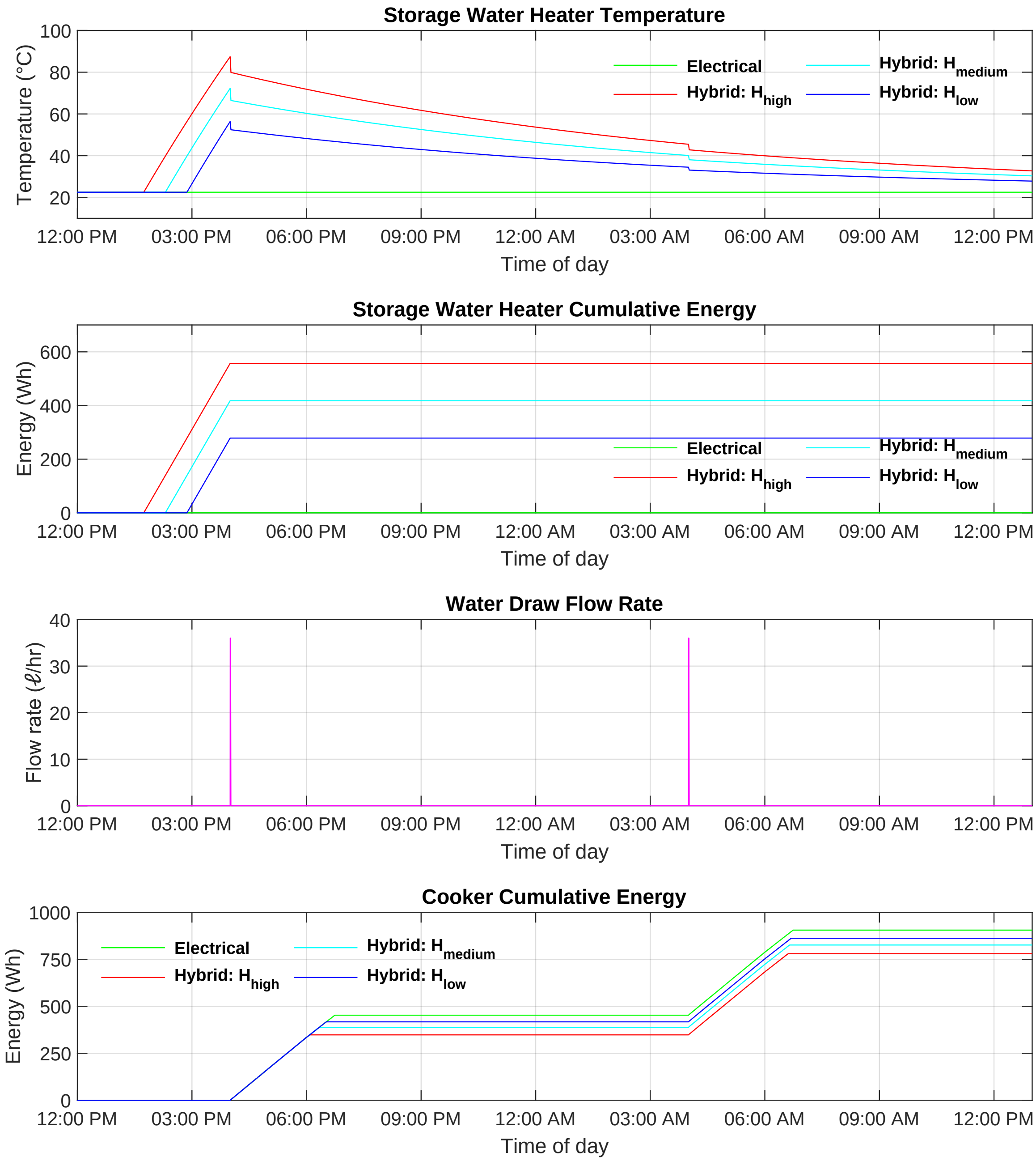

Figure D.2: Results of cooking two meals using an electrical and hybrid system with a piped storage water heater.

the energy and battery sizing results for both systems is presented in *Table D.3*. The preparation of the third meal starts at 10:00 am, after two previous meals were cooked earlier. In scenario $S3$, the water continues to cool after the first two water draws, resulting in lower water to ambient temperature differences of 12.86 °C for H_{high}, 9.853 °C for H_{medium}, and 6.709 °C for H_{low} before cooking the third meal. These temperatures result in electrical energy reductions of

Table D.2: Performance of cooking two meals using electrical and hybrid system with a fixed volume storage water heater.

Parameter	**Electrical**	**Hybrid**		
Daily PV energy level	**-**	**High**	**Medium**	**Low**
Water and ambient temp diff. (1st meal) [°C]	0	64.93	49.74	33.87
Water and ambient temp diff. (2nd meal) [°C]	0	22.98	17.60	11.99
Additional electrical cooking energy [Wh]	908.31	774.53	822.49	856.22
Total electrical energy reduction [%]	0.0%	14.58%	9.290%	5.239%
Battery capacity [Ah]	103.74	88.47	93.94	98.14

Table D.3: Performance of cooking three meals using electrical and hybrid system with a fixed volume storage water heater.

Parameter	**Electrical**	**Hybrid**		
Daily PV energy level	**-**	**High**	**Medium**	**Low**
Water and ambient temp diff. (1st meal) [°C]	0	64.93	49.74	33.87
Water and ambient temp diff. (2nd meal) [°C]	0	22.98	17.60	11.99
Water and ambient temp diff. (3rd meal) [°C]	0	12.86	9.853	6.709
Additional electrical cooking energy [Wh]	1 362.46	1 217.30	1 268.21	1 307.84
Total electrical energy reduction [%]	0.0%	10.50%	6.754%	3.841%
Battery capacity [Ah] (option 1)	155.62	139.04	144.85	149.38
Battery capacity [Ah] (option 2)	103.74	88.47	93.94	98.14

4.88%, 3.46% and 2.14% for cooking. Overall, the combined electrical energy reduction for all three meals ranges from 3.84 to 10.5% compared to the electrical system, which allows for smaller battery capacity of 149.38 to 139.04 Ah to be used, instead of the original 155.62 Ah. Similar to scenario $S2$, the hybrid system with a piped tank produced a slightly lower reduction by 0.1% compared to a non-piped tank (results discussed in *Section 6.2.3*) due to faster cooling trends. However, due to the long 15-hour cooling periods, the temperatures in both tanks end up stabilising close to ambient hence the difference is low. An alternative option for this system is to size the battery for the first two meals that are prepared during off-peak sun hours using the sizing results of scenario $S2$.

D.5 Conclusion

The performance of the hybrid storage cooking system with a fixed volume storage water heater has been explored. The key results reveal significant reductions in electrical energy consumption: up to 24.3% for one meal, up to 14.6% for two meals, and up to 10.5% for three

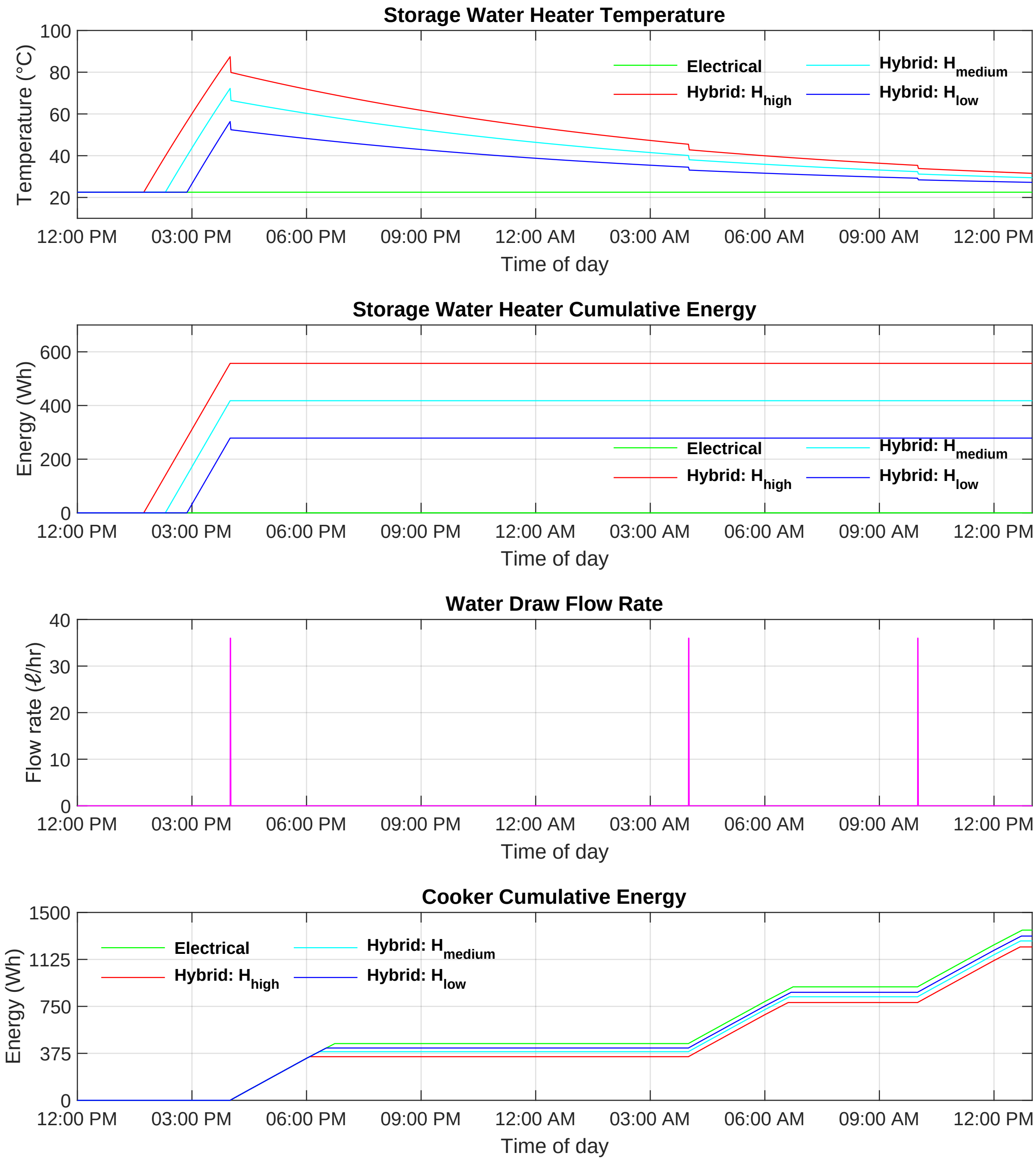

Figure D.3: Results of cooking three meals using an electrical and hybrid system with a piped storage water heater.

meals. Comparing the fixed volume tank with the varying volume tank, it has been observed that the two and three meal preparations exhibit a slightly lower reduction by around 0.1%. This can be attributed to the faster cooling times after the water withdrawal and replacement with water at colder temperatures. Since the difference is minimal between the tanks, the advantage of not having to manually replace water is the key benefit.